AD-A131 324 FATIGUE BEHAVIOR OF LONG AND SHORT CRACKS IN WROUGHT AND POWDER ALUMINUM..(U) CALIFORNIA UNIV BERKELEY DEPT OF MATERIALS SCIENCE AND MINERA.. R O RITCHIE MAY 83 1/2

UNCLASSIFIED UCB/RP/IE/A1013 AFOSR-TR-83-0616 F/G 11/6 NL

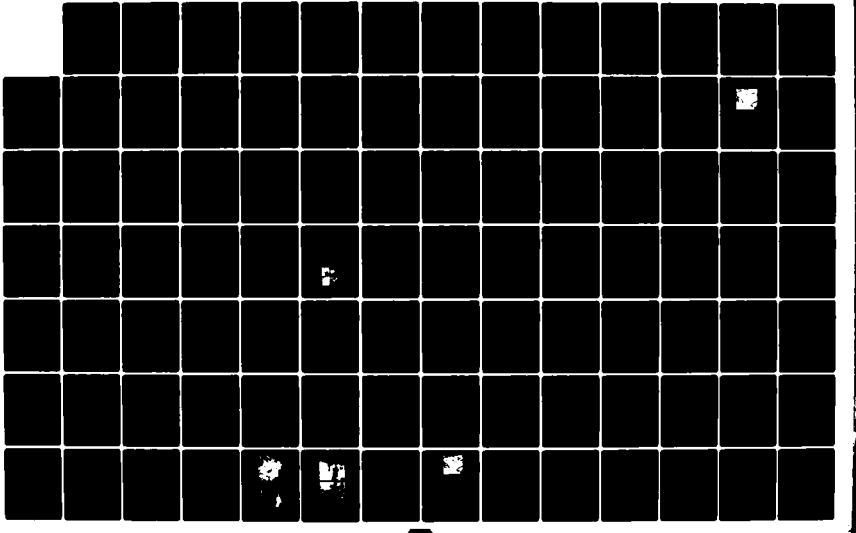

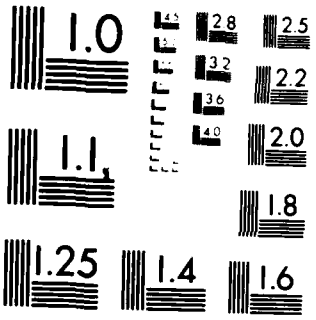

AFOSR-TR- 83 0816

(1)

AD A131324

First Annual Report

to

U.S. Air Force Office of Scientific Research

on

FATIGUE BEHAVIOR OF LONG AND SHORT CRACKS IN WROUGHT AND POWDER ALUMINUM ALLOYS

Grant AFOSR-82-0181

for period 15 April 1982 to 14 April 1983

by

Robert O. Ritchie

May 1983

Report No. UCB/RP/ie/A1013

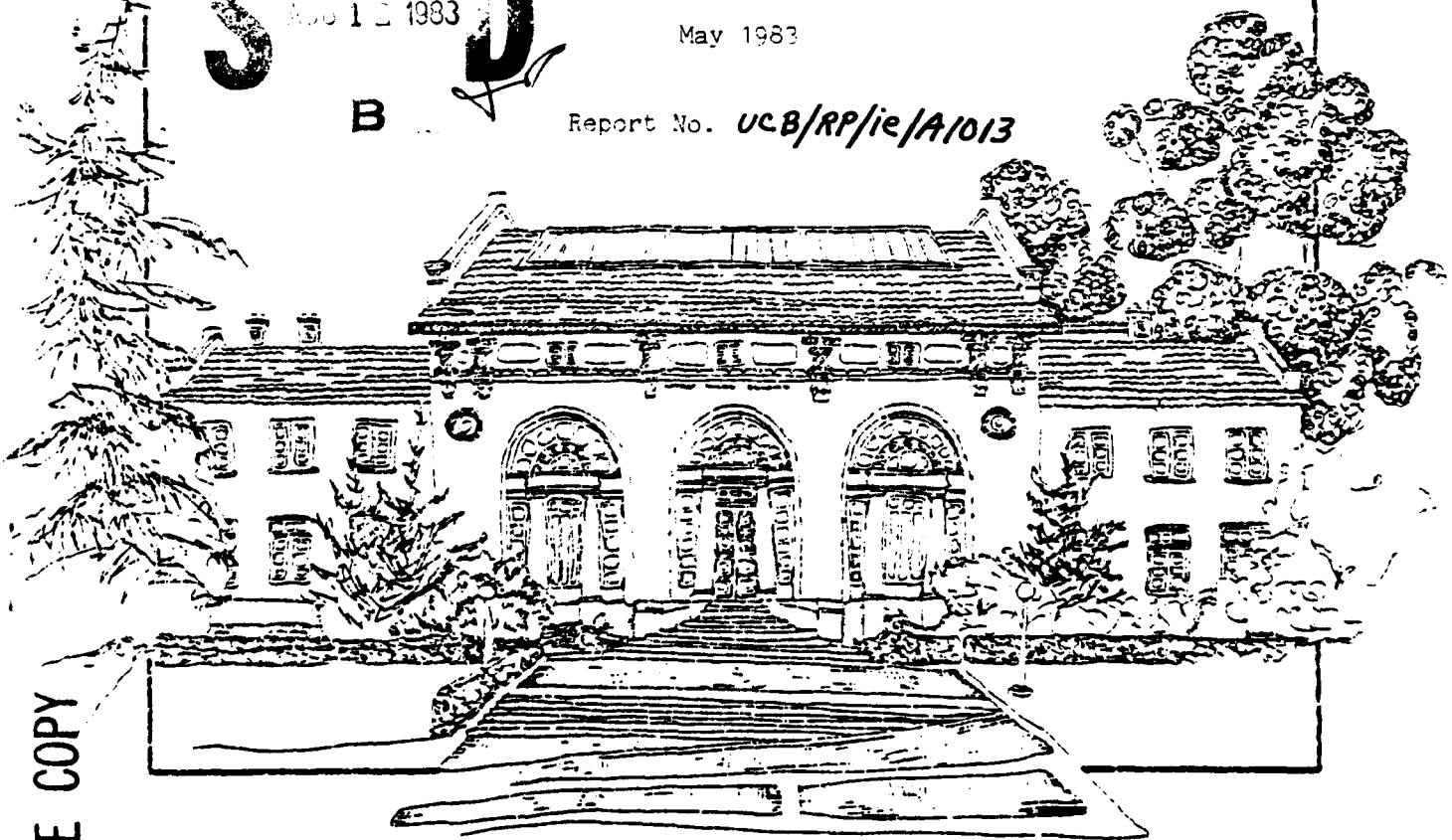

Department of Materials Science and Mineral Engineering

Hearst Mining Building
University of California, Berkeley

Report No. UCB/RP/ie/A1013

First Annual Report

to

U.S. Air Force Office of Scientific Research

on

FATIGUE BEHAVIOR OF LONG AND SHORT CRACKS IN WROUGHT AND POWDER ALUMINUM ALLOYS

Grant AFOSR-82-0181

for period 15 April 1982 to 14 April 1983

submitted to

U.S. Air Force Office of Scientific Research
Bldg. 410, Bolling Air Force Base
Washington, D.C. 20322
Attention: Dr. Alan H. Rosenstein

submitted by

Robert O. Ritchie
Professor of Metallurgy
Department of Materials Science
and Mineral Engineering
University of California
Berkeley, California 94720

May 1983

Unclassified

SECURITY CLASSIFICATION OF THIS PAGE (When Data Entered)

REPORT DOCUMENTATION PAGE		READ INSTRUCTIONS BEFORE COMPLETING FORM
1. REPORT NUMBER **AFOSR-TR- 83-0616**	2. GOVT ACCESSION NO. AD-A131324	3. RECIPIENT'S CATALOG NUMBER
4. TITLE (and Subtitle) FATIGUE BEHAVIOR OF LONG AND SHORT CRACKS IN WROUGHT AND POWDER ALUMINUM ALLOYS		5. TYPE OF REPORT & PERIOD COVERED Annual Report for period 15 April 1982-14 April 1983
		6. PERFORMING ORG. REPORT NUMBER UCB/RP/ie/A1013
7. AUTHOR(s) Robert O. Ritchie		8. CONTRACT OR GRANT NUMBER(s) AFOSR - 82-0181
9. PERFORMING ORGANIZATION NAME AND ADDRESS Robert O. Ritchie, Department of Materials Science and Mineral Engineering, University of California, Berkeley, CA 94720		10. PROGRAM ELEMENT, PROJECT, TASK AREA & WORK UNIT NUMBERS 2306/A1 61102F
11. CONTROLLING OFFICE NAME AND ADDRESS U.S. Air Force Office of Scientific Research, Bldg. 410, Bolling AFB, Washington, D.C. 20322, ATTN: Dr. Alan H. Rosenstein, AFOSR/NE		12. REPORT DATE May 1983
		13. NUMBER OF PAGES
14. MONITORING AGENCY NAME & ADDRESS (if different from Controlling Office) N/A		15. SECURITY CLASS. (of this report) Unclassified
		15a. DECLASSIFICATION/DOWNGRADING SCHEDULE N/A

16. DISTRIBUTION STATEMENT (of this Report)

Approved for public release; distribution unlimited.

17. DISTRIBUTION STATEMENT (of the abstract entered in Block 20, if different from Report)

18. SUPPLEMENTARY NOTES

19. KEY WORDS (Continue on reverse side if necessary and identify by block number)

Fatigue
Defect-tolerant fatigue design
Fatigue in aluminum alloys
Fatigue behavior of long and short cracks
Fatigue cracks: Crack deflection and closure

20. ABSTRACT (Continue on reverse side if necessary and identify by block number)

The fatigue behavior of short cracks, which are small compared to the scale of the microstructure, small compared to the scale of local plasticity or simply physically small (i.e., ≤ 1 mm), must be considered as one of the major factors limiting the application of defect-tolerant fatigue design for airframe and engine components. Accordingly, this program is aimed at identifying factors which govern the growth of such short cracks in a series of commercial aluminum alloys, with specific reference to behavior at near-threshold levels. In this report, the fundamental basis for the study is described in terms of i) a detailed review of

DD FORM 1 JAN 73 1473 EDITION OF 1 NOV 65 IS OBSOLETE

Unclassified

SECURITY CLASSIFICATION OF THIS PAGE (When Data Entered)

Block 20, Abstract (Cont.)

the factors which lead to differences in long and short crack behavior, and ii) a theoretical analysis of the influence of crack deflection and closure mechanisms on long and short crack behavior. It is concluded that many anomalies in the behavior of short fatigue cracks can be traced *primarily* to closure and deflection mechanisms, and accordingly an experimental program is presented with the objective of isolating these effects.

TABLE OF CONTENTS

FATIGUE BEHAVIOR OF LONG AND SHORT CRACKS IN WROUGHT AND POWDER ALUMINUM ALLOYS

R. O. Ritchie

(Grant No. AFOSR-82-0181)

FORWARD

This manuscript constitutes the First Annual Report on Grant No. AFOSR-82-0181, administered by the U.S. Air Force Office of Scientific Research, with Dr. Alan H. Rosenstein as program manager. The work, covering the period April 15, 1982, through April 14, 1983, was performed under the direction of Dr. R. O. Ritchie, Professor of Metallurgy, University of California in Berkeley, and Dr. S. Suresh, Assistant Research Engineer, with assistance from graduate student E. Zaiken and undergraduate student K. A. Johnston.

ABSTRACT

The fatigue behavior of short cracks, which are small compared to the scale of the microstructure, small compared to the scale of local plasticity or simply physically small (i.e., $\leq$ 1 mm), must be considered as one of the major factors limiting the application of defect-tolerant fatigue design for airframe and engine components. Accordingly, the current program is aimed at identifying factors which govern the growth of such short cracks in a series of commercial aluminum alloys, with specific reference to behavior at near-threshold levels (below $\sim 10^{-6}$ mm/cycle). In this first annual report, the fundamental basis for the study is described in terms of i) a detailed review of the factors which lead to differences in long and short crack behavior, with particular regard to the role of crack closure mechanisms, and ii) a theoretical analysis of the influence of crack deflection mechanisms on long and short crack behavior. It is concluded that many anomalies in the behavior of short fatigue cracks can be traced primarily to closure and deflection mechanisms, and accordingly an experimental program is presented with the objective of isolating these effects.

1. INTRODUCTION

The objective of this program is to identify mechanical, microstructural and environmental factors governing the fatigue crack growth of long ($\geq$ 25 mm) and short ($\leq$ 1 mm) cracks in commercial aluminum alloys with specific reference to behavior at ultralow, near-threshold growth rates below typically 10^{-6} mm/cycle. This report covers the initial year of the program of research where attention has been focussed on i) defining factors relevant to the problem (in the form of a literature review), ii) procurement of a series of wrought aluminum alloys, iii) design of a novel test procedure and iv) theoretical analyses of crack closure and crack deflection mechanisms relevant to the behavior of small cracks.

2. REVIEW OF PREVIOUS RESEARCH

Despite an increasing interest, both academically and technologically, in conventional long crack fatigue crack propagation, particularly at near-threshold levels, a major limitation in the application of such information to defect-tolerant design must be regarded as the problem of short flaws. By short flaws, it is implied that flaws are i) small compared with the scale of microstructure, ii) small compared with the scale of local plasticity, or iii) simply physically small (i.e., $\leq$ 0.5 to 1 mm). Design codes at present attempt to predict the growth rates of in-service flaws based on data collected in the laboratory with specimens containing crack sizes of the order of 25 mm. In service, however, initial defects sizes are often far smaller than this. Moreover, in the

few cases where research has been directed towards studying the growth of such small cracks, it has been found, almost without exception, that the growth rate of short cracks is greater than, or equal to, the corresponding growth rate of long cracks at the same nominal driving force[1-17] (Fig. 1). This means that the use of existing fatigue crack propagation data for estimating the structural integrity of certain components using defect-tolerant design may in many cases be non-conservative. Furthermore, it appears, from the limited studies to date,[2,6,10] that the microstructural factors which are known to improve resistance to the growth of long fatigue cracks may be markedly different for short cracks. This clearly poses a difficult problem for the alloy designer in attempting to develop new fatigue-resistant alloys.

To assess the many mechanical, microstructural and environmental factors which may contribute to a lack of correspondence between experimental short crack fatigue data and conventional long crack data, an exhaustive literature survey was performed on the short crack problem, with particular reference to airframe materials. This review is included as the appendix to this report. It was concluded that behavioral differences between the short and long flaw, as shown schematically in Fig. 1, were to be expected, and that such differences could arise from factors which include i) inadequate characterization of crack tip stress and deformation fields of short cracks due to extensive local plasticity, ii) notch tip stress and deformation field effects, iii) interaction of short cracks with microstructural features, i.e., grain boundaries, inclusions, second phases, etc., of dimensions comparable with crack size, iv) differences in crack shape, geometry and distribution, v) differences

in crack extension mechanisms, vi) differences in the contribution from deflection and crack closure mechanisms (specifically plasticity- and roughness-induced) with crack length, and vii) differences in local crack tip environments.

Of these major factors, closure, deflection and environmental mechanisms are considered to be far the most important. Although environmental effects will be examined in future years, our emphasis initially has been on crack closure and crack deflection mechanisms. The application of crack deflection mechanics to the problem of short cracks is relatively new and our theoretical treatment of this topic is described in Section 4. Crack closure mechanisms, on the other hand, have been well documented for long cracks,[16-28] and involve such phenomena as plasticity-induced, oxide-induced and roughness-induced crack closure (Fig. 2). Since these mechanisms act specifically in the wake of the crack tip, and since by definition a short crack will have limited wake, it is reasoned that short cracks will be far less influenced by closure effects. Thus by comparing long and short flaws at the same nominal driving force (e.g., same nominal stress intensity range based on applied stress, geometry and crack length), the short flaw is likely to experience a larger effective, near-tip stress intensity range, and will therefore show a larger crack growth increment, since the crack tip driving force is less limited by premature closure of the crack. Although theoretical studies by Newman[27] have shown that the anomalous near-threshold behavior of short cracks (e.g., in Fig. 1) can be reproduced using a numerical model for fatigue crack advance incorporating a description of plasticity-induced crack

closure,* few if any studies have clearly shown this effect experimentally. Furthermore, in no instances has the influence of microstructural variables been investigated on the origin of such closure at short crack lengths. Since the development of crack closure, or rather the lack of it, for small cracks is considered to be at the heart of the lack of correspondence between long and short flaw data, the initial aim of this program has been to experimentally demonstrate this major influence of closure.

3. EXPERIMENTAL PROCEDURES AND MATERIALS

MATERIALS

The following commercial wrought aluminum alloys, namely 7050, 2024 and 2124, were obtained from ALCOA in the solution treated, quenched and stretched conditions. In addition, a small 2024-T3 heat was acquired from Kaiser Aluminum Company. Nominal chemical compositions are shown below in Table I.

Table I. Nominal Chemical Compositions in wt.% of Alloys

	Si	Fe	Cu	Mn	Mg	Cr	Zn	Ti	Zr	Al
2024	0.50	0.50	4.50	0.50	1.5	0.10	0.25	0.15	--	balance
2124	0.20	0.30	4.50	0.50	1.5	0.10	0.25	0.15	--	balance
7050	0.07	0.10	2.10	--	2.16	--	6.16	0.02	0.13	balance

*In reality, closure principally arises from the oxide and roughness mechanisms under the plane strain conditions near threshold. However, Newman analysis servies to indicate the behavioral patterns which result when any closure mechanism becomes restricted at short crack lengths.

To date, the 2024 and 7050 alloys have been machined into 6.4 mm thick compact C(T) test-pieces for fatigue crack propagation testing and into standard round tensile specimens to determine uniaxial mechanical properties. The test specimens are currently being heat-treated to yield peak-aged (PA) microstructures and underaged (UA) and overaged (OA) microstructures at the same approximate yield strength. The rationale for the latter comparison is that although the UA (i.e., T3) and OA (i.e., T7) microstructures will be of comparable strength, underaged structures are associated with deformation via planar slip due to the coherent nature of the hardening precipitates whereas overaged structures are associated with more wavy slip from the incoherent particle hardening mechanisms. Such differences in slip mode lead to marked differences in fracture morphology which in turn significantly affect the contributions to crack extension from closure and deflection mechanisms. For example, the planar slip characteristics of underaged structures promote a faceted fracture morphology which results in significant crack deflection and roughness-induced crack closure (at least in oxidizing environments). The overaged structure , on the other hand, show a more macroscopically planar fracture morphology which is far less prone to roughness-induced closure, yet, somewhat surprisingly, in 7000 series alloys these structures show significant oxide-induced closure effects.[28] Thus, by variations in microstructure with aging treatment, the hardening mechanism and hence slip mode can be radically changed (at the same strength level) leading to marked differences in the magnitude and source of the operative closure mechanism. The effect of these variations is being examined both for short cracks and long cracks in the near-threshold regime.

TEST PROCEDURES

To obtain a comparison between long and short crack near-threshold behavior and to experimentally demonstrate that the anomalous behavior of short cracks results from a lesser effect of closure in the wake of the crack tip, the following "3 in 1" test specimen/procedure has been devised, as shown schematically in Fig. 3.

Starting with a conventional 1-T compact C(T) test-piece, 6.4 mm thick, long crack threshold tests are performed at 50 Hz using standard load shedding procedures to determine the near-threshold crack growth behavior and the value of the fatigue threshold range ΔK_o for long cracks (A). To demonstrate the effect of closure in the wake of the crack tip, two procedures are then adopted for the long crack arrested at ΔK_o. In certain specimens material is machined away behind the crack tip to "remove" closure in the wake. This has been performed using micro-drilling operations to machine 0.5 mm holes or by removing the entire wake with the aid of a fine jeweller's saw. Conversely, closure is "removed" by applying a single compression overload. In either case, following such procedures, the subsequent growth of the formerly arrested long crack is monitored, under constant ΔK conditions, until closure has once again developed with increase in crack length to again cause arrest (B). The third stage of the test is then to carefully machine away the majority of the test-piece to leave a small crack in a strip of metal (C), which is then tested in three-point bend to investigate near- (and sub-) threshold short crack behavior (D).

Such procedures turn out to be extremely complex to perform in practice due to difficulties in micro-machining and non-uniformity of

crack fronts. Preliminary efforts in 2024-T3, however, appear promising, and full details of the results of these experiments will be reported in future reports.

4. CRACK DEFLECTION

Various arguments have been put forth previously to account for the deceleration of initially high short crack growth and for the existence of a threshold for the arrest of short cracks. Morris et al.[29] suggest that the deceleration and/or arrest of short cracks in the vicinity of a grain boundary occurs because i) the crack does not propagate in an adjacent grain until a "mature" plastic zone develops *and* ii) closure stresses retard crack growth; the extent of closure is determined by the location of the crack tip relative to the grain boundary. Tanaka and co-workers[30] postulate that the crack tip slip bands are *blocked* by the grain boundary; the threshold for the growth of small cracks is determined by whether the slip bands pinned at grain boundaries can propagate into the adjacent grain or not.

Alternative approaches to such previous interpretations of crack tip-grain boundary interactions have recently been proposed[31] by considering the role of crack deflection in influencing the growth of short fatigue cracks. Figure 4 shows the changes in short crack growth direction induced by the grain boundary and the corresponding decrease in crack growth rates in 7075-T6 aluminum alloy (from ref. 32). For a short crack comparable in size to the grain dimensions, the low restraint on cyclic slip will promote a predominantly crystallographic mode of failure, akin to Forsyth's Stage I mechanism (Fig. 5a). On reaching a

grain boundary, the crack tends to re-orient itself in a new crystallographic direction in the adjacent grain to advance by the single slip mechanism and can be considerably deflected by the grain boundaries (Fig. 5b). The extent of deflection is dependent upon the relative orientations of the most favorable slip systems in the adjoining crystals. For an *elastic* short crack, initially inclined to the Mode I growth plane by an angle θ_o and subsequently deflected at the grain boundary by an angle θ_1 (Fig. 5b) the local crack tip stress intensities can be given by (derived in ref. 31):

$$\frac{k_1}{K_I} = \cos^2\theta_o \cos^3(\frac{\theta_1}{2}) + 3 \sin\theta_o \cos\theta_o \sin(\frac{\theta_1}{2}) \cos^2(\frac{\theta_1}{2}) \qquad (1)$$

$$\frac{k_2}{K_I} = \cos^2\theta_o \sin(\frac{\theta_1}{2}) \cos^2(\frac{\theta_1}{2}) - \sin\theta_o \cos\theta_o \cos(\frac{\theta_1}{2}) [1 - 3 \sin^2(\frac{\theta_1}{2})] \quad . \qquad (2)$$

Here, k_1 and k_2 are the *local* Mode I and Mode II stress intensities, respectively, immediately following deflection, and K_I is the *nominal* Mode I stress intensity factor. For typical values of $\theta_o \approx 45°$ and $\theta_1 \approx 90°$ (ref. 32, for example), k_1 and k_2 at the tip of the deflected short crack are found to be about 0.7 K_I and 0.35 K_I. The effective stress intensity factor range Δk_{eff}, obtained from:

$$k_{eff} \approx (k_1^2 + k_2^2)^{\frac{1}{2}} \quad , \qquad (3)$$

is then about 0.78 ΔK_I. Thus, considerations of crack deflection can account for a significant reduction in the driving force during crack-tip-grain boundary interactions. If the extent of deflection at the grain boundary is large, the effective cyclic stresses may be reduced to

a value smaller than the "true threshold" for short crack advance. For such a case, complete crack arrest results. Kitagawa and Takahashi[5] have shown that below a critical crack size (1-10 μm for ultrahigh strength materials and 0.1-1 mm for low strength materials), the "true threshold" for no growth can be characterized by a constant threshold value of cyclic stress $\Delta\sigma_{TH}$, which is roughly equal to the smooth bar fatigue limit $\Delta\sigma_e$. If the effective cyclic stresses are above $\Delta\sigma_{TH}$, no crack arrest occurs. Here, one observes only a deceleration in crack growth which is overcome as the short crack progresses away from the point of deflection. Recent results[32] on 7075-T6 aluminum alloy do indeed show that the minimum in the growth rate of short cracks roughly corresponds to a crack length being equal to the smallest grain dimension.

5. BRIEF SUMMARY OF FUTURE WORK

During the first year of this program a thorough review of previous studies on short crack behavior has highlighted the specific roles of crack closure and crack deflection mechanisms. A theoretical treatment of crack deflection as applied to short crack behavior has been performed to augment prior modelling work on oxide- and roughness-induced crack closure. The immediate emphasis for the current year is to obtain reliable experimental data both for long and short cracks initially on a 7050 alloy in the underaged, peak-aged and overaged conditions, in an attempt to substantiate (or otherwise) our modelling concepts.

6. ACKNOWLEDGEMENTS

The work was supported by the U.S. Air Force Office of Scientific Research under Grant No. AFOSR-82-0181, with Dr. Alan H. Rosenstein as program manager. Thanks are due to Dr. Rosenstein for helpful discussions, and to the Aluminum Company of America and Kaiser Aluminum Company for provision of materials. Particular thanks are due to Alcoa for their interest and support of this program.

7. REFERENCES

1. R. O. Ritchie: International Metals Reviews, 1979, vol. 20, p. 205.

2. M. E. Fine and R. O. Ritchie: in Fatigue and Microstructure, p. 245, American Society for Metals, Metals Park, OH, 1979.

3. S. J. Hudak: J. Eng. Matls. and Tech., Trans. ASME Series H, 1981, vol. 103, p. 26.

4. S. Pearson: Eng. Fract. Mech., 1975, vol. 7, p. 235.

5. H. Kitagawa and S. Takahashi: Proc. 2nd Intl. Conf. on Mech. Beh. of Materials, p. 627, American Society for Metals, Metals Park, OH, 1976.

6. Y. H. Kim, T. Mura and M. E. Fine: Eng. Fract. Mech., 1978, vol. 11, p. 1697.

7. N. E. Dowling: ASTM STP 637, 1978, p. 97.

8. M. H. El Haddad, N. E. Dowling, T. H. Topper and K. N. Smith: Int. J. Fract., 1980, vol. 16, p. 15.

9. R. A. Smith and K. J. Miller: Int. J. Mech. Sci., 1977, vol. 19, p. 11.

10. W. L. Morris: Met. Trans. A, 1980, vol. 11A, p. 1117.

11. B. N. Leis and T. P. Forte: Proc. 13th Natl. Symp. on Fract. Mech., ASTM STP, in press, ASTM, Philadelphia, PA, 1980.

12. S. Usami and S. Shida: Fat. Eng. Matls. and Struct., 1979, vol. 1, p. 471.

13. S. Taira, K. Tanaka and Y. Nakai: Mech. Res. Comm., 1978, vol. 5, p. 375.

14. T. S. Cook, J. Lankford and G. P. Sheldon: Fat. Eng. Matls. and Struct., 1981, vol. 3, p. 219.

15. R. P. Gangloff: Res. Mech. Letters, 1981, vol. 1, p. 299.

16. J. F. McCarver and R. O. Ritchie: Mater. Sci. Eng., 1982, vol. 55, p. 63.

17. R. O. Ritchie and S. Suresh: in Behavior of Short Cracks in Airframe Components, Proc. 55th Specialists Meeting of AGARD Structural and Materials Panel, NATO/AGARD, France, 1982.

18. J. Toplosky and R. O. Ritchie: Scripta Met., 1981, vol. 15, p. 905.

19. R. O. Ritchie, S. Suresh and C. M. Moss: J. Eng. Matls. and Tech., Trans. ASME Series H, 1980, vol. 102, p. 293.

20. S. Suresh, G. F. Zamiski and R. O. Ritchie: Met. Trans. A, 1981, vol. 12A, p. 1435.

21. S. Suresh, D. M. Parks and R. O. Ritchie: in Fatigue Thresholds, Proc. 1st Intl. Conf., Stockholm, vol. 1, p. 391 (EMAS Ltd., Warley, 1982).

22. R. O. Ritchie and S. Suresh: Met. Trans. A, 1982, vol. 13A, p. 937.

23. A. T. Stewart: Eng. Fract. Mech., 1980, vol. 13, p. 463.

24. K. Minakawa and A. J. McEvily: Scripta Met., 1981, vol. 15, p. 633.

25. W. Elber: ASTM STP 486, p. 280, 1971.

26. R. J. Asaro, L. Hermann and J. M. Baik: Met. Trans. A, 1981, vol. 12A, p. 1135.

27. J. C. Newman: in Behavior of Short Cracks in Airframe Components, Proc. 55th Specialists Meeting of AGARD Structural and Materials Panel, NATO/AGARD, France, 1982.

28. A. K. Vasudévan and S. Suresh: Met. Trans. A, 1982, vol. 13A, p. 2271.

29. W. L. Morris, M. R. James and O. Buck: Met. Trans. A, 1981, vol. 12A, p. 57.

30. K. Tanaka, Y. Nakai and M. Yamashita: Int. J. Fract., 1981, vol. 17, p. 519.

31. S. Suresh: "Crack Deflection: Implications for the Growth of Long and Short Fatigue Cracks," U.C. Berkeley Report No. UCB/RP/83/A1011, Feb. 1983, submitted for publication.

32. J. Lankford: Fat. Eng. Mater. Struct., 1982, vol. 5, p. 233.

8. PROGRAM ORGANIZATION AND PERSONNEL

The work described was performed in the Department of Materials Science and Mineral Engineering, University of California in Berkeley, under the supervision of Professor R. O. Ritchie and Dr. S. Suresh, aided by a graduate student research assistant (for M.S. degree) and an undergraduate research helper. The individual personnel are listed below:

i) Professor R. O. Ritchie, Principal Investigator (Department of Materials Science and Mineral Engineering)

ii) Dr. S. Suresh, Assistant Research Engineer (Department of Materials Science and Mineral Engineering)

iii) E. Zaiken, Graduate Student Research Assistant (Department of Mechanical Engineering)

iv) K. A. Johnston, Undergraduate Engineering Aide (Department of Chemical Engineering)

9. PUBLICATIONS

i) R. O. Ritchie and S. Suresh: "The Fracture Mechanics Similitude Concept: Questions Concerning its Application to the Behavior of Short Fatigue Cracks," Materials Science and Engineering, vol. 57, 1983, pp. L27-L30.

ii) R. O. Ritchie and S. Suresh: "Mechanics and Physics of the Growth of Small Cracks," Proceedings of the 55th Meeting of the AGARD Structural and Materials Panel on the Behavior of Short Cracks in Airframe Components, Toronto, AGARD, France, 1983 (Univ. of California Report No. UCB/RP/82/A1001).

iii) S. Suresh: "Crack Deflection: Implications for the Growth of Long and Short Cracks," submitted to Metallurgical Transactions A, 1983 (University of California Report No. UCB/RP/83/A1011).

In Preparation:

i) S. Suresh and R. O. Ritchie: "Propagation of Short Fatigue Cracks," to be submitted to International Metals Reviews.

10. LIST OF FIGURE CAPTIONS

Fig. 1: Schematic representation of typical fatigue crack propagation rate da/dN data for long and short cracks as a function of the alternating stress intensity ΔK for constant amplitude loading with the load ratio R constant.

Fig. 2: Schematic illustration of mechanisms of fatigue crack closure.

Fig. 3: Test geometries, procedures, and expected results for the "3 in 1" specimen developed to experimentally demonstrate the role of closure and the differences between long and short crack behavior.

Fig. 4: a) Micrograph showing the changes in the direction of crack advance when the crack tip encounters a grain boundary; b) abrupt decrease in the rate of short fatigue crack growth due to crack tip-grain boundary interactions in 7075-T6 aluminum alloy (ref. 32).

Fig. 5: Schematic illustrating the growth and deflection of microstructurally-short fatigue cracks and the resultant crack tip displacements and closure.

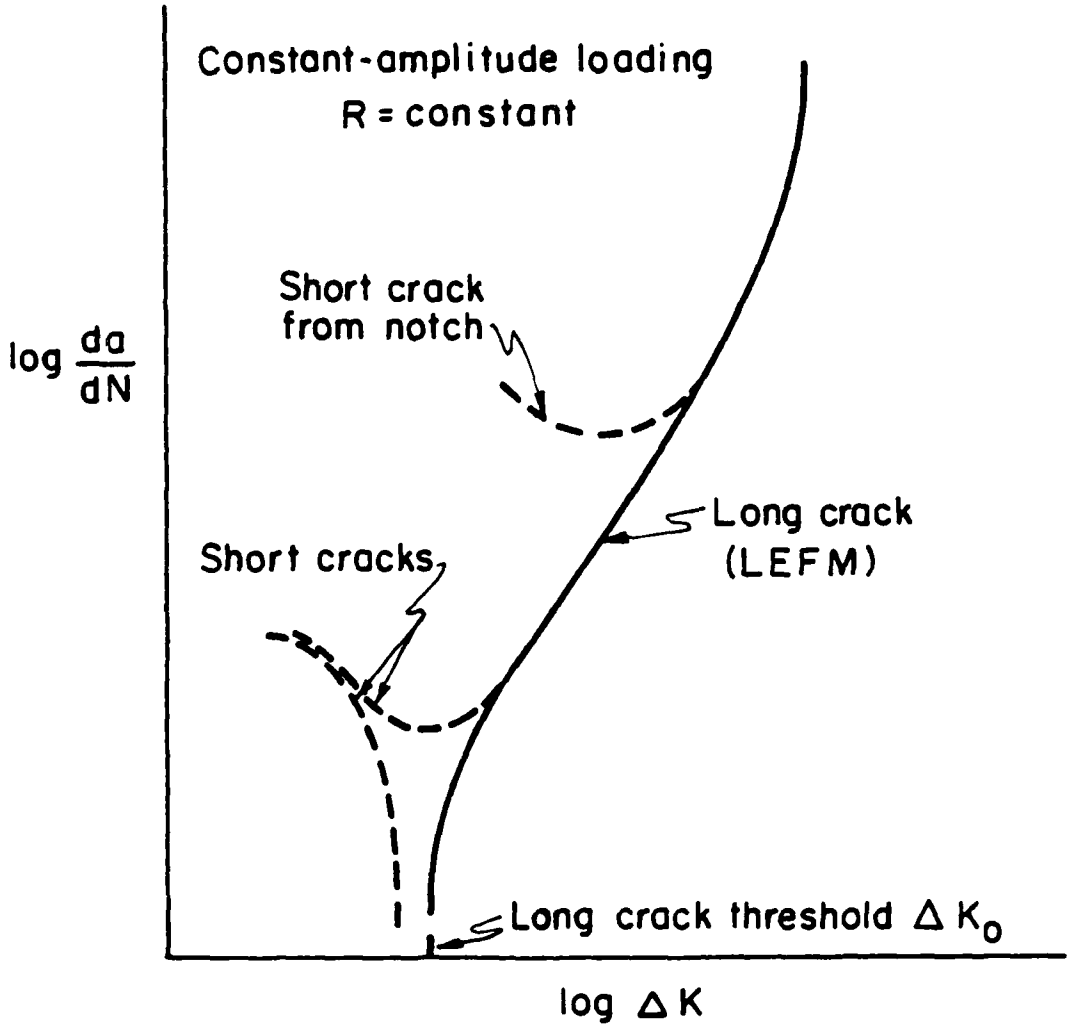

Fig. 1: Schematic representation of typical fatigue crack propagation rate da/dN data for long and short cracks as a function of the alternating stress intensity ΔK for constant amplitude loading with the load ratio R constant.

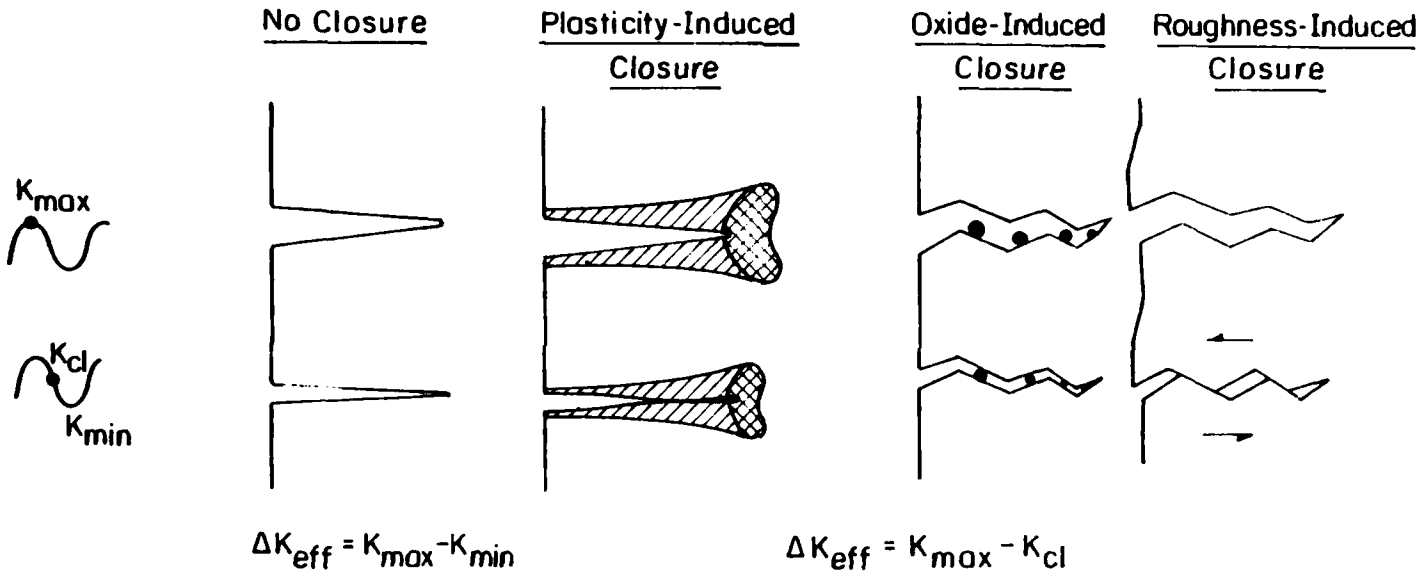

Fig. 2: Schematic illustration of mechanisms of fatigue crack closure.

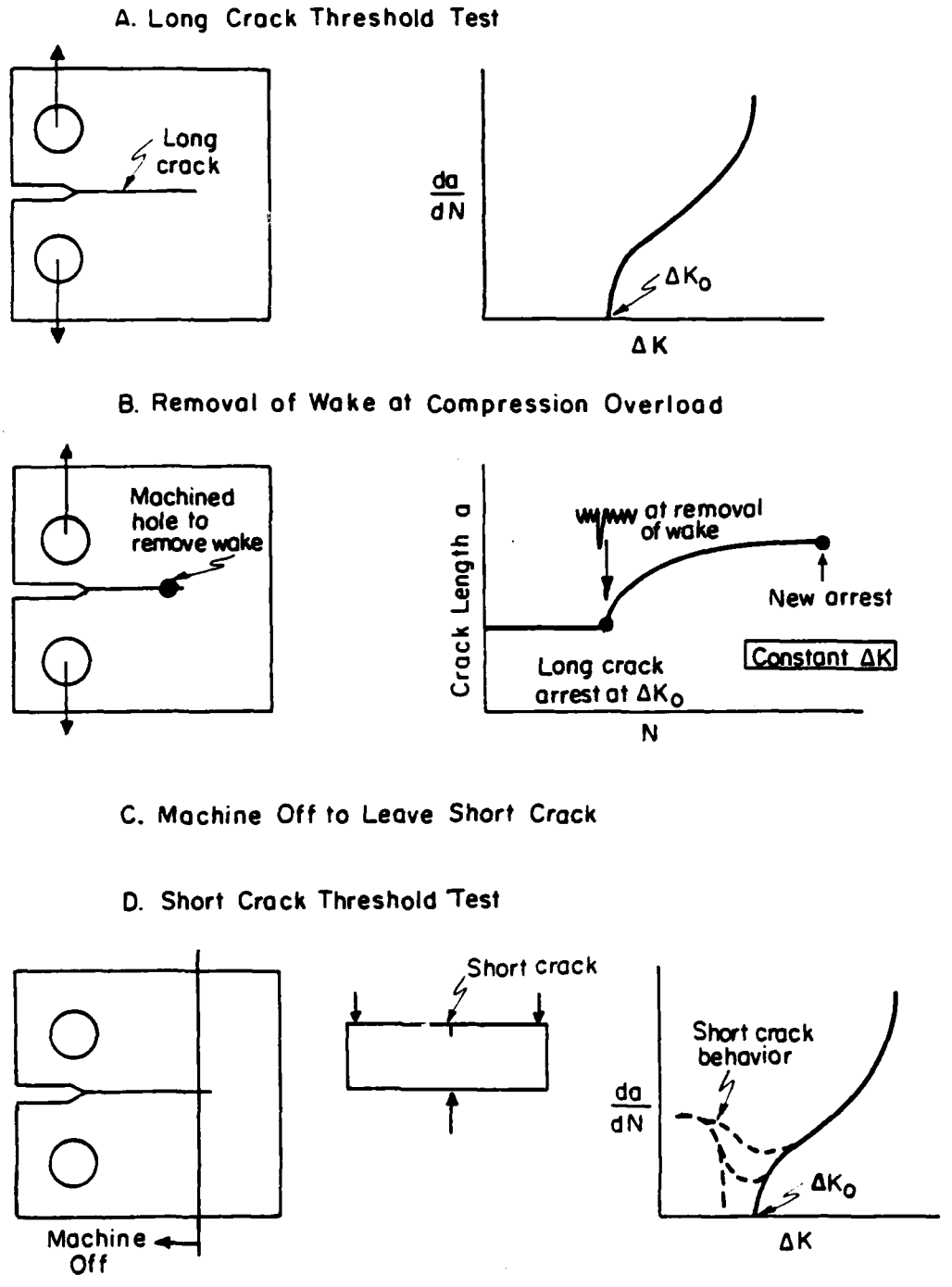

Fig. 3: Test geometries, procedures, and expected results for the "3 in 1" specimen developed to experimentally demonstrate the role of closure and the differences between long and short crack behavior.

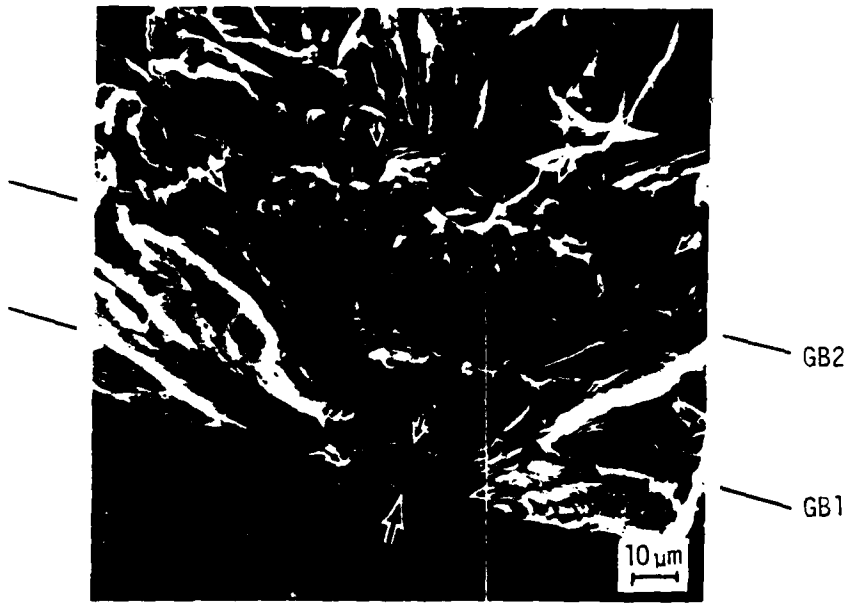

Fig. 4: a) Micrograph showing the changes in the direction of crack advance when the crack tip encounters a grain boundary.

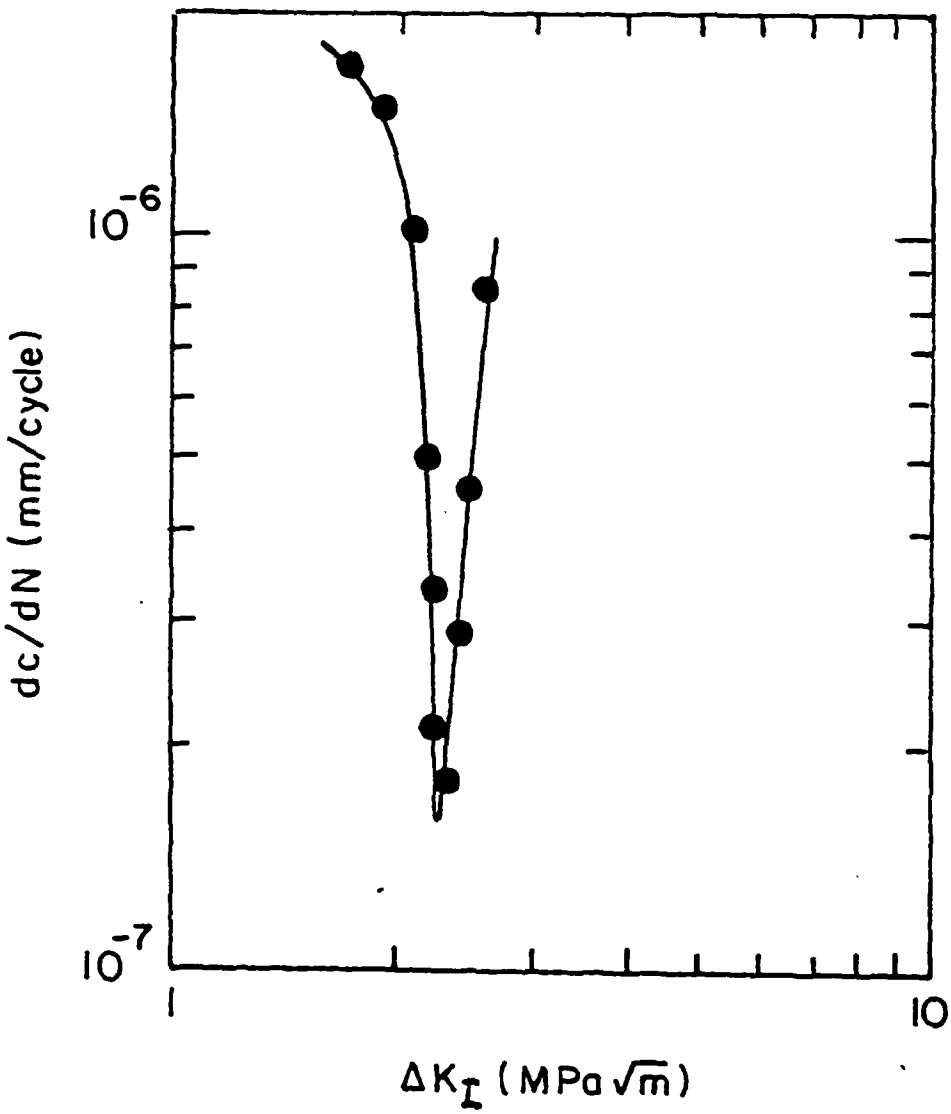

Fig. 4: b) Abrupt decrease in the rate of short fatigue crack growth due to crack tip-grain boundary interactions in 7075-T6 aluminum alloy (ref. 32).

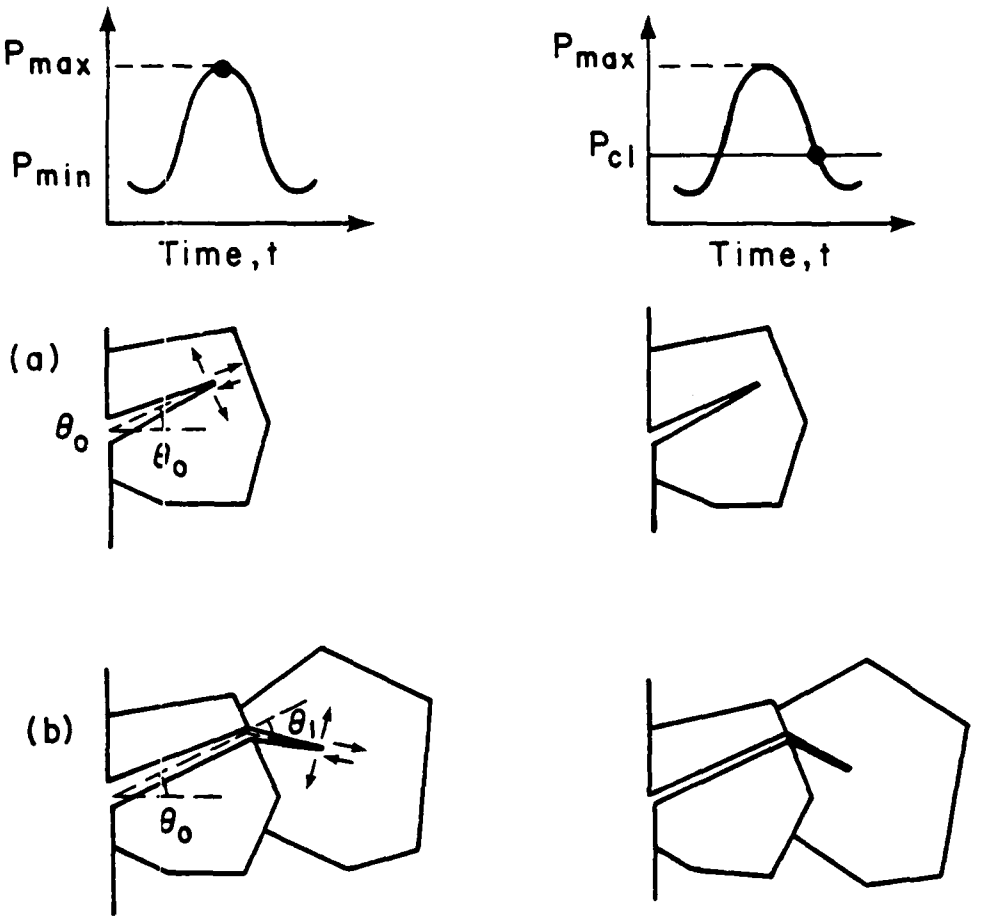

Fig. 5: Schematic illustrating the growth and deflection of microstructurally-short fatigue cracks and the resultant crack tip displacements and closure.

DISTRIBUTION LIST

AFOSR/NE
ATTN: Dr. A. H. Rosenstein
Bldg. #410
Bolling AFB
Washington, D.C. 20332

AFWAL/MLLM
ATTN: Branch Chief
Wright-Patterson AFB, Ohio 45433

AFWAL/MLLS
ATTN: Branch Chief
Wright-Patterson AFB, Ohio 45433

AFWAL/MLLN
ATTN: Branch Chief
Wright-Patterson AFB, Ohio 45433

Dr. Hugh R. Gray
NASA Lewis Research Center
Materials & Structures Division
21000 Brookpark Rd.
Cleveland, Ohio 44135

Dr. R. J. Bucci
Alcoa Technical Center
Alcoa Laboratories
Alcoa Center, PA 15069

APPENDIX

MECHANICS AND PHYSICS OF THE GROWTH OF SMALL CRACKS

by
R. O. Ritchie and S. Suresh
Materials and Molecular Research Division, Lawrence Berkeley Laboratory,
and Department of Materials Science and Mineral Engineering,
University of California
Berkeley, CA 94720
U.S.A.

SUMMARY

The mechanics and physics of the sub-critical propagation of small fatigue cracks are reviewed in terms of reported differences in behavior between long and short flaws based on fracture mechanics, microstructural and environmental viewpoints. Cracks are considered short when their length is small compared to relevant microstructural dimensions (a continuum mechanics limitation), when their length is small compared to the scale of local plasticity (a linear elastic fracture mechanics limitation), and when they are merely physically-small (e.g., <0.5-1 mm). For all three cases, it is shown that, at the same nominal driving force, the growth rates of the short flaws are likely to be greater than (or at least equal to) the corresponding growth rates of long flaws; a situation which can lead to non-conservative defect-tolerant lifetime predictions where existing (long crack) data are utilized. Reasons for this problem of similitude between long and short flaw behavior are discussed in terms of the roles of crack driving force, local plasticity, microstructure, crack shape, crack extension mechanism, premature closure of the crack, and local crack tip environment.

1. INTRODUCTION

Fatigue, involving the progressive failure of materials via the incipient growth of flaws under cyclically-varying stresses, can be regarded as the principal cause of in-service failures in most engineering structures and components. Whether under pure mechanical loading or in association with sliding and friction between surfaces (fretting-fatigue), rolling contact between surfaces (rolling contact fatigue), active environments (corrosion fatigue) or elevated temperatures (creep fatigue), fatigue fractures probably account for over 80% of all service failures. However, the process of these failures can be characterized into several related *phenomena* involving i) initial cyclic damage (cyclic hardening or softening), ii) the formation of initial microscopic flaws (micro-crack initiation), iii) the coalescence of these micro-cracks to form an initial "fatal" flaw (micro-crack growth), iv) the subsequent macroscopic propagation of this flaw (macro-crack growth) and v) final catastrophic failure or instability. In engineering terms, the first three stages, involving deformation and micro-crack initiation and growth, are generally embodied into the single process of (macro-) crack initiation representing the formation of an "engineering-size" detectable crack (i.e., of the order of several grain diameters in length). Thus in such terms, the total fatigue life (N) can be defined as the number of cycles to initiate a (macro-) crack (N_i) plus the number of cycles to propagate it sub-critically to final failure (N_p), i.e.,

$$N = N_i + N_p \quad . \tag{1}$$

From the perspective of fatigue design or lifetime prediction, this distinction between initiation and propagation lives can be critical. Conventional fatigue design approaches, on the one hand, classically involve the use of S-N curves, representing the *total life* N resulting from a stress, or strain, amplitude S, suitably adjusted to take into account effects of mean stress (using, for example, Goodman diagrams), effective stress concentrations at notches (using fatigue-strength reduction factors or local strain analysis), variable-amplitude loading (using the Palmgren-Miner cumulative-damage law or rainflow counting methods), multiaxial stresses, environmental effects, and so forth. Although based on total life, this approach, which is in widespread use, essentially represents design against *crack initiation*, since near the fatigue limit, especially in smooth specimens, the major portion of the lifetime is spent in the formation of an engineering-size crack. For safety-critical structures, especially with welded and riveted components, on the other hand, there has been a growing awareness that the presence of defects in a material below certain size must be assumed and taken into account at the design stage. Under such circumstances, the integrity of a structure will depend upon the lifetime spent in crack propagation, and since the crack-initiation stage will be small, the use of conventional S/N total life analyses may lead to dangerous overestimates of life. Such considerations have led to the adoption of the so-called defect-tolerant approach, where the fatigue lifetime is assessed in terms of the time, or number of cycles, to *propagate* the largest undetected crack (estimated by non-destructive evaluation or proof tests) to failure (defined by the fracture toughness, limit load or some allowable strain criteria). This approach, which is used exclusively for certain applications in the nuclear and aerospace industries, for example, relies on integration of a crack-growth expression, representing a fracture mechanics characterization of relevant fatigue crack propagation data suitably modified to account for mean stress effects (e.g., using the Forman equation), variable-amplitude loading (e.g., using the Wheeler or Willenborg models), environmental effects, and so forth, as required [1]. Since the crack initiation life is taken to be zero, such defect-tolerant life predictions are

assumed to be inherently conservative.

Current practice in the determination of the relevant crack growth law for a particular material in a given application is to utilize the existing data-base of laboratory-determined fatigue crack propagation results, characterized in terms of the linear elastic stress intensity range ΔK. However, the majority of these data has been determined from test-piece geometries containing crack sizes of the order of 25 mm or so, whereas many defects encountered in service are far smaller than this, particularly in turbine disk- and blade applications, for example. In the relatively few instances where the fatigue behavior of such short cracks has been experimentally studied (for reviews see refs. 1-4), it has been found, almost without exception, that at the same nominal driving force, the growth rates of short cracks are greater than (or equal to) the corresponding growth rates of long cracks. This implies a breakdown in the similitude concept generally assumed in fracture mechanics, whereby for, say, nominal linear elastic conditions, different-sized cracks subjected to the same stress intensity K_I will have identical local stress and strain fields at their crack tips and correspondingly should undergo equal amounts of crack extension. Furthermore, it suggests that the use of existing (long crack) data for defect-tolerant life-time calculations in components, where the growth of short flaws represents a large proportion of the life, has the potential for ominously non-conservative life predictions.

There are several factors which constitute a definition of a short crack, namely, i) cracks which are of a length comparable with the scale of microstructure (e.g., $\sim$ grain size, typically $\leq$ 1-50 μm), ii) cracks which are of a length comparable to the scale of local plasticity (e.g., $\sim$ plastic zone size, typically $\leq 10^{-2}$ mm in ultrahigh strength materials to $\leq$ 0.1-1 mm in low strength materials), and iii) cracks which are simply physically small (e.g., $\leq$ 0.5-1 mm). Most investigations to date have focussed on the first two factors which represent, respectively, a continuum mechanics limitation and a linear elastic fracture mechanics (LEFM) limitation to current analysis procedures. Presumably here, with an appropriate micro- or macro-mechanics characterization of crack advance, a correspondence between long and short crack growth rate data should be achieved. However, physically-short flaws, which are "long" in terms of continuum and LEFM analyses, have also been shown to propagate at rates faster than equivalent long cracks (at the same driving force) [4], indicating that the lack of correspondence between results also may reflect basic differences in the physical micro-mechanisms associated with the crack extension of long and short flaws.

In the present paper, we review the existing data on the growth of short fatigue cracks in engineering materials and discuss where behavior may differ from that of equivalent long cracks in terms of i) the appropriate fracture mechanics characterizations and ii) the physics and mechanisms involved in crack advance. In the former case, the short-crack problem is treated in terms of elastic-plastic fracture mechanics (EPFM) analyses which incorporate the effects of local crack tip plasticity and strain fields of notches, whereas in the latter case behavioral differences are examined in terms of the roles of crack size and shape, microstructure, environment, crack closure and crack extension mechanisms. We begin, however, with a brief summary of the fracture mechanics procedures used to characterize fatigue crack propagation for both long and short flaws.

2. FRACTURE MECHANICS CHARACTERIZATION OF FATIGUE CRACK GROWTH

The essential features of fracture mechanics involve characterization of the local stress and deformation fields in the vicinity of the crack tip. Under linear elastic conditions, the local crack tip stresses (σ_{ij}) at a distance r ahead of a nominally stationary crack subjected to tensile (Mode I) opening can be so characterized in terms of the K_I singular field:

$$\sigma_{ij}(r,\theta) \rightarrow \frac{K_I}{\sqrt{2\pi r}} f_{ij}(\theta) , \quad \text{as } r \rightarrow 0 \qquad (2)$$

where K_I is the Mode I stress intensity factor, θ the polar angle measured from the crack plane and f_{ij} a dimensionless function of θ [5]. The use of K_I to uniquely characterize the local linear elastic crack tip field is meaningful only when small-scale yielding conditions exist. This implies that the region of local yielding at the crack tip, denoted by the plastic zone size (r_y),

$$r_y \approx \frac{1}{2\pi}\left(\frac{K_I}{\sigma_o}\right)^2 , \qquad (3)$$

where σ_o is the yield strength of the material, is small compared to the in-plane dimensions of the body, namely crack length (a) and remaining ligament depth (b) [6]. Specifically, small-scale yielding conditions [7], i.e., that a K_I based description of crack tip fields is relevant, requires

$$r_y \ll a,b , \quad \text{typically} < \frac{1}{15}(a,b) . \qquad (4)$$

Under cyclic loading, the range of stress intensity ΔK, given by the difference between the maximum (K_{max}) and minimum (K_{min}) stress intensities in the cycle, is commonly used to correlate to crack extension, through power-laws of the form [8]:

$$\frac{da}{dN} = C\,\Delta K^{m} \quad , \tag{5}$$

where C and m are scaling constants. Here the extent of local yielding is defined in terms of maximum (monotonic) and cyclic plastic zones (r_{max} and r_{Δ}, respectively), given approximately by [7]:

$$r_{max} \approx \frac{1}{2\pi}\left(\frac{K_{max}}{\sigma_o}\right)^2 \quad ,$$

and

$$r_{\Delta} \approx \frac{1}{2\pi}\left(\frac{\Delta K}{2\sigma_o}\right)^2 \quad . \tag{6}$$

The numerical values of the stress intensity factors at the crack tip, i.e., K_I, ΔK, etc., remain undetermined from the asymptotic analysis, yet can be computed from the overall geometry and applied loading conditions. In fact solutions for K_I applicable to a wide variety of situations are now tabulated in handbooks [9]. A useful example of such K_I solutions, which is particularly relevant to the short crack problem, is that of a crack (length ℓ) growing from a notch (length 2c)(Fig. 1) [10]. Assuming a circular hole in an infinite plate under a remotely applied tensile stress σ, the limiting analytical solution for a short crack emanating from the notch is given as:

$$K_s = 1.12\ k_t \sigma\sqrt{\pi \ell} \quad , \tag{7}$$

where k_t is the elastic stress concentration factor (equal to 3 in this case) and 1.12 is the free surface correction factor. However, when the crack becomes long, the limiting stress intensity is obtained by idealizing the geometry so that the notch becomes part of a long crack of dimension $a = c + \ell$, such that

$$K_\ell = F\,\sigma\sqrt{\pi a} \quad , \tag{8}$$

where F is a dimensionless function of geometry, such as a finite width correction factor. The numerically-determined K_I solution for any crack emanating from a notch, shown by the dashed line in Fig. 1, can be seen to be given by these short and long crack limiting cases. As shown by Dowling [10], the transition crack size ℓ_o, which can be interpreted as the extent of the local notch field, can then be obtained by combining Eqs. (7) and (8) as:

$$\ell_o = \frac{c}{(1.12\ k_t/F)^2 + 1} \quad . \tag{9}$$

Values of ℓ_o are generally a small fraction of the notch root radius ρ, and for moderate to sharp notches generally fall in the range $\rho/20$ to $\rho/4$. Dowling [10] has further noted that $k_t\sigma$ values only 20-30% above σ_o are sufficient to generate a notch tip plastic zone which engulfs the small crack region ℓ_o, and thus far small cracks at notches, LEFM analysis will often be suspect.

The above example serves to illustrate one aspect of the short crack problem where the crack length is comparable with the notch tip plastic zone size. A similar situation, where small-scale yielding conditions may not apply, is where the plastic zone at the tip of the fatigue crack itself is comparable with the crack length, i.e., when $a \sim r_y$. Since the use of K_I singular fields is no longer appropriate in such instances, alternative asymptotic analyses have been developed to define the crack tip stress and strain fields in the presence of more extensive local plasticity. Based on the deformation theory of plasticity (i.e., non-linear elasticity), the asymptotic form of these local fields, for non-linear elastic power hardening solids of constitutive law $\sigma = \epsilon^n_{plastic}$, is given by the Hutchinson, Rice, Rosengren (HRR) singularity as [11,12]:

$$\sigma_{ij}(r,\theta) = \left(\frac{E'\,J}{\sigma_o^{\,2}\,r}\right)^{n/n+1} \sigma_o\, f^{I}_{ij}(\theta,n) \quad ,$$

$$\epsilon_{ij}(r,\theta) = \left(\frac{E'\,J}{\sigma_o^{\,2}\,r}\right)^{1/n+1} f^{II}_{ij}(\theta,n) \quad , \tag{10}$$

as $r \to 0$, where n is the work hardening exponent, E' the appropriate elastic modulus ($= E$ for plane stress or $E/(1-\nu^2)$ for plane strain) and f^{I}_{ij}, f^{II}_{ij} are universal functions of their arguments depending upon whether plane stress or plane strain is assumed. The amplitude of this field is the so-called J-integral [13], and analogous to K_I, J uniquely and autonomously characterizes the crack tip field under elastic-plastic conditions *provided some degree of strain hardening exists*. Further, for small-scale

yielding, J can be directly related to the strain energy release rate G, and hence K_I, i.e.,

$$J = G = K_I^2/E' \qquad \text{(linear elastic)} \qquad (11)$$

Despite difficulties in the precise meaning of J as applied to a description of crack growth of cyclically-stressed (non-stationary) cracks, certain authors [14,15] have proposed a power-law correlation of fatigue crack growth rates under elastic-plastic conditions to the range of J, i.e.,

$$\frac{da}{dN} = \Delta J^{m'} \quad . \qquad (12)$$

Provided such analysis is fundamentally justified, the use of ΔJ does present a feasible approach to characterize the growth of short cracks which are comparable in size to the extent of local yielding, as discussed below. However, as alluded to above, the validity of the ΔJ approach is often questioned since it appears to contradict a basic assumption in the definition of J that stress is proportional to the *current* plastic strain. This follows because J is defined from the deformation theory of plasticity (i.e., non-linear elasticity) which does not allow for the elastic unloading and non-proportional loading effects which accompany crack advance [13]. By recognizing, however, that constitutive laws for *cyclic* plasticity (i.e., the cyclic stress-strain curve) can be considered in terms of *stable* hysteresis loops, and that such loops can be mathematically shifted to a common origin after each reversal, the criterion of stress proportional to current plastic strain can be effectively satisfied for cyclic loading [16].

An alternative treatment of elastic/plastic fatigue crack growth, which is not subject to such restrictions required by non-linear elasticity, is to utilize the concept of crack tip opening displacement (CTOD). From Eq. (10), it is apparent that the opening of the crack faces varies at $r \to 0$ as $r^{n/n+1}$, such that this separation can be used to define the CTOD (δ_t) as the opening where 45° lines emanating back from the crack tip intercept the crack faces, i.e.,

$$\delta_t = d(\varepsilon_o, n)\,\frac{J}{\sigma_o} \quad , \qquad \text{(elastic/plastic)} \quad ,$$

$$= \frac{K_I^2}{\sigma_o E'} \quad , \qquad \text{(linear elastic)} \quad , \qquad (13)$$

where d is a proportionality factor (~ 0.3 to 1) dependent upon the yield strain ε_o, the work hardening exponent n, and whether plane stress or plane strain is assumed [17]. Since δ_t, like J, can be taken as a measure of the intensity of the elastic-plastic crack tip fields, it is feasible to correlate rates of fatigue crack growth to the range of δ_t, i.e., the cyclic crack tip opening displacement (ΔCTOD), as

$$\frac{da}{dN} = \Delta\text{CTOD} \quad , \qquad \text{(elastic/plastic)} \quad ,$$

$$= \frac{\Delta K_I^2}{2\sigma_o E'} \quad , \qquad \text{(linear elastic)} \quad . \qquad (14)$$

Approaches based on J and δ_t are basically equivalent, and are of course valid under both elastic/plastic and linear elastic conditions. They therefore are applicable to a continuum description of the growth rate behavior of cracks considered small because their size is comparable with the scale of local plasticity. Thus, for such short cracks, the use of elastic/plastic, rather than linear elastic, fracture mechanics may be expected to normalize differences in behavior between long and short flaws. However, the use of EPFM cannot necessarily be expected to normalize behavior between long and microstructurally-short or physically-short flaws, where other factors are important. These other factors are related to microstructural, environmental and closure effects and are discussed in detail below.

3. REVIEW OF EXPERIMENTAL RESULTS

Microstructural Effects

The first definition of a short fatigue crack involves cracks which are comparable in size with the scale of microstructural features. Several recent experimental studies [1,18-23] on the initiation and growth of cracks in a wide range of materials have revealed that short cracks, initiated near regions of surface roughening caused by the to and fro motion of dislocations or at inclusions and grain boundaries, propagate at rates which are different from those of equivalent long cracks, when characterized in terms of conventional fracture mechanics concepts. For example, it was first shown by Pearson [23] in precipitation hardened alloys that cracks, of a size comparable with the grain size, grew several times faster than long cracks at nominally identical stress intensity values. Such variation in the growth rate behavior of long and microstructurally-short cracks as a function of the stress intensity range is shown in Fig. 2 for 7075-T6

aluminum alloy, taken from the work of Lankford [24]. It is apparent from this figure that the growth rates associated with the short cracks are up to two orders of magnitude faster than those of the long cracks, and further that such accelerated short crack advance occurs at stress intensities well below the so-called fatigue threshold stress intensity range (ΔK_o), below which *long cracks* remain dormant or grow at experimentally-undetectable rates [25]. The initially higher growth rates of the short cracks can be seen to progressively decelerate (and even arrest in certain cases) before merging with the long crack data at stress intensities close to ΔK_o, similar to observations reported elsewhere by Morris et al. [26], Kung et al. [20] and Tanaka et al. [27,28]. Such short crack behavior has been attributed to a slowing down of short crack advance through interaction with grain boundaries [20-22,24,26-28]. Using arguments based on microplasticity and crack closure effects, Morris and co-workers [22,26] have modelled the process in terms of two factors, namely a cessation of propagation into a neighboring grain until a sizeable plastic zone is developed, and a retardation in growth rates due to an elevated crack closure stress. Tanaka et al. [21,27,28] similarly considered the impeded growth of microstructurally-short cracks in terms of the pinning of slip bands, emanating from the crack tip, by grain boundaries. The results of Lankford [24] in Fig. 2 indicate that the crack growth rate minimum corresponds to a crack length roughly equal to the smallest grain dimension (i.e., $a \sim d_g$). Further, the extent, or depth, of the deceleration "well," shown in this figure, appeared to be determined by the degree of microplasticity involved in the crack traversing the boundary. For example, when the orientation between the grain containing the crack and the neighboring grain was similar, little deceleration in growth rates at the boundary was seen to occur. Thus a consensus from these studies is that despite their accelerated propagation rates, compared to long crack data, short cracks are apparently impeded by the presence of grain boundaries, which in general would be unlikely to significantly affect the local propagation rates of long cracks.

From such experimental studies, it is readily apparent that threshold stresses, or stress intensities, associated with long and short cracks are likely to be very different. Although conventional fracture mechanics arguments infer that the threshold stress intensity range (ΔK_{TH}) for a particular material should be independent of crack length (i.e., $\Delta K_{TH} = \Delta K_o$ (the long crack threshold) = constant); Kitagawa and Takahashi [29] first showed that below a critical crack size, the threshold ΔK_{TH} for short cracks actually decreased with decreasing crack length, where the threshold *stress* $\Delta\sigma_{TH}$ approached that of the smooth bar fatigue limit $\Delta\sigma_e$ at very short crack lengths (Fig. 3). Several workers have shown that this critical crack size (below which ΔK_{TH} is no longer constant with crack length) is dependent upon microstructural and mechanical factors [25,28-37], but from continuum arguments it is approximately given by $1/\pi\ (\Delta K_o/\Delta\sigma_e)^2$, where both ΔK_o and $\Delta\sigma_e$ are corrected for a common load ratio. Values of this dimension, which effectively represent the limiting crack size for valid LEFM analysis (see next section), range from typically 1-10 um in ultrahigh strength materials (i.e., $\sigma_o \sim 7000$ MPa) to 0.1-1 mm in low strength materials (i.e., $\sigma_o \sim 200$ MPa).

Based on these results, it has been suggested [30,38,39] that the threshold condition for no growth for long cracks is one of a constant *stress intensity*, i.e., ΔK_o, whereas the threshold condition for short cracks is one of a constant stress, i.e., the fatigue limit $\Delta\sigma_e$ or endurance strength. Such a premise has been shown to be consistent with the modelling studies of Tanaka et al. [28] where the threshold for short crack propagation is governed by whether the crack tip slip bands are blocked, or can traverse, the grain boundary between an adjacent grain.

Local Plasticity Effects

The second definition of a short crack involves cracks which are small compared to the scale of local plasticity, generated either by the crack itself, i.e., the crack tip plastic zone, or by the presence of a larger stress concentrator, i.e., the strain field of a notch. The propagation of such cracks involves crack extension under elastic-plastic conditions, and from comparisons of their behavior with equivalent long cracks using LEFM analyses, i.e., at the same nominal ΔK, it is invariably seen that the short cracks appear to grow much faster [10,31-35,40,41]. However, part of the reason for such results lies not in any physical difference between long and short crack behavior but mostly with the inappropriate use of linear elastic analyses. This was shown particularly clearly by Dowling [40] who monitored the growth of small surface cracks in smooth bar specimens of A533B nuclear pressure vessel steel subjected to fully-reversed strain cycling. By analyzing the growth rates (da/dN) in terms of ΔJ, where J values were computed from the stress-strain hysteresis loops, a closer correspondence was found between long and short crack behavior (Fig. 4). However, even with the more appropriate characterization afforded by elastic-plastic fracture mechanics, it is still apparent in Fig. 4 that short cracks propagate at somewhat faster rates.

In order to account for this apparent breakdown in continuum mechanics concepts, also noticeable in the threshold results in Fig. 3, El Haddad and co-workers [33-35] introduced the notion of an intrinsic crack length a_o. These authors redefined the stress intensity factor in terms of the physical crack length plus a_o, such that the stress intensity range which characterizes the growth of fatigue cracks independent of crack length is given by:

$$\Delta K = Q\ \Delta\sigma \sqrt{\pi(a + a_o)}\ , \qquad (15)$$

where Q is the geometry factor. The material-dependent constant a_o was estimated from the limiting conditions of crack length where the nominal stress $\Delta\sigma^{\infty}$ approaches the fatigue limit $\Delta\sigma_e$ when $a \to 0$ and $\Delta K = \Delta K_o$, i.e.,

$$a_o \approx \frac{1}{\pi}\left(\frac{\Delta K_o}{\Delta\sigma_e}\right)^2 \quad . \tag{16}$$

and can be seen to be equivalent to the critical crack size (above which $\Delta K_{TH} = \Delta K_o$) in Fig. 3. By recomputing both ΔK and ΔJ to include this a_o concept, these authors [33] re-analyzed the short crack data of Dowling [40], shown in Fig. 4, and claimed to achieve a closer correspondence between long and short crack growth results [35].

Although such intrinsic crack length arguments successfully rationalize many apparent anomalies between the growth rate kinetics of long and short cracks limited by LEFM analyses, there is currently no available physical interpretation for the parameter a_o. Comparisons of a_o with the characteristic scales of microstructural dimensions have failed to reveal any convincing correspondence.

A somewhat different approach to rationalizing the behavior of long and short cracks, specifically with respect to the threshold condition, was presented by Usami and co-workers [36,37]. To replace the notion that the threshold condition for short cracks was one of a constant stress, compared to one of a constant stress intensity range for long cracks, these authors proposed a single criterion that the cyclic plastic zone dimension (r_Δ) at the threshold is a material constant. Using the Dugdale solution to approximate plastic zone sizes, this approach was shown to reproduce the form of the $\Delta\sigma_{TH}$ vs. a curves shown in Fig. 3 and further to rationalize effects of stress ratio and yield strength on short crack behavior. However, experimental conformation of the constancy of r_Δ at the threshold for long and short cracks was not presented.

Effects of local plasticity also play an important role in influencing the initiation and growth of short cracks emanating from notches, where cracks are considered short when their lengths are comparable in size to the extent of the strain field of the notch tip plastic zone (Fig. 5). The linear elastic K_I solutions for such short flaws have been discussed previously in Section 2. Phillips, Frost and others [42,43] first showed that such cracks initiated from notches can arrest completely and become so-called non-propagating cracks (NPC) after growing a short distance. Many subsequent studies [31,32, 35,44-47] have confirmed the existence of such NPC's although a precise understanding of the mechanisms for their occurrence is still lacking. Stress-strain/life analyses, however, have revealed that NPC's only form at sharp notches above a critical stress concentration factor k_t [47]. Hammouda and Miller [32] argue that the total plastic shear displacement, which is taken as the sum of the shear displacement arising from (notch) bulk plasticity and that due to the local crack tip plastic zone for LEFM controlled growth, determines the growth kinetics of such short cracks. Where the crack is completely submerged in the notch tip plastic zone (Fig. 5), bulk plasticity conditions dominate behavior. Here it is argued that the growth rates of the short cracks will progressively decrease until they arrest or merge with the long crack LEFM curve where behavior is dominated by local plasticity conditions within the crack tip plastic zone (Fig. 6). Several continuum mechanics explanations for such observations of decreasing growth rates of short cracks within the notch tip plastic zone have been claimed based on the above total plastic shear displacement argument [32], on elastic-plastic J-based analyses incorporating the a_o concept [45] and on the concept that the reversed plastic zone size is a material concept (independent on crack length) [37]. The physical reasons for such behavior, however, are difficult to comprehend, particularly since a striking similarity exists between Fig. 6 and Fig. 2. In the latter case the progressive deceleration in short crack growth rates was reported [24] in the absence of a notch and attributed to impeded growth at grain boundaries. With this in mind, we must conclude that the precise mechanism for the occurrence of decelerated short crack growth and NPC's is currently unclear but we do recognize that factors such as notch-tip plasticity, micro-plasticity, grain boundary blocking of slip-bands, cessation of growth and crystallographic reorientation of growth at grain boundaries, and crack closure (see Section 4) all may play a significant role. In this regard, it has been claimed that since small cracks are capable of propagating below the long crack threshold ΔK_o value, they may propagate for some distance until the combination of their size and local stress cause them to arrest at or below the ΔK_o value [2]. Although this is a convenient statement to rationalize the behavior schematically illustrated in Figs. 2 and 6, physically based mechanistic interpretations of such behavior are still uncertain.

Physically-Short Flaws

The third definition of a short crack, and perhaps the most ominous from a design viewpoint, is the physically-short flaw where the crack is long compared to both the scale of microstructure and the scale of local plasticity, yet simply physically small, i.e., typically less than 0.5-1 mm in length. Since both continuum mechanics and LEFM characterizations of the behavior of such flaws would be expected to be valid, it is perhaps surprising to find that under certain circumstances [4,48-52] even physically-short cracks show growth rates in excess of those of long cracks under nominally identical driving force conditions (i.e., at the same ΔK). This realization represents a significant breakdown in the similitude argument engrained in fracture mechanics analyses of sub-critical crack growth and has been currently attributed to two basic factors. The first of these pertains to the phenomenon of crack closure where, due to interference

and physical contact between mating fracture surfaces in the *wake* of the crack tip, the crack can be effectively closed at positive loads during the fatigue cycle. Since the crack cannot propagate whilst it remains closed, the net effect of closure is to reduce the nominal stress intensity range (ΔK), computed as $K_{max} - K_{min}$ from applied loads and crack length measurements, to some lower effective value (ΔK_{eff}) actually experienced at the crack tip, i.e., $\Delta K_{eff} = K_{max} - K_{cl}$, where K_{cl} is the stress intensity at closure ($\geq K_{min}$) [53]. Closure can arise from a number of sources, such as the constraint of surrounding elastic material on the residual stretch in material elements previously plastically-strained at the tip (plasticity-induced closure) [53], the presence of corrosion debris within the crack (oxide-induced closure) [54-56], and the contact at discrete points between faceted or rough fracture surfaces where significant Mode II crack tip displacements are present (roughness-induced closure) [52,56-60]. These mechanisms of crack closure are schematically illustrated in Fig. 7 [59], and are particularly relevant to short crack behavior simply because their action predominates in the *wake* of the crack tip. Since for small cracks the extent of this wake is limited, it is to be expected that the effect of crack closure will be different for long and short cracks, and specifically that the short crack is likely to be subjected to a smaller influence of closure. Evidence for the extent of crack closure being a function of crack size has been reported by Morris et al. [51] for the growth of short flaws in titanium alloys. Here, by monitoring the surface crack opening displacement (at zero load) for crack sizes ranging from 50 to 500 μm (Fig. 8), these authors concluded that for cracks less than approximately 160 μm in length, the extent of crack closure, specifically roughness-induced, decreased with decreasing crack length. A further influence of roughness-induced closure was inferred in the work of McCarver and Ritchie [50] on the crystallographic growth of long and physically-short fatigue cracks in René 95 nickel-base superalloy. In this latter study, threshold ΔK_{TH} values for short cracks ($a \sim 0.01$-0.20 μm) at low mean stresses ($R = 0.1$) were found to be 60% smaller than for long cracks ($a \sim 25$ mm), yet at high mean stresses ($R = 0.7$) where closure effects are minimal, this difference was not apparent. Thus, at equivalent nominal ΔK levels, physically-short flaws may be expected to propagate faster (and show lower thresholds) than corresponding long flaws simply due to a smaller influence of closure producing larger effective stress intensity ranges at the crack tip. Specific mechanisms for this effect are discussed in more detail in the following section.

However, a second factor which may also produce accelerated growth rates for short cracks is associated with chemical and electrochemical effects and is relevant to the growth of physically-short flaws in differing environments [4,48,49,61]. Experiments by Gangloff [4,48] on high strength 4130 steels tested in NaCl solution revealed corrosion fatigue crack propagation rates of short cracks (0.1-0.8 mm) to be up to two orders of magnitude faster than corresponding rates of long cracks (25-60 mm) at the same ΔK level, although behavior in inert atmospheres was essentially similar (Fig. 9). A complete understanding of this phenomenon is as yet lacking but preliminary analysis indicated that the effect could be attributed to differences in the local crack tip environments in the long and short flaws, principally resulting from different electrochemically-active surface-to-volume ratios of the cracks and from the influence of crack length on the solution renewal rate in the crack tip region [48].

4. DISCUSSION

In this paper, an attempt has been made to draw from the literature the salient points relevant to the mechanics and physics of the growth of short fatigue cracks. From the preceding discussion it is apparent that such cracks may present difficulties in fatigue design simply because their growth rate behavior is somewhat unpredictable when based on current (long crack) analyses and methodologies (e.g., using long crack LEFM data). It is also apparent that the latter procedures are liable to yield non-conservative predictions of lifetimes in the presence of short flaws because, at the same nominal driving force, the short crack invariably propagates at a faster rate than the corresponding long crack. This problem of similitude between long and short crack behavior can be considered to arise for a number of reasons, such as i) local plasticity effects resulting in the inappropriate characterization of the crack driving force for short cracks, ii) local microstructural features which in general do not perturb macro-crack growth yet which are of a size that they can interact strongly with the growth of small cracks, iii) similitude of crack shape and geometry, iv) interaction with other micro-cracks, v) similitude of crack extension mechanism, vi) crack closure effects, and vii) differences in the local crack tip environments. We now examine each of these factors in turn.

Questions concerning the inappropriate use of linear elastic fracture mechanics to characterize the growth of short cracks in the presence of extensive plasticity have been largely resolved through the use of J, or CTOD-based, methodologies, as evidenced by the results of Dowling [40] in Fig. 4. It is now apparent that much earlier data indicating differences in long and short crack behavior can be traced to the fact that growth rates were compared at equivalent ΔK values, and that the use of this LEFM parameter did not provide an adequate characterization of the short crack tip fields where $a \sim r_y$. However, for the case of short cracks emanating from notches, where initial growth is occurring within the plastic zone of the notch (Fig. 5), a continuum mechanics description of behavior is less clear. Certainly there is experimental evidence that such short cracks can propagate below the long crack threshold at progressively decreasing growth rates (Fig. 6) and even arrest to form non-propagating cracks [31,32,45], but such behavior has been also shown in the absence of a notch and attributed alternatively to

microstructural factors (Fig. 2) [24]. Certainly no linear elastic analysis of the case of a notch plus short crack [62] has demonstrated that the crack driving force (e.g., K_T) goes through a minimum, as the crack extends from the notch, to rationalize such behavior, and to our knowledge there is no formal elastic-plastic analysis available which similarly predicts the appropriate variation in crack driving force (without incorporation of crack closure effects). Whilst we cannot refute the experimental data on short crack growth at notches, in the absence of a complete continuum mechanics analysis we must conclude that part of the reason for the differing growth rate behavior of the short cracks in this instance may similarly result from the interaction of the short flaw with microstructural features and from the role of crack closure, as described below.

With respect to microstructural features, it is generally accepted that the presence of grain boundaries, hard second phases, inclusions, etc. play a somewhat minimal role in influencing the growth of long fatigue cracks [25] (at least over the range of growth rates below $\sim 10^{-3}$ mm/cycle), because behavior is governed primarily by average bulk properties. However, this clearly will not be the case for small micro-cracks whose length will be comparable to the size of these microstructural features. For example, for micro-cracks contained within a single grain, cyclic slip will be strongly influenced by the crystal orientation and the proximity of the grain boundary, resulting in locally non-planar crack extension [3]. There is now a large body of evidence that shows that the growth of small cracks is impeded by the presence of grain boundaries by such mechanisms as the blocking of slip bands [21] or containment of the plastic zone [22] within the grain, reorientation and re-initiation of the crack as it traverses the boundary [24], and simply cessation of growth at the boundary [22]. The latter effect has also been demonstrated for the presence of harder second phases, where in duplex ferritic-martensitic steels, micro-cracks were observed to initiate and grow in the softer ferrite only to arrest when they encountered the harder martensite [63]. Such considerations do not explain why short cracks can propagate below the long crack threshold ΔK_o, yet they do provide a feasible interpretation for the progressively decreasing growth rates observed in this region (Fig. 2).

A further factor which may contribute to differences in the behavior of long and short cracks is the question of crack shape [3]. Even long cracks, which encompass many grains, are known to possess certain irregularities in their geometry (*on a microscale level*) due to local interactions with microstructural features [64], yet, at a given ΔK, the overall growth behavior would be expected to be similar. However, on comparing a macro-crack and a micro-crack contained within a few grains, this similarity would seem to be questionable. Moreover, the early stages of fatigue damage often involve the multi-initiation of micro-cracks such that the subsequent growth of a particular small flaw is likely to be strongly influenced by the presence of other micro-cracks [1,19].

Differences in the behavior of long and short cracks may also result from the fact that, at the same nominal ΔK, the crack extension mechanisms may be radically different. As pointed out by Schijve [3], the restraint of the elastic surrounding on a small crack near a free surface is very different from that experienced at the tip of a long crack inside the material. For a small grain-sized crack, the low restraint on cyclic slip will predominately promote single slip on the system with the highest critical resolved shear stress resulting in a Mode II + Mode I slip band cracking mechanism akin to Forsyth's Stage I. For the long crack, however, which spans many grains, maintaining such slip-band cracking in a single direction in each grain is incompatible with a coherent crack front. The resulting increased restraint on cyclic plasticity will tend to activate further slip-systems leading to a non-crystallographic mode of crack advance by alternating or simultaneous shear, commonly referred to as striation growth (Forsyth's Stage II). At near-threshold levels where the extent of local plasticity is contained within a single grain, even long cracks propagate via this single shear mechanism but, in contrast to the short crack case, the orientation of the slip-band cracking will change at each grain boundary leading to a faceted or zig-zag crack path morphology (Fig. 10) [3,59]. As discussed below, the occurrence of this shear mode of crack extension, together with the development of a faceted fracture surface, has major implications with respect to the magnitude of crack closure effects [59,60], which further may lead to differences in long and short crack behavior [50].

The origin of the differences in behavior resulting from the contribution from crack closure arises from the fact that such closure effects predominate in the *wake* of the crack tip. Since short cracks by definition will possess a limited wake, it is to be expected that in general such cracks will be subjected to less closure. Thus, at the same *nominal* ΔK, short cracks may experience a larger *effective* ΔK compared to the equivalent long crack. As outlined in Section 3, this can arise from two sources. First, with respect to plasticity-induced closure, plastic deformation in the wake of the crack has to build up before it can be effective in reducing ΔK_{eff}. From analogous studies of the role of dilatant inelasticity (generated by phase transformations) on reducing the effective stress intensity at the crack tip in ceramics [65], it has been found that the full effect of this closure is only felt when the transformed zone extends a distance five times its forward extent in the wake of the crack. Although this analysis has not been performed for plastic deformation in metals, it is to be expected that the role of the compressive stresses in the plastic zone encompassing the wake of the crack would be limited for small cracks of a length comparable with the forward extent of this zone (i.e., for $a \sim r_y$). We believe that this is one of the major reasons (at least from the perspective of continuum mechanics) for non-propagating cracks and why short cracks and cracks emanating from notches can propagate below the long crack threshold ΔK_o. Essentially they can initiate and grow at nominal stress intensities below ΔK_o due to the absence of closure effects, but, as they increase in length, the build-up of plasticity in their wake promotes a

contribution from crack closure, which progressively decreases the effective ΔK experienced at the crack tip resulting in a progressive reduction in crack growth rate and sometimes complete arrest.

An analogous situation can arise due to the contribution from roughness-induced crack closure promoted by rough, irregular fracture surfaces, particularly where the crack extension mechanism involves a strong single shear (Mode II + Mode I) component [50,59,60]. Since a crack of zero length can have no fracture surface and hence no roughness-induced closure, it is to be expected that the development of such closure will be a strong function of crack size [50-52], as demonstrated by the experimental data of Morris et al. [51] in Fig. 8. A lower bound estimate for the transition crack size below which roughness-induced closure will be ineffective (at near-threshold levels) can be appreciated from Fig. 11 [50]. The long crack, which encompasses several grains, will at near-threshold levels have developed a faceted morphology and, due to incompatibility between mating crack surfaces from the Mode II crack tip displacements, will be subjected to roughness-induced closure in the manner depicted in Fig. 7. The short crack, however, will be unable to develop such closure whilst its length remains less than a grain diameter since, although it is advancing via the same single shear mechanism, it will not have changed direction at a grain boundary and accordingly will not have formed a faceted morphology.

In general, since the majority of results showing differences in long and short crack growth rates have been observed at low stress intensity ranges, and since the fatigue crack propagation behavior of long cracks in this near-threshold regime is known to be strongly influenced by crack closure effects, it is our belief that the major reason for the faster growth of short cracks and the fact that they can propagate below the long crack threshold ΔK_o is associated with a decreasing role of closure at decreasing crack sizes. In this regard it would be useful to compare short crack data with data for long cracks *at high load ratios*, since closure effects are minimal here even for long cracks. Where this has been done, i.e., for crystallographic near-threshold fatigue in nickel-base alloys [50], the threshold for short cracks, despite being 60% smaller than the long crack threshold at $R = 0.1$, was approximately equal to the long crack threshold at $R = 0.7$.

Finally, large differences in the behavior of long and short cracks can arise at stress intensities well outside the threshold regime due to environmental factors [4,48,49]. As shown in Fig. 9, the results of Gangloff [4,48] have demonstrated that the corrosion fatigue crack growth rates of physically-short cracks in 4130 steel tested in aqueous NaCl solution can be 1-2 orders of magnitude faster than the corresponding growth rates of long cracks at the same ΔK value. This unique environmentally-assisted behavior of short cracks was attributed to differing local crack tip environments as a function of crack size. Specifically, the local concentration of the embrittling species within the crack was reasoned to depend on the surface to volume ratio of the crack, on the diffusive and convective mass transport to the crack tip, and on the distribution and coverage of active sites for electrochemical reaction, all processes sensitive to crack depth, opening displacement and crack surface morphology [48]. Analogous, yet less spectacular, environmental crack size effects may also arise in gaseous environments, where for example the presence of hydrogen may induce an intergranular fracture mode. The rough nature of this failure mechanism would promote roughness-induced closure which again act to primarily influence the long crack behavior by reducing ΔK_{eff}.

These examples of the differences in behavior of fatigue cracks of varying size are a clear indication of where the fracture mechanics similitude concept can break down. The stress intensity, although adequately characterizing the mechanical driving force for crack extension, cannot account for the chemical activity of the crack tip environment, or the *local* interaction of the crack with microstructural features. Since these factors, together with the development of crack closure, are a strong function of crack size, it is actually unreasonable to expect identical crack growth behavior for long and short cracks. Thus, in the absence of the similitude relationship, the analysis and utilization of laboratory fatigue crack propagation data to predict the performance of in-service components, where short cracks are present, becomes an extremely complex task, a task which immediately demands a major effort in fatigue research from both academics and practical engineers alike.

5. CONCLUDING REMARKS

The problem of short cracks must now be recognized as one of the most important topics facing current researchers in fatigue. Not only is it a comparatively unexplored area academically, but it raises doubts in the universal application of fracture mechanics to the characterization of sub-critical flaw growth and accordingly has the potential, from the engineering viewpoint, for creating unreliable, non-conservative defect-tolerant lifetime predictions. In the current paper, we have attempted to provide an overview of the recent experimental studies on the growth of small fatigue cracks, and specifically to outline the mechanical, metallurgical and environmental reasons, as to why the behavior of *such cracks should differ from the* behavior of long cracks. Our intent was not to present a formal analysis of each of these factors, since in most cases such analysis simply does not exist, but rather to thoroughly review the many inter-disciplinary factors which may be relevant. We conclude that behavioral differences between the short and long flaw are to be expected, and such differences can arise from a number of distinct phenomena, namely: i) inadequate characterization of the crack tip stress and deformation fields of short cracks due to extensive local plasticity, ii) notch tip stress and

deformation field effects, iii) interaction of short cracks with microstructural features, e.g., grain boundaries, inclusions, second phases, etc., of dimensions comparable in size with the crack length, iv) differences in crack shape and geometry, v) differences in crack extension mechanisms, vi) differences in the contribution from crack closure mechanisms (specifically plasticity- and roughness-induced) with crack length, and finally vii) differences in the local crack tip environments. Each of these factors represents a formidable challenge in fatigue research, because of the complex nature of both experimental and theoretical studies, yet their importance is undeniable. We trust that the proceedings of this conference will provide a significant step in increasing our understanding of this important topic.

6. REFERENCES

1. M.E. Fine and R. O. Ritchie: "Fatigue-Crack Initiation and Near-Threshold Crack Growth," in Fatigue and Microstructure, Amer. Soc. Metals, Metals Park, OH, 1968, pp. 245-278.
2. S. J. Hudak: "Small Crack Behavior and the Prediction of Fatigue Life," J. Eng. Matls. Tech., Trans. ASME Ser. H, vol. 103, 1981, pp. 26-35.
3. J. Schijve: "Differences between the Growth of Small and Large Fatigue Cracks: The Relation to Threshold K-Values," in Fatigue Thresholds, eds. J. Bäcklund, A. Blom, and C. J. Beevers, EMAS Ltd., Warley, U.K., vol. 2, 1981, pp. 881-908.
4. R. P. Gangloff: "Electrical Potential Monitoring of the Formation and Growth of Small Fatigue Cracks in Embrittling Environments," in Advances in Crack Length Measurement, ed. C. J. Beevers, EMAS Ltd., Warley, U.K., 1982, in press.
5. M. L. Williams: "On the Stress Distribution at the Base of a Stationary Crack," J. Appl. Mech., vol. 24, 1957, pp. 109-117.
6. G. R. Irwin: "Fracture Mechanics," in Structural Mechanics, Proc. 1st. Symp. on Naval Structural Mechanics, eds. J. Goodier and N. Huff, Pergamon Press, New York, 1960.
7. J. R. Rice: "Mathematical Analysis in the Mechanics of Fracture," in Fracture: An Advanced Treatise, ed. H. Liebowitz, Academic Press, New York, vol. 2, 1968, pp. 191-311.
8. P. C. Paris and F. Erdogan: "A Critical Analysis of Crack Propagation Laws," J. Basic Eng., Trans. ASME Ser. D, vol. 85, 1963, pp. 528-534.
9. H. Tada, P. C. Paris, and G. R. Irwin: in The Stress Analysis of Cracks Handbook, Del Research Corp., Hellertown, PA, 1973.
10. N. E. Dowling: "Notched Member Fatigue Life Predictions Combining Crack Initiation and Propagation," Fat. Eng. Matls. Struct., vol. 2, 1979, pp. 129-138.
11. J. W. Hutchinson: "Singular Behavior at the End of a Tensile Crack in a Hardening Material," J. Mech. Phys. Solids, vol. 16, 1968, pp. 13-31.
12. J. R. Rice and G. R. Rosengren: "Plane Strain Deformation Near a Crack Tip in a Power Hardening Material," J. Mech. Phys. Solids, vol. 16, 1968, pp. 1-12.
13. J. R. Rice: "A Path Independent Integral and the Approximate Analysis of Strain Concentration by Notches and Cracks," J. Appl. Mech., vol. 35, 1968, pp. 379-385.
14. N. E. Dowling: "Geometry Effects and the J-Integral Approach to Elastic-Plastic Fatigue Crack Growth," in Cracks and Fracture, ASTM STP 601, Am. Soc. Test. Matls., 1976, pp. 19-32.
15. N. E. Dowling and J. A. Begley: "Fatigue Crack Growth During Gross Plasticity and the J-Integral," in Mechanics of Crack Growth, ASTM STP 590, Am. Soc. Test. Matls., 1976, pp. 82-103.
16. R. O. Ritchie: "Why Ductile Fracture Mechanics?," J. Eng. Matls. Tech., Trans. ASME Ser. H, vol. 104, 1982, in press.
17. C. F. Shih: "Relationships Between the J-Integral and Crack Opening Displacement for Stationary and Extending Cracks," J. Mech. Phys. Solids, vol. 29, 1981, pp. 305-330.
18. A. R. Jack and A. T. Price: "The Initiation of Fatigue Cracks from Notches in Mild Steel Plates," Acta Met., vol. 6, 1970, pp. 401-409.
19. Y. H. Kim, T. Mura, and M. E. Fine: "Fatigue Crack Initiation and Microcrack Growth in 4140 Steel," Met. Trans. A, vol. 9A, 1978, pp. 1679-1683.
20. C. Y. Kung and M. E. Fine: "Fatigue Crack Initiation and Microcrack Growth in 2024-T4 and 2124-T3 Aluminum Alloys," Met. Trans. A, vol. 10A, 1979, pp. 603-610.
21. S. Taira, K. Tanaka and M. Hoshina: "Grain Size Effect on Crack Nucleation and Growth in Long-Life Fatigue of Low Carbon Steel," in Fatigue Mechanisms, ASTM STP 675, Am. Soc. Test. Matls., 1979, pp. 135-173.
22. W. L. Morris: "The Noncontinuum Crack Tip Deformation Behavior of Surface Microcracks," Met. Trans. A, vol. 11A, 1980, pp. 1117-1123.
23. S. Pearson: "Initiation of Fatigue Cracks in Commercial Aluminum Alloys and the Subsequent Propagation of Very Short Cracks," Eng. Fract. Mech., vol. 7, 1975, pp. 235-247.

24. J. Lankford: "The Growth of Small Fatigue Cracks in 7075-T6 Aluminum," Fat. Eng. Matls. Struct., vol. 5, 1982, in press.

25. R. O. Ritchie: "Near-Threshold Fatigue Crack Propagation in Steels," Intl. Metals Rev., vol. 20, 1979, pp. 205-230.

26. W. L. Morris, M. R. James, and O. Buck: "Growth Rate Models for Short Surface Cracks in Al 2219-T851," Met. Trans. A, vol. 12A, 1981, pp. 57-64.

27. S. Taira, K. Tanaka, and Y. Nakai: "A Model of Crack Tip Slip Band Blocked by Grain Boundary," Mech. Res. Comm., vol. 5, 1978, pp. 375-381.

28. K. Tanaka, Y. Nakai, and M. Yamashita: "Fatigue Growth Threshold of Small Cracks," Intl. J. Fract., vol. 17, 1981, pp. 519-533.

29. H. Kitagawa and S. Takahashi: "Applicability of Fracture Mechanics to Very Small Cracks or the Cracks in the Early Stage," in Proc. 2nd Intl. Conf. on Mech. Beh. of Materials, 1979, pp. 627-631.

30. R. A. Smith: "On the Short Crack Limitations of Fracture Mechanics," Intl. J. Fract., vol. 13, 1977, pp. 717-719.

31. R. A. Smith and K. J. Miller: "Prediction of Fatigue Regimes in Notched Components," Intl. J. Mech. Sci., vol. 20, 1978, pp. 201-206.

32. M. M. Hammouda and K. J. Miller: "Elastic-Plastic Fracture Mechanics Analyses of Notches," in Elastic-Plastic Fracture, ASTM STP 668, Amer. Soc. Test. Matls., 1979, pp. 703-719.

33. M. H. El Haddad, K. N. Smith, and T. H. Topper: "Fatigue Crack Propagation of Short Cracks," J. Eng. Matls. Tech., Trans. ASME Ser. H, vol. 101, 1979, pp. 42-46.

34. M. H. El Haddad, T. H. Topper, and B. Mukherjee: "Review of New Developments in Crack Propagation Studies," J. Test. Eval., vol. 9, 1981, pp. 65-81.

35. M. H. El Haddad, N. E. Dowling, T. H. Topper, and K. N. Smith: "J-Integral Applications for Short Cracks at Notches," Intl. J. Fract., vol. 16, 1980, pp. 15-30.

36. S. Usami and S. Shida: "Elastic-Plastic Analysis of the Fatigue Limit for a Material with Small Flaws," Fat. Eng. Matls. Struct., vol. 1, 1979, pp. 471-481.

37. S. Usami: "Applications of Threshold Cyclic-Plastic-Zone-Size Criterion to Some Fatigue Limit Problems," in Fatigue Thresholds, eds. J. Bäcklund, A. Blom, and C. J. Beevers, EMAS Ltd., Warley, U.K., vol. 1, 1982, pp. 205-238.

38. R. O. Ritchie: "Discussion on Microstructural Aspects of the Threshold Condition for Nonpropagating Fatigue Cracks in Martensitic-Ferritic Structures," in Fatigue Mechanisms, ASTM STP 675, Amer. Soc. Test. Matls., 1979, pp. 364-366.

39. J. Lankford: "On the Small Crack Fracture Mechanics Problem," Intl. J. Fract., vol. 16, 1980, pp. R7-R9.

40. N. E. Dowling: Crack Growth During Low Cycle Fatigue of Smooth Axial Specimens," in Cyclic Stress-Strain and Plastic Deformation Aspects of Fatigue Crack Growth, ASTM STP 637, Amer. Soc. Test. Matls., 1977, pp. 97-121.

41. R. A. Smith and K. J. Miller: "Fatigue Cracks at Notches," Intl. J. Mech. Sci., vol. 19, 1977, pp. 11-22.

42. C. E. Phillips: "Discussion on Non-Propagating Fatigue Cracks in Low-Carbon Steel," in Proc. Colloquium on Fatigue, IUTAM Stockholm, 1955, Springer, Berlin, 1956, p. 210.

43. N. E. Frost and D. S. Dugdale: "Fatigue Tests on Notched Mild Steel Plates with Measurement of Fatigue Cracks," J. Mech. Phys. Solids, vol. 5, 1957, pp. 182-192.

44. P. Lukáš and M. Klesnil: "Fatigue Limit of Notched Bodies," Mater. Sci. Eng., vol. 34, 1978, pp. 61-66.

45. M. H. El Haddad, K. N. Smith, and T. H. Topper: "Prediction of Non-Propagating Cracks," Eng. Fract. Mech., vol. 11, 1979, pp. 573-584.

46. B. N. Leis and T. P. Forte: "Fatigue Growth of Initially Physically Short Cracks in Notched Aluminum and Steel Plates," in Fracture Mechanics, ASTM STP 743, Amer. Soc. Test. Matls., 1982, pp. 100-124.

47. N. E. Frost, K. J. Marsh, and L. P. Pook: in Metal Fatigue, Clarendon Press, Oxford, 1974.

48. R. P. Gangloff: "The Criticality of Crack Size in Aqueous Corrosion Fatigue," Res. Mech. Let., vol. 1, 1981, pp. 299-306.

49. B. F. Jones: "The Influence of Crack Depth on the Fatigue Crack Propagation Rate for a Marine Steel in Seawater," J. Matls. Sci., vol. 17, 1982, pp. 499-507.

50. J. F. McCarver and R. O. Ritchie: "Fatigue Crack Propagation Thresholds for Long and Short Cracks in René 95 Nickel-Base Superalloy," Mater. Sci. Eng., vol. 55, 1982, pp. 63-67.

51. W. L. Morris, M. R. James, and O. Buck: "A Simple Model of Stress Intensity Range Threshold and Crack Closure Stress," Eng. Fract. Mech., vol. 14, 1982, in press.

52. M. R. James and W. L. Morris: "Effect of Fracture Surface Roughness on Short Fatigue Crack Growth," Met. Trans. A, vol. 13A, 1982, in press.

53. W. Elber: "The Significance of Fatigue Crack Closure," in Damage Tolerance in Aircraft Structures, ASTM STP 486, Amer. Soc. Test. Matls., 1971, pp. 230-242.

54. R. O. Ritchie, S. Suresh, and C. M. Moss: "Near-Threshold Fatigue Crack Growth in 2¼Cr-1Mo Pressure Vessel Steel in Air and Hydrogen," J. Eng. Matls. Tech., Trans. ASME Ser. H, vol. 102, 1980, pp. 293-299.

55. A. T. Stewart: "The Influence of Environment and Stress Ratio on Fatigue Crack Growth at Near-Threshold Stress Intensities in Low-Alloy Steels," Eng. Fract. Mech., vol. 13, 1980, pp. 463-478.

56. S. Suresh, G. F. Zamiski, and R. O. Ritchie: "Oxide-Induced Crack Closure: An Explanation for Near-Threshold Corrosion Faitgue Crack Growth Behavior," Met. Trans. A, vol. 12A, 1981, pp. 1435-1443.

57. N. Walker and C. J. Beevers: "A Fatigue Crack Closure Mechanism in Titanium," Fat. Eng. Matl. Struct., vol. 1, 1979, pp. 135-148.

58. K. Minakawa and A. J. McEvily: "On Crack Closure in the Near-Threshold Regime," Scripta Met., vol. 15, 1981, pp. 633-636.

59. R. O. Ritchie and S. Suresh: "Some Considerations on Fatigue Crack Closure at Near-Threshold Stress Intensities Due to Fracture Surface Morphology," Met. Trans. A, vol. 13A, 1982, pp. 937-940.

60. S. Suresh and R. O. Ritchie: "A Geometric Model for Fatigue Crack Closure Induced by Fracture Surface Roughness," Met. Trans. A, vol. 13A, 1982, in press.

61. J. Lankford: "The Effect of Environment on the Growth of Small Fatigue Cracks," Fat. Eng. Matls. Struct., vol. 5, 1982, in press.

62. J. Schijve: "The Stress Intensity Factor of Small Cracks at Notches," Fat. Eng. Matls. Struct., vol. 5, 1982, pp. 77-90.

63. T. Kunio and K. Yamada: "Microstructural Aspects of the Threshold Condition for Non-Propagating Fatigue Cracks in Martensitic-Ferritic Structures," in Fatigue Mechanisms, ASTM STP 675, Amer. Soc. Test. Matls, 1979, pp. 342-370.

64. J. Schijve: "The Effect of an Irregular Crack Front on Fatigue Crack Growth," Eng. Fract. Mech., vol. 14, 1981, pp. 467-475.

65. R. M. McMeeking and A. G. Evans: "Mechanics of Transformation-Toughening in Brittle Materials," J. Amer. Cer. Soc., vol. 65, 1982, pp. 242-246.

7. ACKNOWLEDGEMENTS

The work was performed under Grant No. AFOSR-82-0181 from the Air Force Office of Scientific Research. The authors wish to thank Dr. Alan Rosenstein of AFOSR for his support and encouragement, and Kimberly A. Johnston and Madeleine M. Penton for their help in preparing the manuscript.

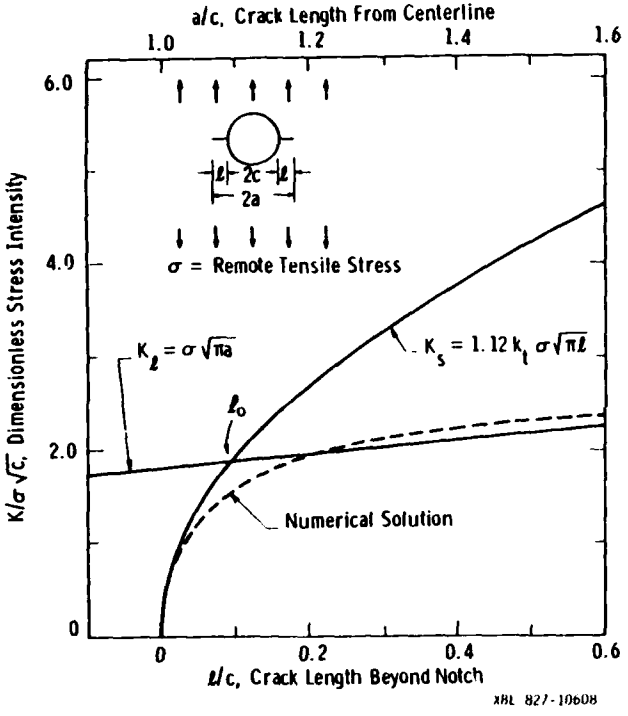

Fig. 1: Linear elastic K_I solutions for a crack, length ℓ, emanating from a circular notch, radius c, in an infinite plate subjected to a remotely applied uniaxial tensile stress σ. Short (K_S) and long ($K\ell$) crack limiting solutions and numerical solution are shown. After Dowling (1978).

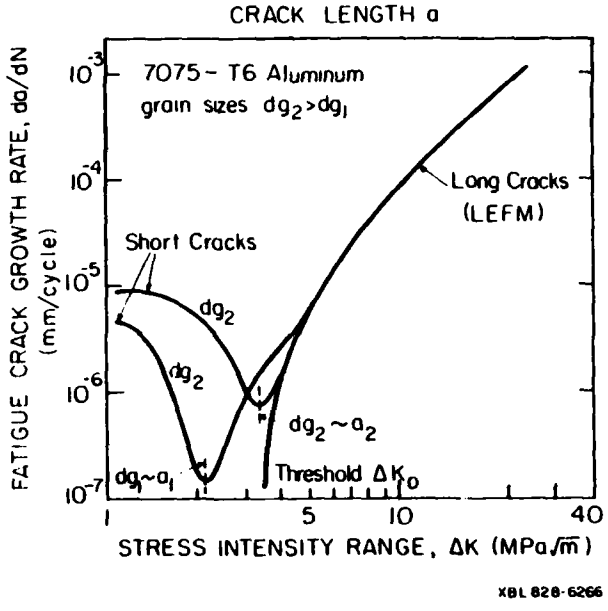

Fig. 2: Effect of grain size (d_g) on the growth of microstructurally-short fatigue cracks in 7075-T6 aluminum alloy (σ_o = 515 MPa). Micro-crack growth rate (da/dN) data, for two grain sizes ($dg_2 > dg_1$), show growth rate minima approximately where crack length $a \sim d_g$, below the long crack threshold ΔK_o. After Lankford (1982).

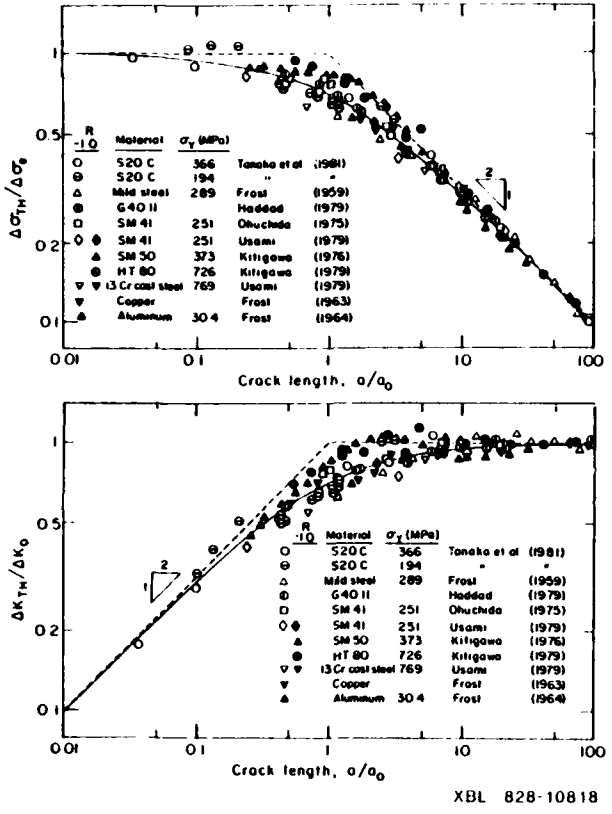

Fig. 3: Variation of threshold stress ($\Delta\sigma_{TH}$), normalized with respect to the smooth bar fatigue limit ($\Delta\sigma_e$), and threshold stress intensity (ΔK_{TH}), normalized with respect to the long crack threshold (ΔK_o), with crack length (a), normalized with respect to the intrinsic crack length ($a_o = 1/\pi[\Delta K_o/\Delta\sigma_e]^2$). After Tanaka et al. (1981).

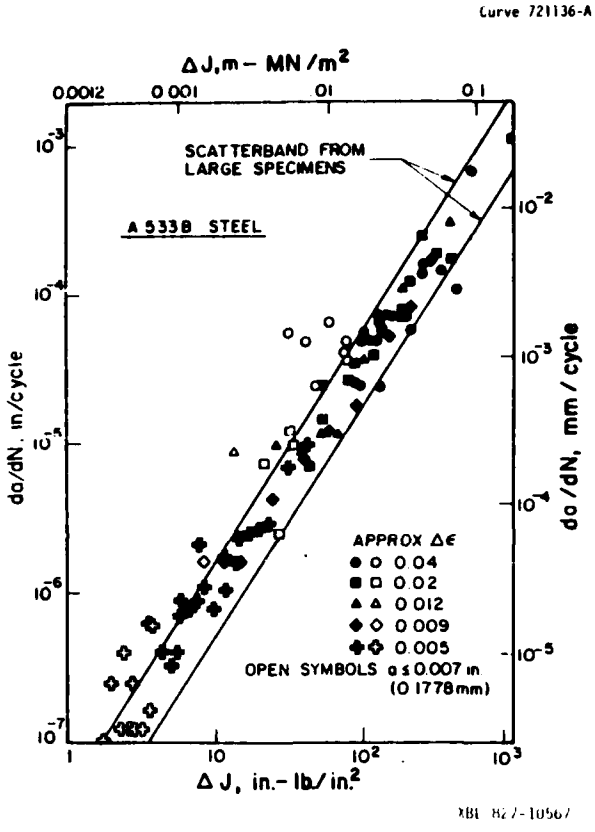

Fig. 4: Variation of fatigue crack growth rate (da/dN) for long ($a \gtrsim 25$ mm) and short ($a \lesssim 0.18$ mm) cracks in A533B steel (σ_o = 480 MPa) under plastic loading, where data are analyzed in terms of ΔJ. After Dowling (1977).

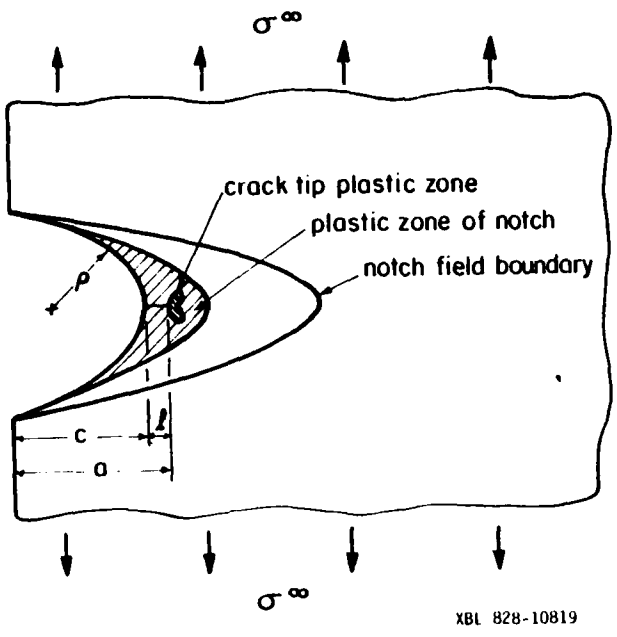

Fig. 5: Schematic illustration of crack tip and notch plastic strain field associated with the growth of a short crack, length ℓ, emanating from a notch of depth c and root radius ρ. After Hammouda and Miller (1979).

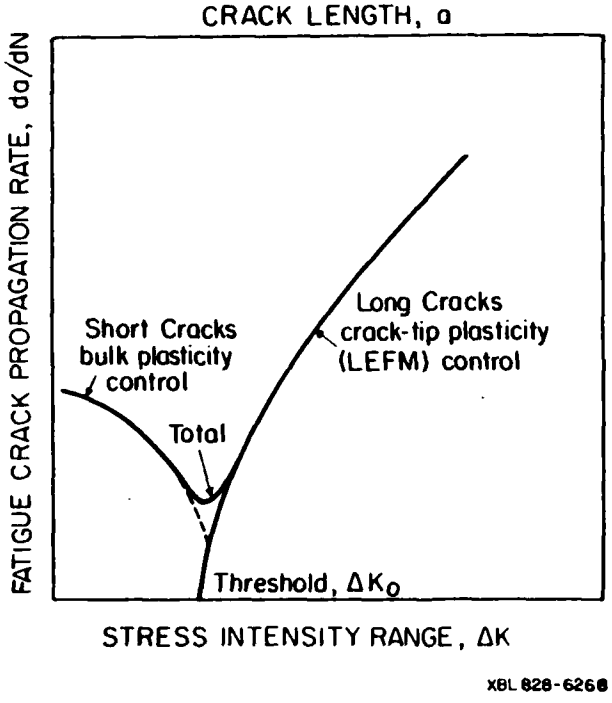

Fig. 6: Schematic illustration of the elastic-plastic and linear elastic characterization of the kinetics of crack growth for a short crack propagating from a notch (as shown in Fig. 5). After Hammouda and Miller (1979).

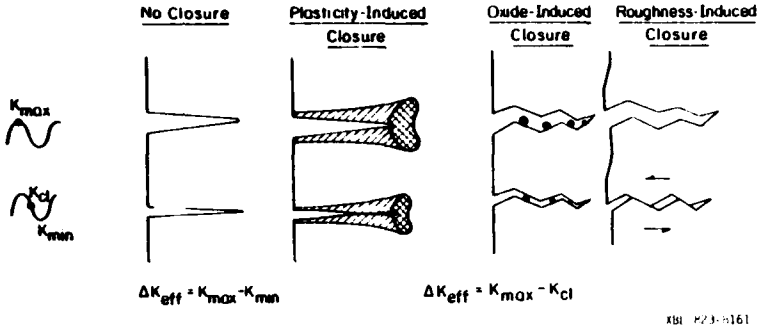

Fig. 7: Schematic illustration of the mechanisms of fatigue crack closure induced by plasticity effects, corrosion debris and rough fracture morphologies. ΔK_{eff} is the effective stress intensity range, defined as $K_{max} - K_{cl}$, where K_{cl} is the stress intensity to close the crack ($K_{cl} \geq K_{min}$). After Ritchie and Suresh (1982).

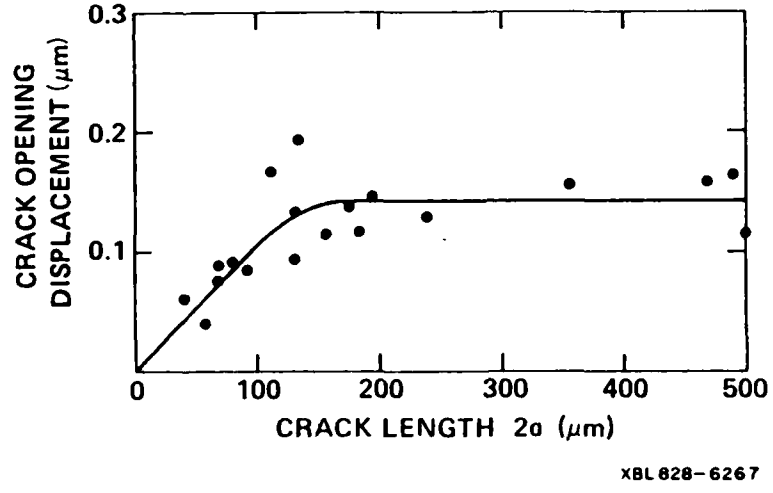

Fig. 8: Variation in crack mouth opening displacement (at zero load), with crack length a, of small surface cracks in 6Al-2Sn-4Zn-6Mo titanium alloy (σ_o = 1140 MPa, primary α grain size - 4 μm, β grain size = 12 μm), showing reduction in crack closure with decreasing crack size. After Morris et al. (1982).

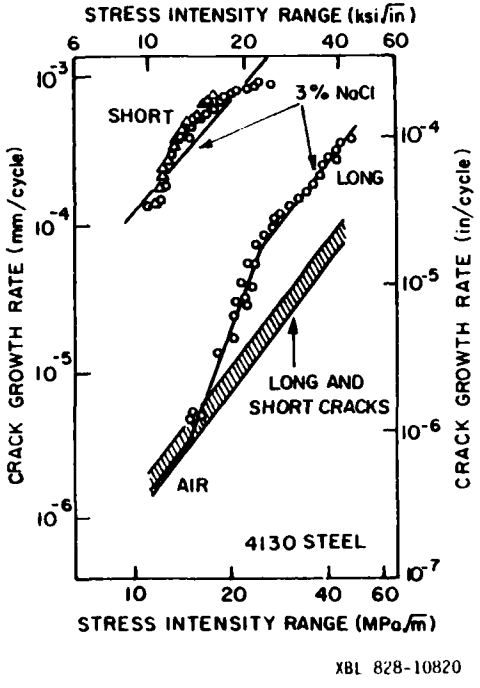

Fig. 9: Variation in fatigue crack growth rate (da/dN) as a function of ΔK for long (a ∿ 50 mm) and physically short (a = 0.1-0.8 mm) cracks in 4130 steel (σ_o = 1300 MPa) tested in moist air and aqueous 3% NaCl solution. After Gangloff (1981).

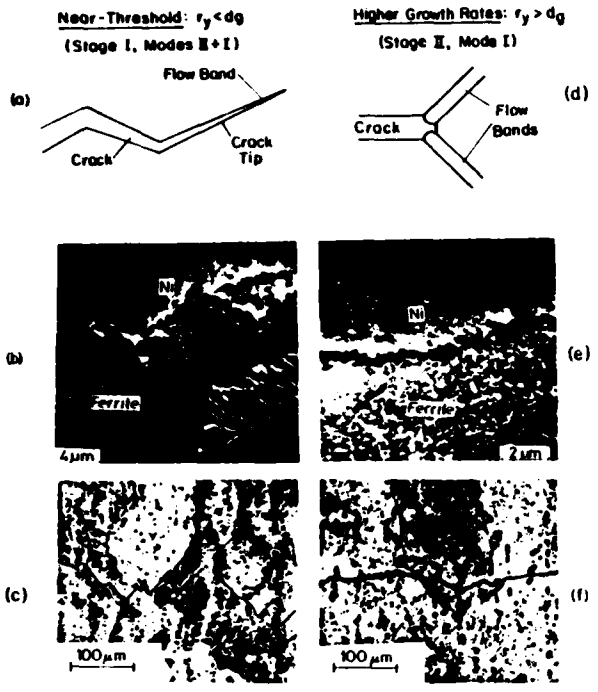

Fig. 10: Crack opening profiles and resulting long crack path morphologies for (a), (b), (c) near-threshold (Stage I) and (d), (e), (f) higher growth rate (Stage II) fatigue crack propagation. (b) and (e) are nickel-plated fracture sections in 1018 steel (after Minakawa and McEvily, 1981), and (c) and (f) are metallographic sections in 7075-T6 aluminum alloy (after Louwaard, 1977, quoted in ref. 3). After Suresh and Ritchie (1982).

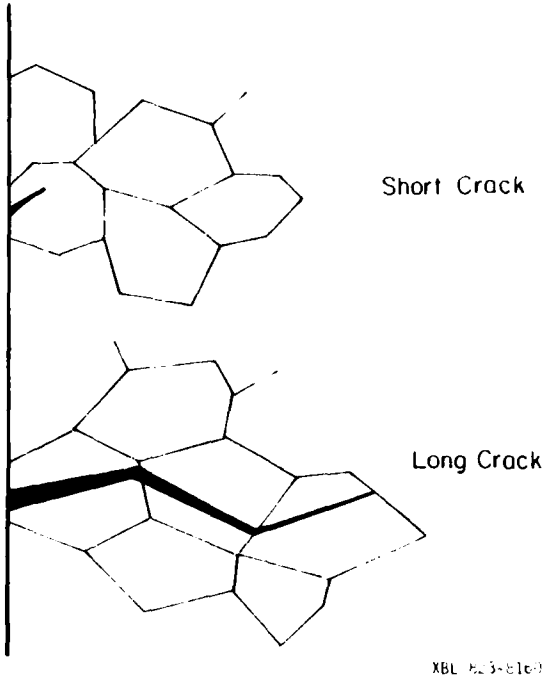

Fig. 11: Idealization of a microstructurally-short and microstructurally-long crack propagating at near-threshold levels by single-shear Stage I mechanism. Note, with reference to Fig. 7, how roughness-induced crack closure will be promoted only in the long crack case. After Suresh and Ritchie (1982).

Paper No. UCB/RP/83/A1011

CRACK DEFLECTION: IMPLICATIONS FOR THE GROWTH OF LONG AND SHORT FATIGUE CRACKS

S. Suresh

Department of Materials Science and Mineral Engineering
and Lawrence Berkeley Laboratory,
University of California, Berkeley, CA 94720

February 1983

CRACK DEFLECTION: IMPLICATIONS FOR THE GROWTH OF LONG AND SHORT FATIGUE CRACKS

S. Suresh

Department of Materials Science and Mineral Engineering
and Lawrence Berkeley Laboratory,
University of California, Berkeley, CA 94720

ABSTRACT

Mechanistic implications associated with the deflection of *nominally* Mode I fatigue cracks are examined. Previous theoretical analyses for deflected cracks are reviewed. Approximate stress intensity solutions are developed to characterize some special cases of multiple kinks in crack path. Experimental results of crack deflection are described for a dual-phase steel and an aluminum alloy subjected to Mode I constant and variable amplitude fatigue cycles. Simple models to predict fatigue crack growth rates are presented for various degrees of deflection. It is demonstrated with the aid of elastic analyses and experimental information that crack deflection models offer a physically-appealing rationale for several fatigue characteristics of metals and alloys. The implications of the deflection of Mode I fatigue cracks are discussed in terms of the *local* mode of crack advance, microstructure, effective driving force, growth mechanisms, mean stress, slip characteristics and crack closure.

INTRODUCTION

Characterization of fatigue crack advance under nominally Mode I loading conditions using the elastic stress intensity factor range is generally based on the premise that the path of the crack is linear and that its plane of growth is normal to the loading axis. It is, however, well known that on a microscopic level, cracks seldom propagate in such a linear fashion. In addition to the normal undulations in the fatigue crack path caused by the particular growth mechanism, pronounced deflection or branching of the crack can occur due to factors such as stress state (1), environment (2), load excursions (3,4) and local microstructural discontinuities (5,6) like second phase particles and grain boundaries. There is a growing interest in the mechanics associated with the non-linearities in crack path (7-10), and an understanding of the crack deflection characteristics is considered essential for a variety of applications including toughening of brittle solids (11), improving the fatigue resistance of commercial alloys (5,12), environmentally-assisted fracture (1,13) and variable amplitude loading (4,14).

Non-linearities in crack path are generally ignored in the characterization of fatigue behavior because of the difficulties in incorporating crack meandering effects in estimates of the driving force, i.e., the stress intensity factor range. In addition, such local variations in the path of a long crack are normally overcome during subsequent propagation over a short distance. Existing evidence from both theoretical (7-10) and experimental studies (4,14), however, clearly indicates that deflections in crack profile can result in marked alterations in fracture

behavior in certain cyclic loading situations where crack growth along the deflected trajectory occurs over several thousand cycles. For example, deflection of cracks resulting in low effective stress intensity values (e.g., in near-threshold and post-overload fatigue crack growth regions) can induce substantial changes in the failure mechanism.

It is known from many investigations that severe crack deflection can occur due to mixed-mode loading (15-18). Moreover, contradicting experimental results variously reveal (16) that the propagation rates of a Mode I fatigue crack can decrease, remain unchanged or increase, when biaxial stresses are superimposed externally. Several recent studies have attempted to characterize the fatigue crack propagation behavior of engineering materials under such externally-imposed mixed-mode fatigue conditions involving either initially inclined cracks (19-21) or multi-axial loads (15-18). However, the important problem of local (near-tip) mixed-mode growth characteristics of (nominally) pure Mode I fatigue cracks, induced solely by crack deflection, has received very little attention (22,23). The purpose of this paper is to examine specifically the role of crack deflection in influencing the growth of long and microstructurally-short fatigue cracks subjected to purely tensile (Mode I) external (far-field) loading conditions.

2. REVIEW OF PRIOR WORK

Figure 1 schematically shows two dimensional models of various crack deflection processes typically encountered during fatigue crack propagation in metals and alloys and the corresponding linear elastic stress intensity factors at the crack tip. As indicated in this figure, deflection of cracks can result in kinked, forked, multiple-kinked (double-kinked or zig-zag) or twisted profiles. The effective driving force for such branched cracks can be substantially different from that observed for a linear crack of the same length.

Solutions of simple two dimensional deflection models are considered here to examine the effects of variations in crack profiles on the growth of linear elastic cracks. When a crack is deviated from its main path (as shown in Fig. 1), it undergoes both tensile opening and sliding displacements locally at the crack tip, even though the far field loading may be purely tensile. For the general case of an elastic crack subjected to both tensile and shear loads, the Mode I and Mode II stress intensity factors k_1 and k_2, respectively, at the deflected crack tip can be expressed (8) as functions of the corresponding stress intensity factors for a linear crack of the same length, K_I and K_{II}, respectively, such that

$$k_1 = a_{11}(\theta)\, K_I + a_{12}(\theta)\, K_{II} \qquad (1a)$$

$$k_2 = a_{21}(\theta)\, K_I + a_{22}(\theta)\, K_{II} \qquad (1b)$$

Here, θ is the angle denoting the extent of branching (Fig. 1a and 1b) and $a_{ij}(\theta)$ are the angular functions associated with the deflected crack. First order solutions (10) for $a_{ij}(\theta)$ yield

$$a_{11}(\theta) = \cos^3(\theta/2) \tag{2a}$$

$$a_{12}(\theta) = -3\sin(\tfrac{\theta}{2})\cos^2(\tfrac{\theta}{2}) \tag{2b}$$

$$a_{21}(\theta) = \sin(\tfrac{\theta}{2})\cos^2(\tfrac{\theta}{2}) \tag{2c}$$

$$a_{22}(\theta) = \cos(\tfrac{\theta}{2})[1 - 3\sin^2(\tfrac{\theta}{2})] \tag{2d}$$

The functions $a_{ij}(\theta)$ in eq. 2 are analogous to the angular dependence of the normal and shear stresses in the near-tip field (ref. 24, for example) and are equivalent to the exact solutions presented by Bilby et al. (8).

Several fracture criteria have been proposed over the years to predict the direction of crack advance and effective driving force for mixed mode conditions based on maximum tangential stress (1), strain energy release rate (for coplanar (25) or non-coplanar (26) growth), strain energy density factor (27) or maximum crack growth rates (15). There is presently some controversy as to the ability of these various criteria to characterize successfully the effective driving force and the direction of further growth. A comparison of the estimates of such failure criteria with experimental data by Petrovic and Mendiratta (28) showed that the simple coplanar strain energy release rate theory (25) yielding

$$k_{eff} \approx \{k_1^2 + k_2^2\}^{\frac{1}{2}} \tag{3}$$

provides reasonable predictions of the effective driving force for brittle materials. The recent results of Hua et al. (16) for 316 stainless steel reveal that fatigue cracks loaded in Mode I and Mode II could grow over a

short distance in the same plane as the initial precrack, instead of deflecting. Moreover, in situations where deflections of monotonically loaded fatigue cracks due to microstructure, environment or load excursions cause local mixed-mode growth, the coplanar approximation (eq. 3) may provide somewhat realistic estimates of effective stress intensities since crack advance can occur in the direction of initial kink over a considerable number of fatigue cycles (3-6,12-14).

For the case of a kinked crack (Fig. 1a), estimates of k_1 and k_2 values at the tip of the kink can be obtained from the work of Bilby et al. (8) for situations where the length of the kink, b, is much smaller than the length of the main crack, a. For Mode I external loading ($K_{II} = 0$) and $b << a$, the normalized crack tip stress intensities k_1/K_I and k_2/K_I for the kinked crack are shown in Fig. 2 for various angles of deflection θ (3).

As the branched crack advances at an angle to the main crack (i.e., as b increases in Figure 1a), the values of k_1 and k_2 change and their relative magnitudes can be obtained from the work of Kitagawa et al. (9). Figure 3 shows the variation of the ratio of Mode II to Mode I stress intensity factors at the crack tip (9) as a function of $\frac{b}{a}$ for various values of θ. The most important inference from this figure is that the Mode II stress intensity k_2 can be over twice as much as the Mode I stress intensity k_1 locally at the tip of a deflected crack, even though the far-field loading is purely in Mode I. Similar analyses are also presently available (8,9) for forked elastic cracks shown in Figure 1b.

2.1 Three-Dimensional Analysis of Crack Deflection

The tilted crack, discussed thus far, has Mode I (tensile opening) and Mode II (sliding) components to its effective stress intensity, whereas a twisted crack (shown schematically in Fig. 1e) incorporates both Mode I and Mode III (tearing) components, k_1 and k_3, respectively. For a crack undergoing pronounced tilting and twisting deflections, the coplanar crack advance can be assumed (24) to be governed by the strain energy release rate, G, for each deflected trajectory,

$$EG = k_1^2(1 - \nu^2) + k_2^2(1 - \nu^2) + k_3^2(1 + \nu) \qquad (4)$$

under plane strain conditions. Here, E and ν are the Young's modulus and Poisson's ratio of the material, respectively. In the present paper, only deflections occurring through the majority of specimen cross section (tilting deflections) are considered.

3. MULTIPLE-KINKS IN CRACK PATH

Approximate stress intensity factor solutions for some special cases of multiple kinks in crack path are derived in this section. Based on the "criterion of local symmetry" (10), the deflected crack loaded in tension (Mode I), tends to return to its main path so that $k_2 = 0$ (Fig. 1c). Even if the plane of crack advance is dictated by external environments or the growth mechanism (e.g., crystallographic mode of propagation, where crack advance can occur along the kink over distances of the order of a grain diameter), further changes in crack profile can take place as the crack tip encounters a grain boundary or second phase particle. Thus, a doubly-kinked crack profile schematically shown in Fig. 1c, is developed.

With the development of a second kink in crack path, the crack tip stress intensities undergo additional changes and can be estimated as follows.

Just prior to the development of the second kink (location A in Fig. 1c), the Mode I and Mode II crack tip stress intensities for farfield tensile loading conditions ($K_{II} = 0$) are given by eqs. 1 and 2.

$$k_{1_A} = \cos^3(\tfrac{\theta}{2})\, K_I \tag{5a}$$

$$k_{2_A} = \sin(\tfrac{\theta}{2}) \cos^2(\tfrac{\theta}{2})\, K_I \tag{5b}$$

for $b \ll a$. As the second kink of length b' develops ($b' \ll b$), the stress intensities k_1 and k_2 at the tip of the doubly-kinked crack are obtained by substituting k_{1_A} and k_{2_A} from eq. 5 for K_I and K_{II}, respectively, in eq. 1 and by setting $\theta = -\alpha$. Thus, combining eqs. 1, 2 and 5, for the doubly-kinked crack profile subjected to tensile loading only, yields

$$k_1 = K_I\left\{\cos^3(\tfrac{\theta}{2}) \cos^3(\tfrac{\alpha}{2}) + 3\sin(\tfrac{\theta}{2}) \cos^2(\tfrac{\theta}{2}) \sin(\tfrac{\alpha}{2}) \cos^2(\tfrac{\alpha}{2})\right\} \tag{6a}$$

$$k_2 = K_I\left\{\cos^3(\tfrac{\theta}{2}) \sin(\tfrac{\alpha}{2}) \cos^2(\tfrac{\alpha}{2}) - \sin(\tfrac{\theta}{2}) \cos^2(\tfrac{\theta}{2}) \cos(\tfrac{\alpha}{2})\left[1 - 3\sin^2(\tfrac{\alpha}{2})\right]\right\} \tag{6b}$$

Here, θ and α are the angles representing the extent of the first and second kinks in crack path, respectively (Fig. 1c), and K_I is the nominal stress intensity factor for a linear crack of the same length. The magnitudes of k_1/K_I and k_2/K_I from eq. 6 are plotted in Fig. 4 for various combinations of θ and α. The value of k_1/K_I (which can be substantially smaller than 1) initially increases with α at lower values of α (Fig. 4a), before decreasing rapidly at higher values of α. The ratio k_2/K_I plotted in

Fig. 4b suggests that Mode II stress intensities at the tip of a doubly-kinked crack can vary from zero to considerably higher values, depending on the combination of θ and α. (Note that for $\alpha = 0°$, the k_1/K_I and k_2/K_I values are the same as those presented in Fig. 2 for a kinked crack, from the exact solutions of Bilby et al. (8)). Even as the deflected crack tends to return to its main growth direction, the Mode I stress intensity k_1 remains smaller than that for a linear crack (Fig. 4a), for $b_1 << b$. Thus, even for cases of double deflection where $k_2 = 0$, k_1 approaches K_I only after the crack grows away from the location of the second deflection. These results imply that deflected cracks with a zig-zag profile around their nominal Mode I crack plane (schematically illustrated in Fig. 1d) can lead to effective tensile opening stress intensities smaller than K_I as long as the tip of the crack is inclined to the loading axis.

4. IMPLICATIONS OF FATIGUE CRACK DEFLECTION: MECHANISTIC ASPECTS

The process of crack deflection, detailed in the previous sections, has the following effects on the growth behavior of fatigue cracks.

a) With changes in crack profile, the *effective* stress intensity range value responsible for crack advance can be *reduced* considerably from the nominal stress intensity range. The Mode II stress intensity value k_2 at the tip of a deflected crack can be much higher than the Mode I stress intensity k_1 even though the external loading may be purely tensile (Mode I). The magnitude of k_2 is dependent upon the angle of

diversion of the crack tip from the Mode I growth direction. For certain values of such angles, the magnitude of k_2 may be zero even though considerable crack deflection is observed (Fig. 4b). Even when $k_2 = 0$, the value of k_1 immediately following deflection can be substantially smaller than K_I.

b) The lowering of crack driving force due to deflection occurs during the *entire* fatigue cycle. The stress intensity range is modified from a nominal value of

$$\Delta K_I = [K_I]_{max} - [K_I]_{min} \tag{7}$$

to an effective value of

$$\Delta k_{eff} = k_{max} - k_{min} \tag{8}$$

where k_{max} and k_{min} are the effective maximum and minimum stress intensity factor values (eq. 3) for a deflected crack.

c) With changes in crack morphology, the mean stress of the fatigue cycle is altered from the nominal load ratio of

$$R = [K_I]_{min}/[K_I]_{max} \tag{9}$$

to an actual load ratio of

$$\bar{R} = k_{min}/k_{max} \tag{10}$$

d) An ideal elastic crack would close completely at zero load irrespective of the magnitude of Mode I and Mode II displacements at the crack tip. Such a crack would not undergo any closure at tensile loads. However, in practical terms, a linear elastic fatigue crack undergoes irreversible deformation which results in permanent residual strains in

the wake of the crack (29). In addition, irreversibility of slip can occur during the unloading portion of the fatigue cycle due to oxidation of slip steps in moist media (30). A large volume of results (4,14,31-34) indicates that a combination of these factors leads to irreversibility of crack tip displacements and mismatch between fracture surface asperities during the unloading portion of the fatigue cycle, thereby leading to roughness-induced crack closure (31). The Mode II crack tip stress intensities arising from deflections in crack path primarily determine the extent of roughness-induced closure. The relative sliding between crack faces arising from crack deflection also causes enhanced oxide formation on the fractured faces thereby promoting oxide-induced closure (31). An experimental study of fatigue crack tip movement in aluminum alloys using stereoimaging techniques (22) has revealed that the sliding displacements can be substantially larger than tensile opening displacements, even though the external loading is tensile. Moreover, the ratio of such Mode II to Mode I displacements is found to be a function of environment.

e) The premature closure of the fracture surfaces arising as a result of asperity contact *raises* the effective minimum load of the fatigue cycle. Thus, the actual load ratio is increased under the combined effects of crack deflection and fracture surface mismatch to a value of

$$\bar{R} = k_{cl}/k_{max} \qquad (11)$$

where k_{cl} is the effective stress intensity factor for the deflected crack at the point of first asperity contact.

f) Pronounced crack deflection *during fatigue* can lower the effective stress intensity range to such an extent that significant

changes in crack growth mechanism (or even complete crack arrest) can occur. Such effects typically involve near-threshold or post-overload crack growth regions and are examined in the following.

5. DEFLECTION OF LONG FATIGUE CRACKS

The propagation of fatigue cracks in many engineering materials invariably involves undulations and deflections in crack path. Such variations from a linear morphology are normally overcome during subsequent growth over a few fatigue cycles and are insignificant from the point of view of the measurement of overall fatigue crack growth rates. However, marked deflections in crack path do occur as a result of microstructure, environment or changes in the magnitude or direction of applied loads and for these situations, subsequent crack propagation can take place along the kink over several thousand fatigue cycles. Under such circumstances, both the value of the stress intensity factor (computed for a linear crack profile) and the measured crack propagation rates (which ignore deflections in crack path) are substantially in error. For example, several experimental studies on titanium alloys (e.g., ref. 35) have reported sudden arrest of constant amplitude fatigue cracks at nominal stress intensities well above the threshold ΔK_o value. Such anomalous and unreproducible results can often be traced back to abrupt crack deflections.

5.1 Growth Rate Predictions

Linear elastic models, accounting for changes in crack tip driving force and growth rates, are developed here to demonstrate the

role of crack deflection in influencing the fatigue behavior of engineering materials. The thick solid lines (corresponding to $\theta = 0°$) in Figs. 5b-5d show the typical room temperature crack growth behavior (for $R = 0.05$ at 50 Hz) of steels with yield strength values around 600 MPa, such as the fully martensitic 2¼Cr-1Mo steel (ASTM A542 Class 2, 690°C temper (ref. 31)) or the intermediate-quenched* Fe/2Si/0.1C ferrite-martensite dual phase steel (ref. 36). Such steels show predominantly linear fatigue crack profiles during the entire range of crack propagation rates. However, if deflections are introduced in the fatigue crack path of these materials through microstructural modifications, pronounced changes are observed in the apparent crack growth behavior. Fig. 5a shows an idealization of such a deflected crack profile. Here θ denotes the angle of deflection, D the distance over which the tilted crack advances along the kink and S the distance over which linear (Mode I) crack growth occurs. The deflection behavior of this model crack is repeated in each segment comprising a total growth distance of D + S, which is much smaller than the total length of the crack. The extent of deflections in two adjoining segments is the same although the deflections occur in opposite directions (Fig. 5a). The ratio $\frac{D}{D + S}$ signifies the extent of crack deflection.

Variations in the fatigue behavior arising from the deflections of this idealized crack can be estimated for various values of θ and $\frac{D}{D + S}$ using the following procedures and assumptions: i) The crack driving

*Austenitized at 1150°C, brine quenched and subsequently heated to 1020°C ($\alpha + \gamma$ range) before quenching, thereby obtaining a microstructure of fine fibrous α' in α matrix.

force for coplanar growth along the deflected trajectory can be characterized by eqs. 3 and 8, with k_1 and k_2 calculated from eqs. 1 and 2. ii) The effective driving force in each segment is represented by the weighted average of the effective stress intensity factor values for the deflected span, D, and the straight span, S, i.e., the average stress intensity range in each segment equals

$$\overline{\Delta K_I} = (D\Delta k_{eff} + S\Delta K_I)/(D + S) \qquad (12)$$

iii) The effects of prior deflections in crack path become negligible as the crack grows along the linear segment S, away from the point of deflection. iv) Crack growth rates are determined by the effective value of the stress intensity factor range Δk_{eff}; for an undeflected crack tip ($\theta = 0°$) the nominal (apparent) stress intensity factor range $\Delta K_I = \Delta k_{eff}$, whereas for a deflected crack tip ($\theta \neq 0°$), $\Delta K_I > \Delta k_{eff}$. v) The nominal Mode I crack propagation rate in each segment is determined by the weighted average of the growth along the projection of the deflected trajectory spanning a distance of D cosθ and the straight span, S, i.e.,

$$(\overline{\frac{dc}{dN}}) = (\frac{D\cos\theta + S}{D + S})(\frac{dc}{dN}) \qquad (13)$$

Here $(\overline{\frac{dc}{dN}})$ is the measured average growth rate of a deflected crack in each segment and $(\frac{dc}{dN})$ the growth rate of an undeflected crack. In other words, the measured growth rates of a deflected crack are always apparently lower than those for an undeflected crack at the same value of Δk_{eff}, if the deflections in crack path are not taken into consideration.

The above procedure for estimating the crack growth rates of a deflected crack can be illustrated for the conditions of $\theta = 60°$ and $\frac{D}{D+S} = 0.5$. Substitution of $\theta = 60°$ and $K_{II} = 0$ in eqs. 1-2 yields $k_1 \approx 0.65\ K_I$ and $k_2 \approx 0.375\ K_I$. Using these values of mixed-mode local stress intensity factors in eqs. 3 and 8 provides an apparent stress intensity factor for the deflected path, $\Delta k_{eff} \approx 0.75\ \Delta K_I$. Substituting this value of Δk_{eff} and $\frac{D}{D+S} = 0.5$ in eq. 12, one obtains the weighted average the effective stress intensity factor in each segment $\overline{\Delta K_I} \approx 0.875\ \Delta K_I$. While $\overline{\Delta K_I} = \Delta K_I = \Delta k_{eff}$ for the undeflected crack, an externally applied driving force of $\Delta K_I = (0.875)^{-1}\ \Delta k_{eff}$ is required to propagate the deflected crack at the same rate. Similarly, eq. 13 provides $(\overline{\frac{dc}{dN}}) \approx 0.75(\frac{dc}{dN})$. In other words, a deflected crack with $\theta = 60°$ and $\frac{D}{D+S} = 0.5$, has an apparent driving force 1.14 times greater than an undeflected crack (at equal growth rates) and propagates at apparently 25% slower rate in the Mode I growth direction (at equal values of Δk_{eff}).

Figs. 5b-5d show the predicted changes in the fatigue behavior for various degrees of deflection denoted by θ and $\frac{D}{D+S}$. It is noted from these figures that increasing values of θ and $\frac{D}{D+S}$ shift the crack propagation curve further to the right of the fatigue curve for an undeflected crack ($\theta = 0°$).

5.2 Experimental Observations

5.2.1 Steel:

The recent results of McEvily and co-workers (37,38), Wasynczuk (39) and Dutta et al. (40) on ferrite-martensite duplex steels reveal that significant improvements in fatigue response can be accomplished without sacrificing tensile strength properties. These studies have found considerably higher threshold ΔK_o values and slower fatigue crack growth rates in certain duplex microstructures capable of inducing nonlinearities

in crack path, as compared to conventional steels of comparable strength levels. The predicted variations (Figs. 5b-5d) in fatigue behavior arising from deflection are compared here with the recent experimental results of the author and co-workers (40) for the Fe/2Si/0.1C dual phase steel. The intermediate-quenched condition of this steel resulting in a ferrite-martensite duplex microstrucutre (with 58% α' and a yield strength of approximately 600 MPa) leads to a predominantly linear crack profile during fatigue cycling. The fatigue behavior for this heat treatment was modelled as a reference for an undeflected crack ($\theta \approx 0$) in Figs. 5b-5d and is also shown in Fig. 6. Changing the heat treatment of this steel by a step-quenching procedure* (with about 32% α' and a yield strength of 635 MPa) has been observed to cause pronounced deflections in crack path during the entire range of fatigue crack propagation. A typical example of the tortuous crack path for this material is illustrated in Fig. 7a which shows the crack profile with deflection at $\Delta K \approx \Delta K_o$. The fatigue crack growth resistance of the step-quenched condition is also substantially better than that of the intermediate-quenched condition, as evident from the data in Fig. 6. Measurements of crack closure for the two heat treatments (40) reveal that 30-50% of the difference in fatigue behavior (Fig. 6) between the two heat treatments can be accounted for by crack closure phenomena. Considering the pronounced deflections in crack path in the step-quenched conditions and taking typical values (40) of angles of tilt $\theta \approx 45°\text{-}75°$ (occurring over several grains through the specimen cross section) and $\frac{D}{D+S} \approx 0.25\text{-}0.5$, it can be inferred from the

*Austenitized at 1150°C, air cooled to 910°C and subsequently brine quenched, thereby obtaining a microstructure of coarse α' in continuous α.

predictions of Figs. 5b and 5c that the remainder of the differences in the fatigue behavior of these two materials is accounted for by crack deflection phenomena. Thus, non-linearities in crack path seem to cause a substantial influence on the *apparent* fatigue growth characteristics (consistent with the predictions of the deflection models), in addition to the effects of the ensuing crack closure and intrinsic microstructural factors. The fatigue data obtained for such duplex steels show considerable scatter and poor reproducibility (37-40). This appears to be due to the fact that the effective driving force is strongly dictated by crack deflection which in turn is controlled by *local* microstructural features. The metallurgical aspects governing crack path in this dual phase steel will be discussed in detail in a forthcoming paper (40).

5.2.2 Aluminum Alloy:

Figure 7b shows the abrupt deflection ($\theta \simeq 75°$) of a crack when it encounters a grain boundary in 2020-T6 aluminum (Al-4.5Cu-1.1Li-0.5Mn-0.2Cd) alloy at $\Delta K_I \simeq 7.7$ MPa$\sqrt{m}$. Results obtained by the author and colleagues (5) reveal that the crack propagation rates for this alloy are up to 4-5 times slower (at room temperature) than those for the 7075-T6 alloy (41) of about the same strength level, even when the differences in the elastic modulii are incorporated in the analyses. A primary reason for this improved fatigue resistance of the 2020 alloy seems to arise from the highly tortuous fatigue crack path in this alloy. Approximate estimates of the effective driving force using the prediction of the crack deflection models in Figs. 5b-5d suggest that the majority of the differences in crack propagation rates between the two high strength aluminum alloys can be traced back to the differences in crack deflection characteristics (5).

5.3 Crack Deflection During Variable Amplitude Fatigue

Deflection of a crack, induced by overloads, may also considerably alter the fatigue crack growth characteristics. Figure 8 shows the non-linearity induced in the crack path when an 80% single peak overload is applied to a 2020-T6 aluminum alloy at a baseline stress intensity range of 7.7 MPa$\sqrt{m}$. Figure 8a is the crack profile at the specimen surface immediately following the application of overload, whereas Figure 8b reveals the crack morphology and coplanar growth along the kink at center thickness section after 9000 constant amplitude cycles following the overload. Estimates of crack tip stress intensity factors based on elastic kinked crack models (schematically represented in Fig. 1a, with $\theta \simeq 45°$) yield $k_1 \simeq 0.79\ K_I$, $k_2 \simeq 0.33\ K_I$ and $k_{eff} \simeq 0.86\ K_I$ from eqs. 1-3. This suggests that crack deflection alone accounts for a 14% reduction in the effective driving force in the post-overload region. If the extent of crack deflection and overload-induced changes in crack-tip plasticity is so pronounced that the post-overload *effective* driving force is smaller than the threshold ΔK_o, complete crack arrest is observed (14).

6. DEFLECTION OF SHORT FATIGUE CRACKS

Cracks are considered short when a) their length is small compared to relevant microstructural dimensions (a continuum mechanics limitation), b) their length is small compared to the scale of local plasticity (a linear elastic fracture mechanics limitation) and c) they are merely physically small (i.e., crack length $\leq$ 0.5-1 mm). Recent studies have shown (6,42-52) that short cracks grow substantially faster than long cracks when characterized in terms of the same nominal elastic stress

intensity factor range, ΔK_I. Figure 9 schematically shows the typical variation of fatigue crack growth rates dc/dN as a function of ΔK for both long and short cracks. It is noted from this figure that accelerated short crack advance occurs at stress intensities lower than the threshold stress intensity range ΔK_o, below which long cracks do not propagate or grow at experimentally undetectable rates. Figure 9 also reveals that the initially faster growth of short cracks progressively decelerates (or even arrests completely, in some cases) before merging with the long crack data.

Various arguments have been put forth previously to account for the deceleration of initially high short crack growth and for the existence of a threshold for the arrest of short cracks. Morris et al. (42) suggest that the deceleration and/or arrest of short cracks in the vicinity of a grain boundary occurs because i) the crack does not propagate in an adjacent grain until a "mature" plastic zone develops *and* ii) closure stresses retard crack growth; the extent of closure is determined by the location of the crack tip relative to the grain boundary. Tanaka and co-workers (49) postulate that the crack tip slip bands are *blocked* by the grain boundary; the threshold for the growth of small cracks is determined by whether the slip bands pinned at grain boundaries can propagate into the adjacent grain or not.

Alternative approaches to such previous interpretations of crack tip-grain boundary interactions can be developed by considering the role of crack deflection in influencing the growth of short fatigue cracks. Figure 10 shows the changes in short crack growth direction induced by the grain boundary and the corresponding decrease in crack growth rates in

7075-T6 aluminum alloy (from ref. 6). For a short crack comparable in size to the grain dimensions, the low restraint on cyclic slip will promote a predominantly crystallographic mode of failure, akin to Forsyth's Stage I mechanism (51) (Fig. 11a). On reaching a grain boundary, the crack tends to re-orient itself in a new crystallographic direction in the adjacent grain to advance by the single slip mechanism and can be considerably deflected by the grain boundaries (Fig. 11b). The extent of deflection is dependent upon the relative orientations of the most favorable slip systems in the adjoining crystals. It is the inference of the present study that crack deflection processes play a major role in influencing the behavior of short fatigue cracks (described in Figs. 9 and 10), as indicated by the models presented earlier. The mechanistic implications associated with the non-linearities in crack path discussed earlier are also applicable to the growth of short cracks. Approximate expressions to estimate the crack tip stress intensity factors for deflected short cracks are derived in the Appendix.

The values of normalized local stress intensity factors k_1/K_I and k_2/k_1, *immediately after* deflection, are plotted in Figure 12 from the equation developed in the Appendix for various combinations of the short crack initiation and deflection angles, θ_0 and θ_1, respectively. For typical values of $\theta_0 \simeq 45°$ and $\theta_1 \approx 90°$ (ref. 6, for example), k_1 and k_2 at the tip of the deflected short crack are found to be about 0.7 K_I and 0.35 K_I (from eqs. A3 and A4 in the Appendix). The effective stress intensity factor range Δk_{eff}, then, is obtained from eq. 3 to be about 0.78 ΔK_I. Thus, considerations of crack deflection can account for a significant reduction in the driving force during crack-tip-grain boundary interactions. If the extent of deflection at the grain boundary is large, the effective

cyclic stresses may be reduced to a value smaller than the "true threshold" for short crack advance. For such a case, complete crack arrest results (as denoted by curve A in Fig. 9). Kitagawa and Takahashi (43) have shown that below a critical crack size (1-10 μm for ultrahigh strength materials and 0.1-1 mm for low strength materials), the "true threshold" for no growth can be characterized by a constant threshold value of cyclic stress $\Delta\sigma_{TH}$, which is roughly equal to the smooth bar fatigue limit $\Delta\sigma_e$. If the effective cyclic stresses are above $\Delta\sigma_{TH}$, no crack arrest occurs (as denoted in point B in Fig. 9). Here, one observes only a deceleration in crack growth which is overcome as the short crack progresses away from the point of deflection. Recent results (6) on 7075-T6 aluminum alloy do indeed show that the minimum in the growth rate of short cracks roughly corresponds to a crack length being equal to the smallest grain dimension.

It is appropriate, at this point, to consider the limitations involved in the application of fracture mechanics concepts to the short crack problem. Recently several authors (42,44,46,49,50) have used the linear elastic stress intensity factor to characterize the growth of short cracks. Although such results remain controversial, alternative attempts (e.g., 45) to characterize short crack growth using the J-integral or CTOD concepts are still questionable since they also do not consider the role of closure of the fractured faces of the wake. In addition, there is currently no physical interpretation for the intrinsic crack length arguments (50) proposed to rationalize the apparent anomalies between the growth kinetics of long and short cracks. The deflection models are presented here using stress intensity factors to rationalize previously

published results (42,44,46,49) of apparent thresholds for short cracks. It is noted that although such elastic calculations are questionable in view of the paucity of a reliable parameter to characterize the mechanics of short crack growth, the mechanisms underlying such analyses are physically realistic irrespective of the choice of the characterization parameter.

In addition to the major role of the deflection of short cracks arising from the growth mechanism and crack tip-grain boundary interactions, other factors should also be considered to rationalize the differences in the fatigue behavior of long and short cracks. It is now established that crack closure due to i) residual plastic deformation left in the wake of a growing crack (29), ii) formation of enlarged corrosion deposits on the fracture surface in moist environments (31,41,53) and iii) premature fracture surface asperity contact (31-34), can impede the growth of long cracks. The work of Newman (54) has indicated that, at equivalent stress intensity factor levels, small cracks in plates and at notches grow faster than long cracks because the applied stress needed to open a small crack is less than that needed to open a long crack. Newman's finite-element analyses (54) specifically examined the role of residual plastic deformation behind the crack tip in causing closure. Although such plasticity-induced closure may be less significant for short cracks, other forms of closure are also of importance for short crack growth. For example, irreversibility of slip steps and surface oxidation can lead to nonuniform tensile opening and shear displacements of short cracks. Given the presence of serrated fracture surfaces and Mode II crack tip displacements due to deflection, such nonuniformities in crack

opening and sliding, in reality, result in premature asperity contact resulting in roughness-induced crack closure. (A perfectly elastic crack would not result in any roughness-induced closure irrespective of the extent of deflection.) Experimental measurements of crack closure (42) do indeed show that even short cracks (spanning only a few grain diameters) can close above the minimum load of the fatigue cycle. Such closure processes during the growth of short cracks are modelled in Figure 11. Thus, it is inferred that crack deflection can influence the growth of short cracks through reductions in the effective driving force as well as the resultant roughness-induced closure.

7. CONCLUDING REMARKS

As seen in the earlier sections, a consideration of the deflection of fatigue cracks is of paramount importance to gain an insight into the various mechanistic aspects as well as to rationalize several apparent anomalies in the fatigue characteristics of metals and alloys. The simple elastic models for deflection do provide an indication of the nature of local mixed-mode growth and the role of microstructure, environment and stress state. However, they do not take into consideration the size of the plastic zone at the tip of the deflected crack. In metals and alloys, the scale of the crack tip process zone may be comparable to the length of the kink. There have been some recent attempts to characterize the mechanics of crack deflection in terms of elastic-plastic analyses using the J-integral (55). Such an approach, however, does not significantly improve the prediction of crack tip driving force since it also does not account for the contact between crack faces

(closure) *behind* the crack tip. The process of crack deflection plays a substantial role in enhancing crack closure. The analyses presented in this work have a greater accuracy at the lower crack propagation rates (e.g., near-threshold regime) where the size of the process zone induced by the *effective* stress intensity range is very small. The elastic models discussed earlier incorporate only a two dimensional analysis although the deflection of fatigue cracks is a three dimensional problem. Statistical approaches to estimate the improvements in toughness of brittle materials have recently become available, where three dimensional crack deflection models incorporate both tilting and twisting of cracks for various size, shape and distribution of secondary particles (11). Similar analyses for metals become extremely difficult because of the strong dependence of deflection characteristics on the slip behavior, orientation of the slip systems with respect to the crack plane, inter-metallic particles, grain boundaries, environmental influences and the loading patterns. For situations involving predominantly tilting deflections (e.g., Figs. 5-8), and pronounced growth along the kinked path, the present analyses based on two-dimensional models result in a high degree of accuracy. It should be pointed out that the calculation using only the surface measurements of crack profiles provide a lower bound estimate of the reduction in effective driving force due to deflection.

In many cyclic loading situations involving *local* mixed mode crack advance over several thousand cycles, characterization of fatigue data

using the *nominal* Mode I stress intensity factor alone will result in erroneous predictions of the driving force and crack propagation rates. Moreover, a neglect of local crack deflection processes in both long and short fatigue crack problems leads to a *nonconservative* estimate of the *effective* threshold stress values. Such non-conservative estimates based on the nominal Mode I stress intensity factor are often somewhat experimentally unreproducible and show considerable scatter (as indicated by several studies on the threshold fatigue behavior in dual phase steels and titanium alloys, for example) because of the dependence of crack deflection on local microstructural features, loading history and environment. Thus it is recommended that corrections to the driving force based on the deflections in crack path be incorporated in the fatigue data wherever possible. In this light, it is interesting to note that crack deflection processes seem to offer substantial improvements in the fatigue crack growth resistance of engineering alloys, as evidenced by the unusually lower fatigue crack propagation rates and higher threshold ΔK_o values of certain dual phase steels.

ACKNOWLEDGMENTS

This work was supported by the Air Force Office of Scientific Research under Grant No. AFOSR-82-0181. Thanks are due to Professor A. G. Evans for his many valuable discussions and suggestions during the course of this work. The author is grateful to his colleagues, Mr. V. B. Dutta and Dr. A. K. Vasudevan, for their help in obtaining and permission to use some of the micrographs in this paper. The author is also thankful to Professor R. O. Ritchie for his continued support, encouragement and suggestions.

NOMENCLATURE

a	length of the main crack
a_{ij}	angular functions
b	length of the first kink
b_1	length of the fork
b^1	length of the second kink
b_{ij}	angular functions relating k_1, k_3 and K_I
c	nominal length of a fatigue crack
c_{ij}	constants relating strain energy density factor and stress intensity factors
D	length of the deflected segment
dc/dN	nominal crack growth rate
$\overline{dc}/dN$	growth rate of a deflected crack
E	Young's modulus
G	strain energy release rate
h	average asperity height
k_{eff}	effective stress intensity factor for a deflected crack
k_1	Mode I stress intensity factor for a deflected crack
$\bar{k}_1$	Mode I stress intensity factor for an inclined crack
K_I	Mode I stress intensity factor for a linear crack
k_2	Mode II stress intensity factor for a deflected crack
$\bar{k}_2$	Mode II stress intensity factor for an inclined crack
K_{II}	Mode II stress intensity factor for a linear crack
k_3	Mode III stress intensity factor for a deflected crack
N	number of fatigue cycles
R	nominal load ratio ($= (K_I)_{min}/(K_I)_{max}$)
$\bar{R}$	load ratio accounting for crack deflection ($= k_{min}/k_{max}$)

$\bar{R}$	load ratio accounting for crack deflection and crack closure ($= k_{cl}/k_{max}$)
S	length of the linear segment
w	average asperity width
α	angle of second deflection for long tilted crack
γ	angle at which normal stress or strain energy release rate is a maximum
Δk	effective stress intensity factor range
ΔK_I	nominal Mode I stress intensity factor range
$\overline{\Delta K_I}$	average stress intensity factor range in a segment
ϕ	angle of deflection for a twisted crack
θ	angle of first deflection for a long crack
θ_o	angle of initial inclination for a short crack
θ_1	angle of first deflection for a short crack
$\sigma_{\theta\theta}$	normal stress
$\sigma_{r\theta}$	shear stress
$\Delta\sigma_e$	fatigue limit
$\Delta\sigma_{TH}$	threshold cyclic stress range for short cracks
ν	Poisson's ratio

APPENDIX

Stress intensity solutions are presented here for the ideal case of the deflection of an initially inclined crack in a perfectly elastic medium. When such a crack is inclined at an angle θ_o to the Mode I growth plane (Fig. 12a), the tensile and shear stress intensity factors at the crack tip, $\bar{k}_1$ and $\bar{k}_2$, respectively are obtained from resolving the stresses in the direction of kink so that

$$\bar{k}_1 = K_I \cos^2\theta_o \tag{A1}$$

$$\bar{k}_2 = K_I \sin\theta_o \cos\theta_o \tag{A2}$$

When such an *elastic* crack is deflected by an angle θ_1 (Fig. 12b), the stress intensity factors k_1 and k_2 immediately following deflection (Fig. 12b) can be obtained by substituting $\bar{k}_1$ and $\bar{k}_2$ for K_I and K_{II} in eq. (1) and by setting $\theta = -\theta_1$ in eq. (2) for angular functions a_{ij}. Thus,

$$k_1/K_I = \cos^2\theta_o \cos^3(\tfrac{\theta_1}{2}) + 3\sin\theta_o \cos\theta_o \sin(\tfrac{\theta_1}{2}) \cos^2(\tfrac{\theta_1}{2}) \tag{A3}$$

$$k_2/K_I = \cos^2\theta_o \sin(\tfrac{\theta_1}{2}) \cos^2(\tfrac{\theta_1}{2}) - \sin\theta_o \cos\theta_o \cos(\tfrac{\theta_1}{2})[1 - 3\sin^2(\tfrac{\theta_1}{2})] \tag{A4}$$

REFERENCES

1. F. Erdogan and G. C. Sih, J. Basic Eng., 1963, vol. 85, p. 519.

2. W. W. Gerberich and K. A. Peterson, in Micro and Macro Mechanics of Crack Growth, K. Sadananda, B. B. Rath and D. J. Michel, eds., The Metallurgical Society of AIME, Warrendale, PA, 1982, p. 1.

3. J. Lankford and D. L. Davidson, in Advances in Fracture Research, D. Francois, ed., Pergamon Press, Oxford, 1981, vol. 4, p. 899.

4. S. Suresh, Scripta Met., 1982, vol. 16, p. 995.

5. S. Suresh and A. K. Vasudevan, unpublished research, University of California, Berkeley, 1983.

6. J. Lankford, Fat. Eng. Mater. Struct., 1982, vol. 5, p. 233.

7. S. N. Chatterjee, Int. J. Solids Struct., 1975, vol. 15, p. 521.

8. B. A. Bilby, G. E. Cardew and I. C. Howards, in Fracture 1977, D. M. R. Taplin, ed., University of Waterloo Press, 1977, vol. 3, p. 197.

9. H. Kitagawa, R. Yuuki and T. Ohira, Eng. Fract. Mech., 1975, vol. 7, p. 515.

10. B. Cotterell and J. R. Rice, Int. J. Fract., 1980, vol. 16, p. 155.

11. K. T. Faber and A. G. Evans, Acta Met., 1983, in press.

12. E. W. Lee, C. J. Beevers and E. A. Starke, paper presented at AIME Annual Meeting, Atlanta, GA, 1983.

13. M. O. Speidel, NATO Conference, Ericeira, 1971.

14. S. Suresh, Eng. Fract. Mech., 1983, vol. 15, in press.

15. F. Hourlier and A. Pineaux, in Advances in Fracture Research, D. Francois, ed., Pergamon Press, Oxford, 1981, vol. 4, p. 1833.

16. G. Hua, M. W. Brown and K. J. Miller, Fat. Eng. Mater. Struct., 1982, vol. 5, p. 1.

17. M. Truchon, M. Amestoy and K. Dang-Van, in Advances in Fracture Research, D. Francois, ed., Pergamon Press, Oxford, 1981, vol. 4, p. 1841.

18. A. Otsuka, K. Mori, T. Ohshima and S. Tsuyama, ibid, 1981, p. 1851.

19. R. Badaliance, Eng. Fract. Mech., 1980, vol. 13, p. 657.

20. A. B. Patel and R. K. Pandey, Fat. Eng. Mater. Struct., 1981, vol. 4, p. 65.

21. K. Tanaka, Eng. Fract. Mech., 1974, vol. 6, p. 493.

22. D. L. Davidson and J. Lankford, SWRI Report, 1982.

23. D. L. Davidson, Fat. Eng. Mater. Struct., 1981, vol. 3, p. 229.

24. B. R. Lawn and T. R. Wilshaw, Fracture of Brittle Solids, Cambridge University Press, 1975.

25. P. C. Paris and G. C. Sih, Stress Analysis of Cracks, ASTM STP 381, 1965, p. 30.

26. M. A. Hussain, S. L. Pu and J. Underwood, ASTM STP 560, 1974, p. 2.

27. G. C. Sih, Int. J. Fract., 1974, vol. 10, p. 305.

28. J. J. Petrovic and M. G. Mendiratta, J. Am. Ceramic Soc., 1977, vol. 60, p. 463.

29. W. Elber, ASTM STP 486, 1971, p. 230.

30. R. M. N. Pelloux, Eng. Fract. Mech., 1970, vol. 1, p. 697.

31. S. Suresh, G. F. Zamiski and R. O. Ritchie, Met. Trans. A, 1981, vol. 12A, p. 1435.

32. N. Walker and C. J. Beevers, Fat. Eng. Mater. Struct., 1979, vol. 1, p. 135.

33. K. Minakawa and A. J. McEvily, Scripta Met., 1981, vol. 15, p. 633.

34. S. Suresh and R. O. Ritchie, Met. Trans. A, 1982, vol. 13A, p. 1627.

35. J. Chesnutt, Rockwell International Science Center Report, 1978.

36. V. B. Dutta, M.S. Thesis, University of California, Berkeley, 1983.

37. H. Suzuki and A. J. McEvily, Met. Trans. A, 1979, vol. 10A, p. 475.

38. K. Minakawa, Y. Matsuo and A. J. McEvily, Met. Trans. A, 1982, vol. 13A, p. 439.

39. J. Wasynczuk, M.S. Thesis, University of California, Berkeley, 1982.

40. V. B. Dutta, S. Suresh and R. O. Ritchie, unpublished research, 1983.

41. A. K. Vasudévan and S. Suresh, Met. Trans. A, 1982, vol. 13A, p. 2270.

42. W. L. Morris, M. R. James and O. Buck, Met. Trans. A, 1981, vol. 12A, p. 57.

43. H. Kitagawa and S. Takahashi, in Proc. 2nd Intl. Conf. on Mech. Beh. Mater., 1979, p. 717.

44. S. J. Hudak, Jr., J. Eng. Mater. Tech., Trans. ASME, Ser. H, 1981, vol. 103, p. 26.

45. N. Dowling, in Cracks and Fracture, ASTM STP 601, Amer. Soc. Test. Mater., 1976, p. 17.

46. D. Taylor and J. F. Knott, Fat. Eng. Mat. Struct., 1981, vol. 4, p. 220.

47. J. Schijve, in Fatigue Thresholds, Blom et al., eds., EMAS Ltd., Warley, 1982, vol. 2, p. 881.

48. R. O. Ritchie and S. Suresh, in Proc. 55th Meeting of the AGARD Structural and Materials Panel on "Behavior of Short Cracks in Airframe Components," Toronto, Canada, 1982.

49. K. Tanaka, Y. Nakai and M. Yamashita, Int. J. Fract., 1981, vol. 17, p. 519.

50. M. H. El-Haddad, K. N. Smith and T. H. Topper, J. Eng. Mater. Tech., Trans. ASME, Ser. H, 1979, vol. 101, p. 42.

51. P. J. E. Forshyth, in Proc. of Symposium on Crack Propagation, Cranfield, England, 1961.

52. S. Pearson, Eng. Frac. Mech., 1975, vol. 7, p. 235.

53. P. K. Liaw, S. J. Hudak, Jr. and J. K. Donald, Met. Trans. A, 1982, vol. 13A, p. 1633.

54. J. C. Newman, Jr., in Proc. 55th Meeting of the AGARD Structural and Materials Panel on "Behavior of Short Cracks in Airframe Components," Toronto, Canada, 1982.

55. H. Ishikawa, H. Kitagawa and H. Okamura, in Proc. ICM3, Pergamon Press, Oxford, 1979, vol. 3, p. 447.

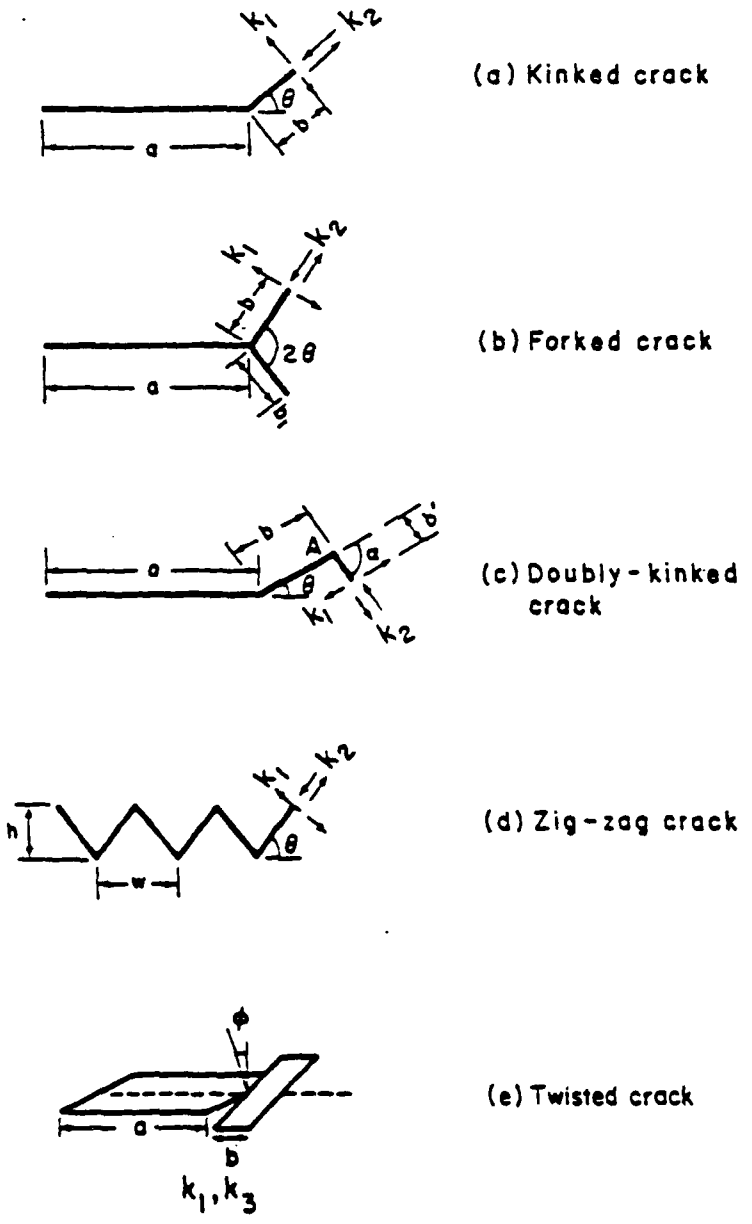

Fig. 1. Schematic showing possible types of fatigue crack deflection and the corresponding nomenclature to describe stress intensity factors.

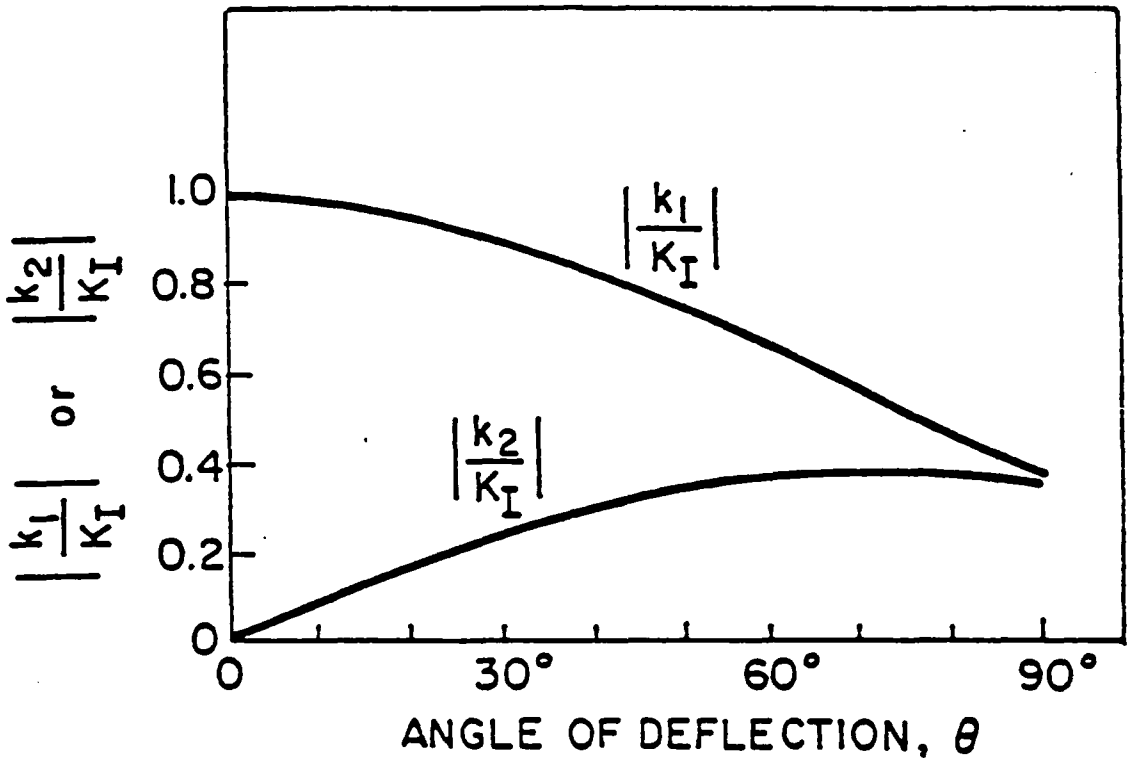

Fig. 2. Variation of the normalized crack tip stress intensity factors for a kinked crack (Fig. 1a) loaded in tension, as a function of the angle of deflection (ref. 8).

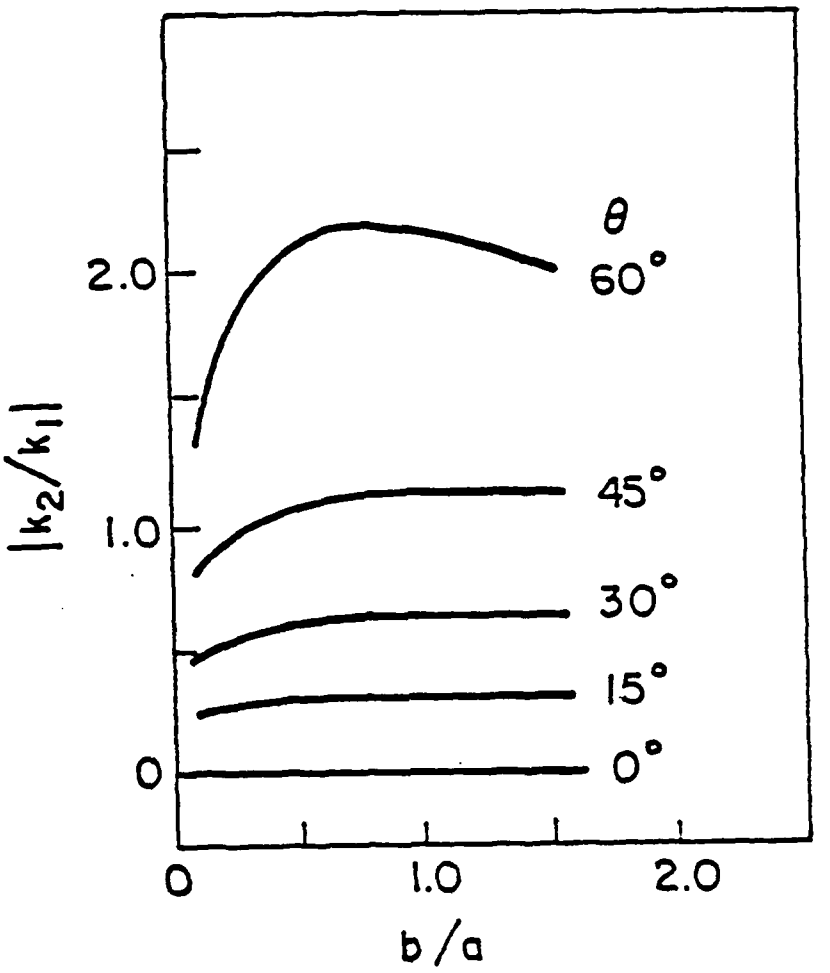

Fig. 3. Variation of the ratio of Mode II to Mode I stress intensity factors at the tip of a kinked crack (Fig. 1a) loaded in tension, as a function of the angle of deflection (ref. 9).

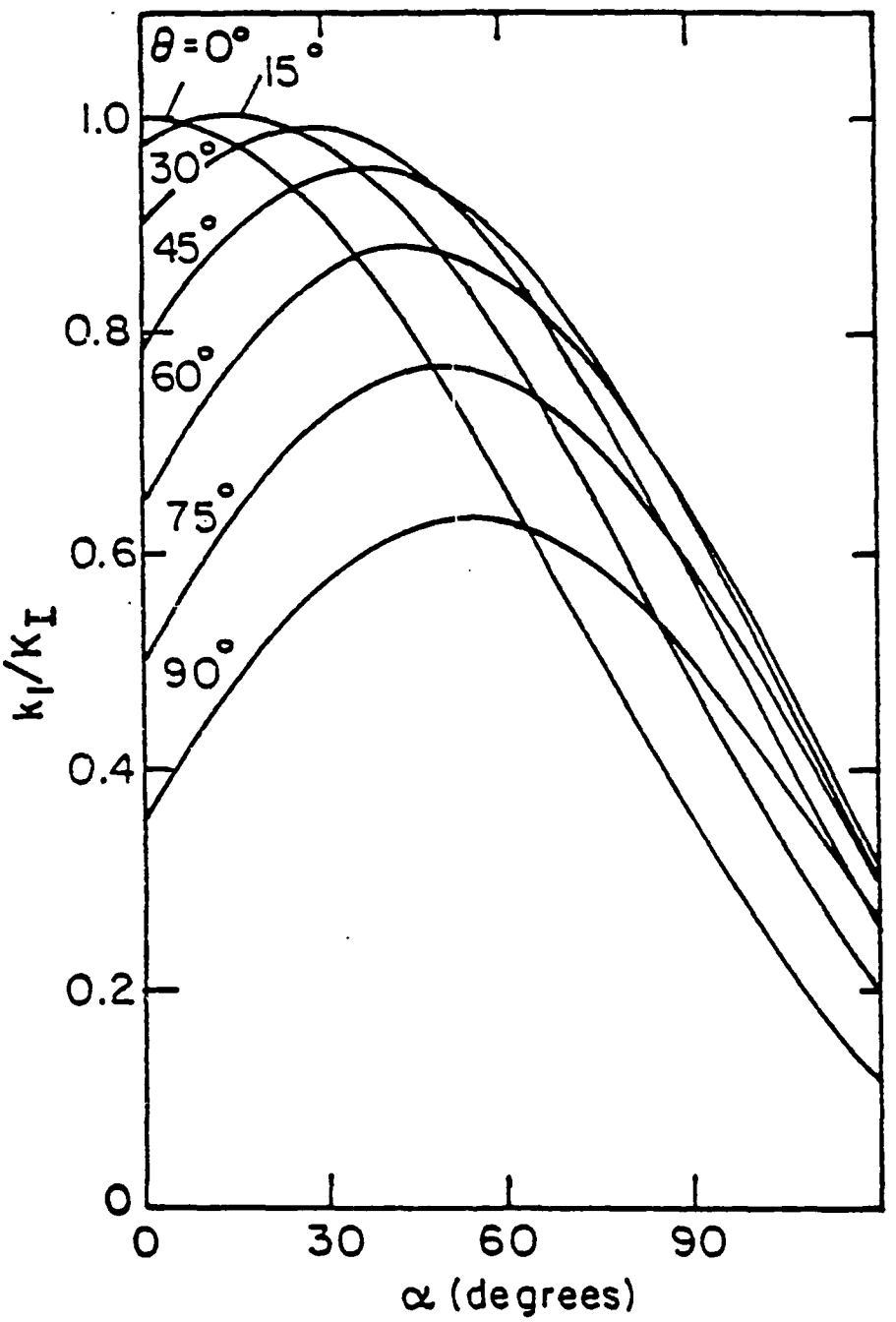

XBL 832-7852

Fig. 4a

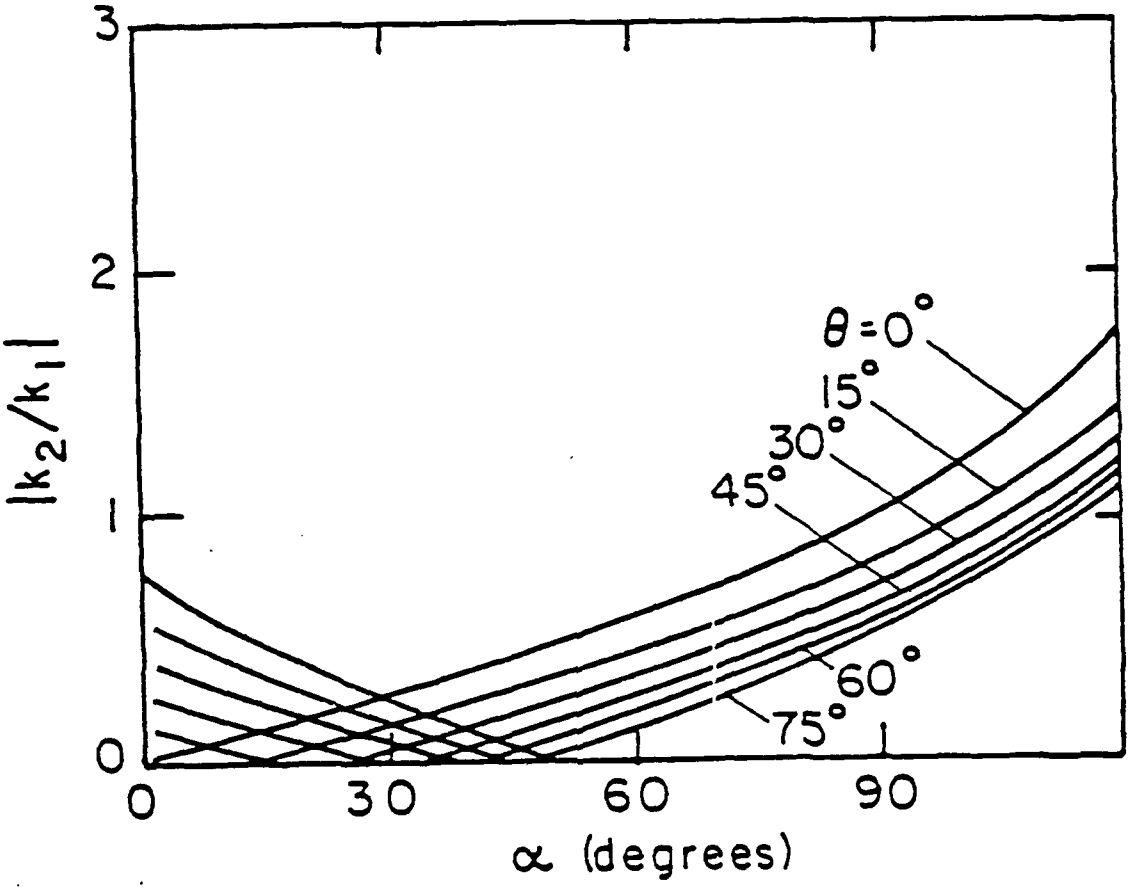

(b)

Fig. 4. Predicted variation (eq. 6) of the crack tip stress intensity factors at the tip of the doubly-kinked crack, as a function of θ and α, the angles of first and second deflection, respectively; a) normalized Mode I stress intensity factor and b) ratio of Mode II to Mode I stress intensity factors.

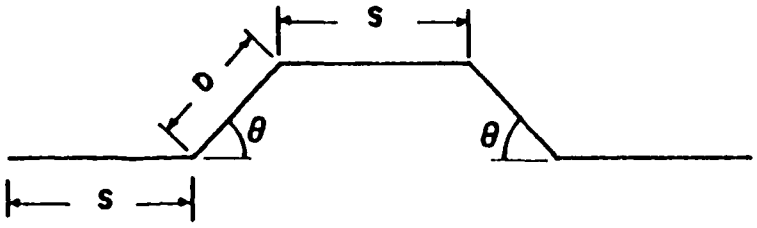

(a)

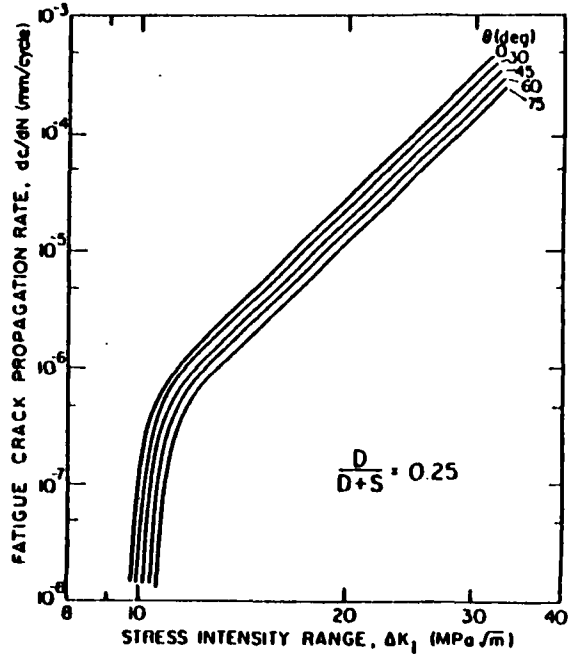

(b)

XBL 833-8868

Fig. 5

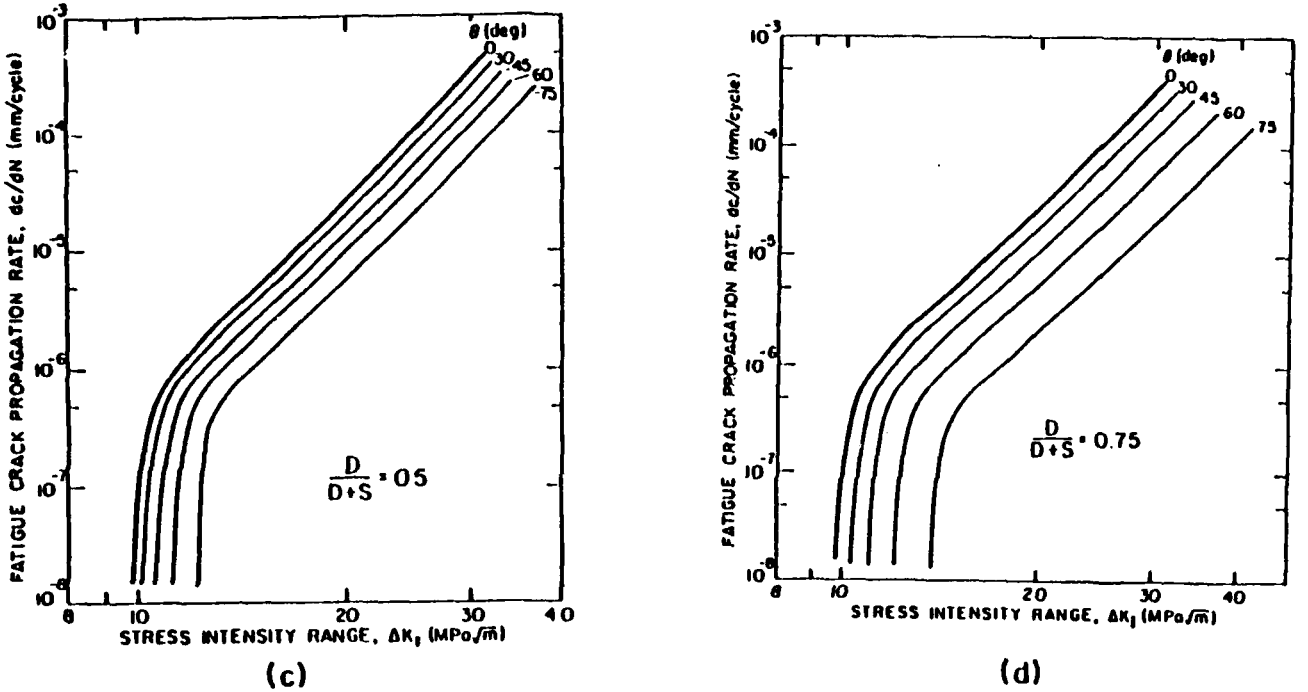

Fig. 5. a) Model profile of a segment of a deflected crack with the associated nomenclature (see text for detailed descriptions). b) - d) Predicted crack propagation rates for deflected cracks as functions of the angle of deflection, θ, and the extent of deflection, D/D + S.

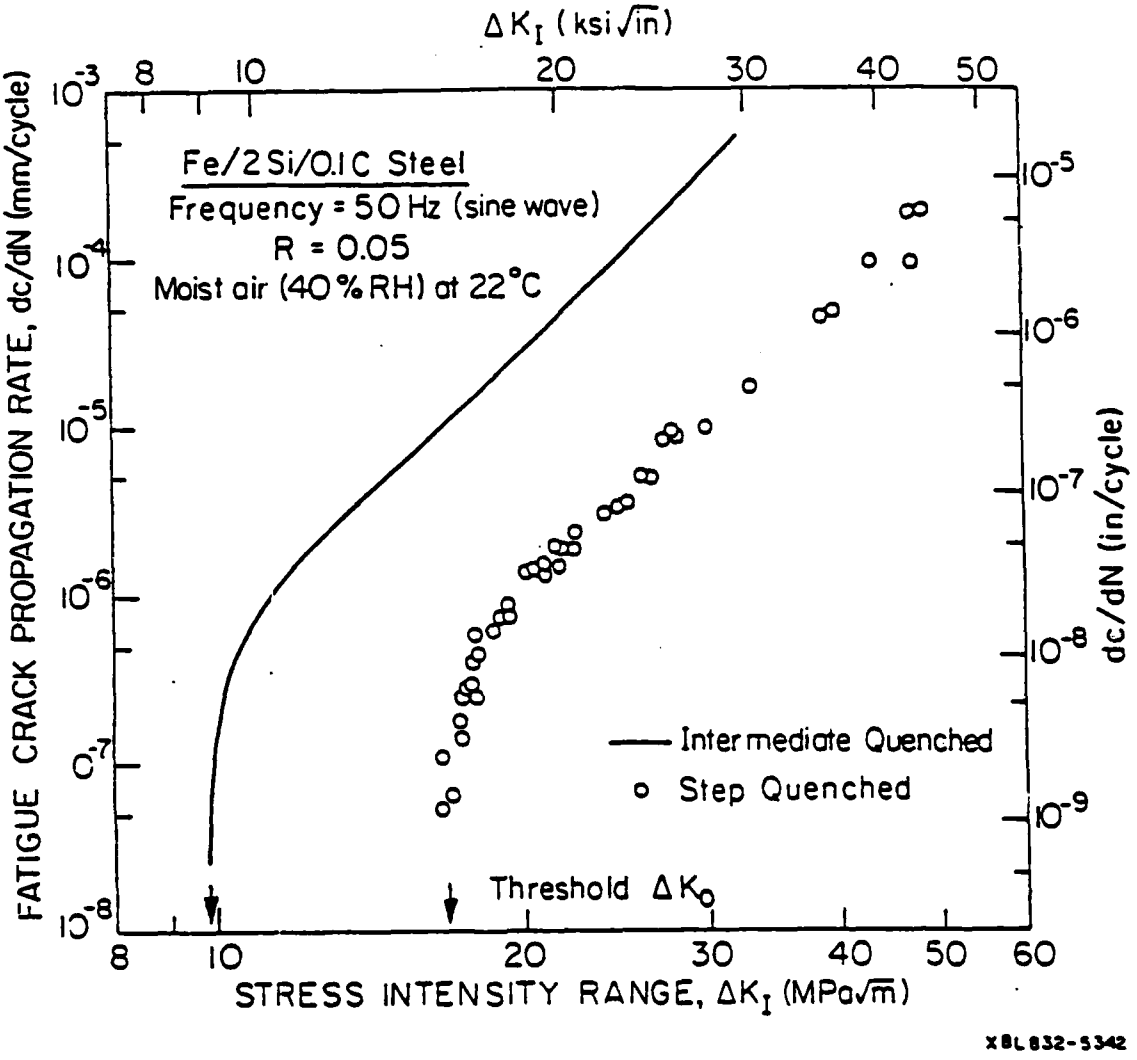

Fig. 6. Fatigue crack propagation data for the intermediate-quenched and step-quenched conditions of Fe/2Si/0.1C duplex steel (40).

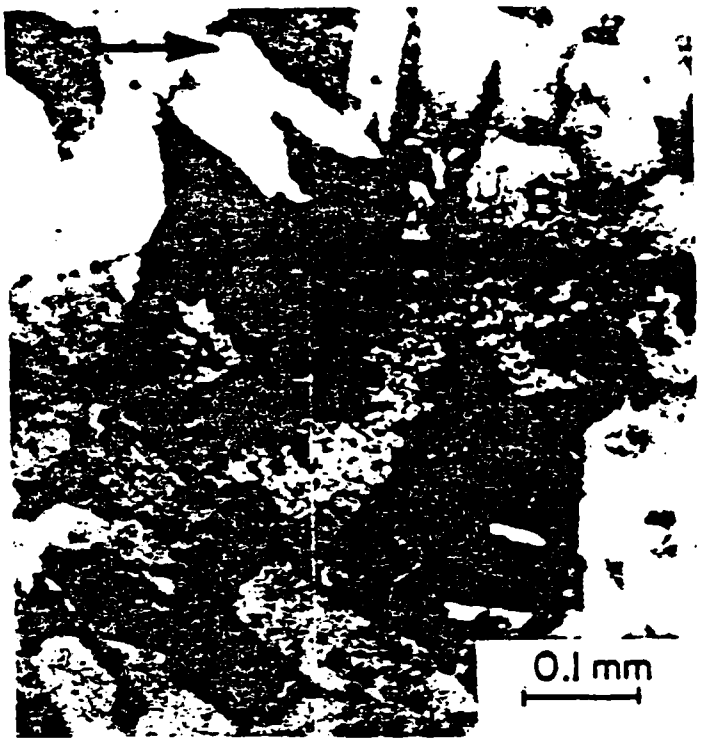

(a)

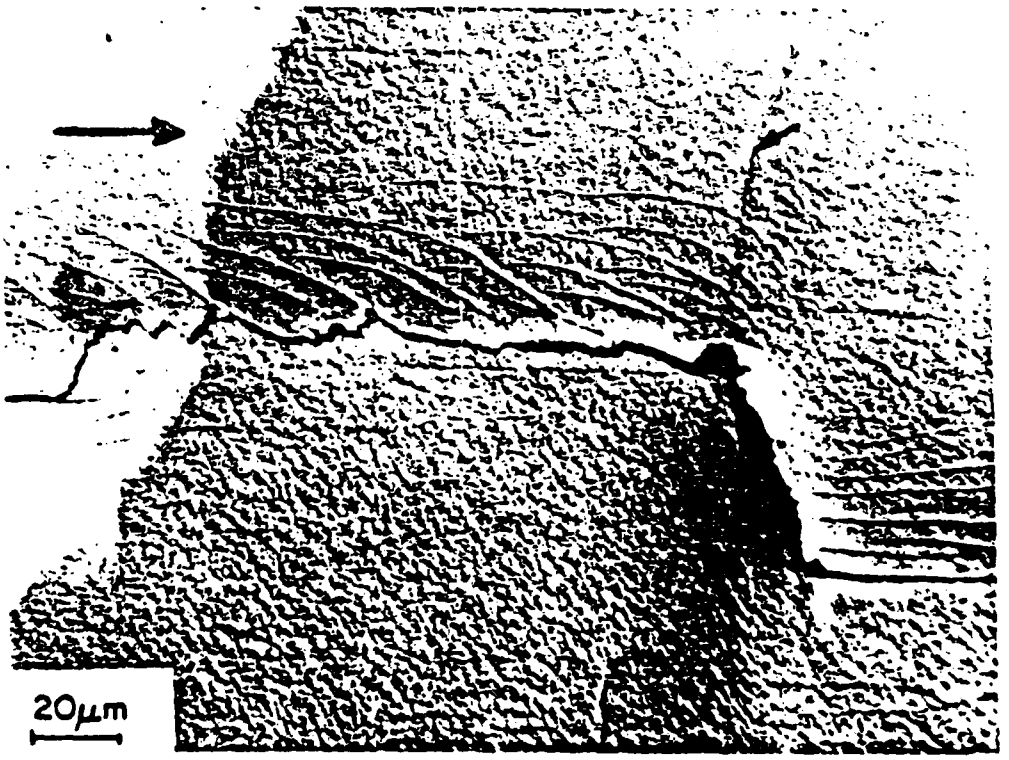

(b)

Fig. 7. a) Profile of a deflected crack in Fe/2Si/0.1C duplex steel; A denotes the near-threshold growth regime; deflection at $\Delta K_I \simeq \Delta K_o$; B denotes growth at higher stress intensities. b) Deflection of a Mode I fatigue crack on encountering a grain boundary (smaller arrow) in 2020-T651 aluminum alloy at $\Delta K_I \simeq 7.7$ MPa$\sqrt{m}$; larger arrows in both figures indicate crack growth direction.

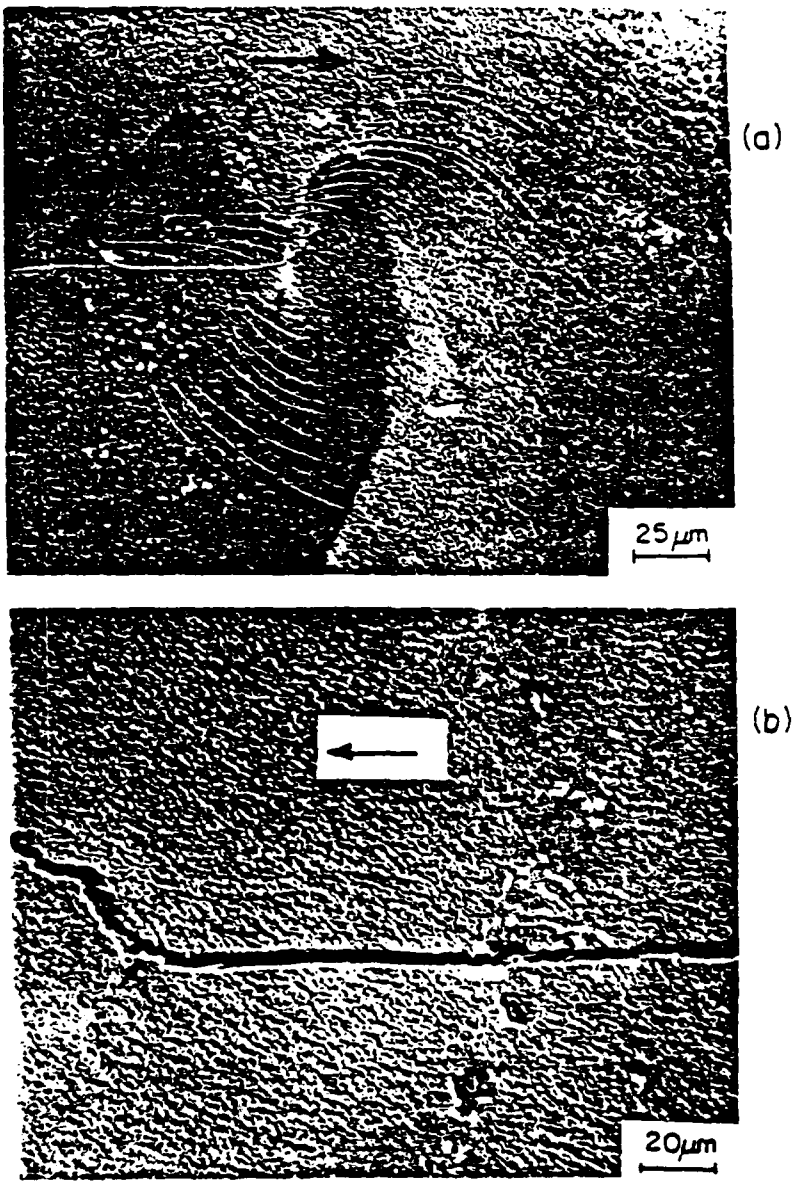

Fig. 8. a) Surface profile of deflection of a Mode I fatigue crack immediately after the application of 80% overload in 2020-T651 aluminum alloy at $\Delta K_I \approx 7.7$ MPa$\sqrt{m}$. b) Crack profile at specimen center thickness at 9000 cycles of constant amplitude loading following the overload in 2020-T651 alloy; smaller arrows indicate crack tip location at which overload was applied. Larger arrows indicate crack growth direction.

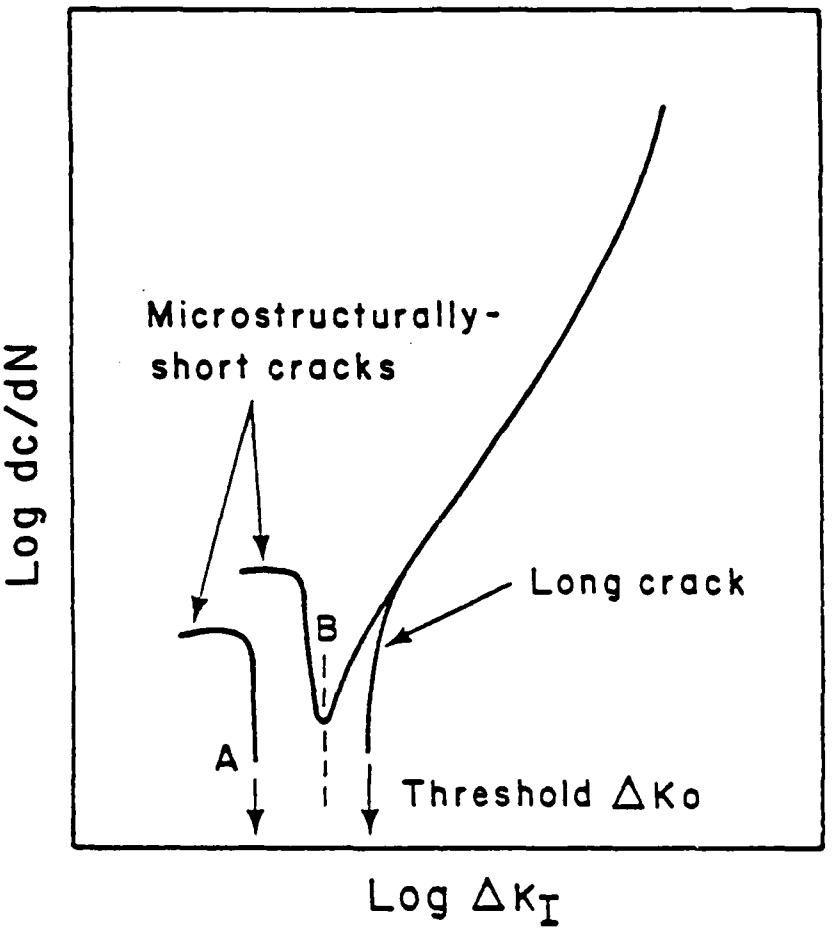

Fig. 9. Schematic showing the typical variation of fatigue crack growth rates dc/dN as a function of ΔK for both long and short fatigue cracks.

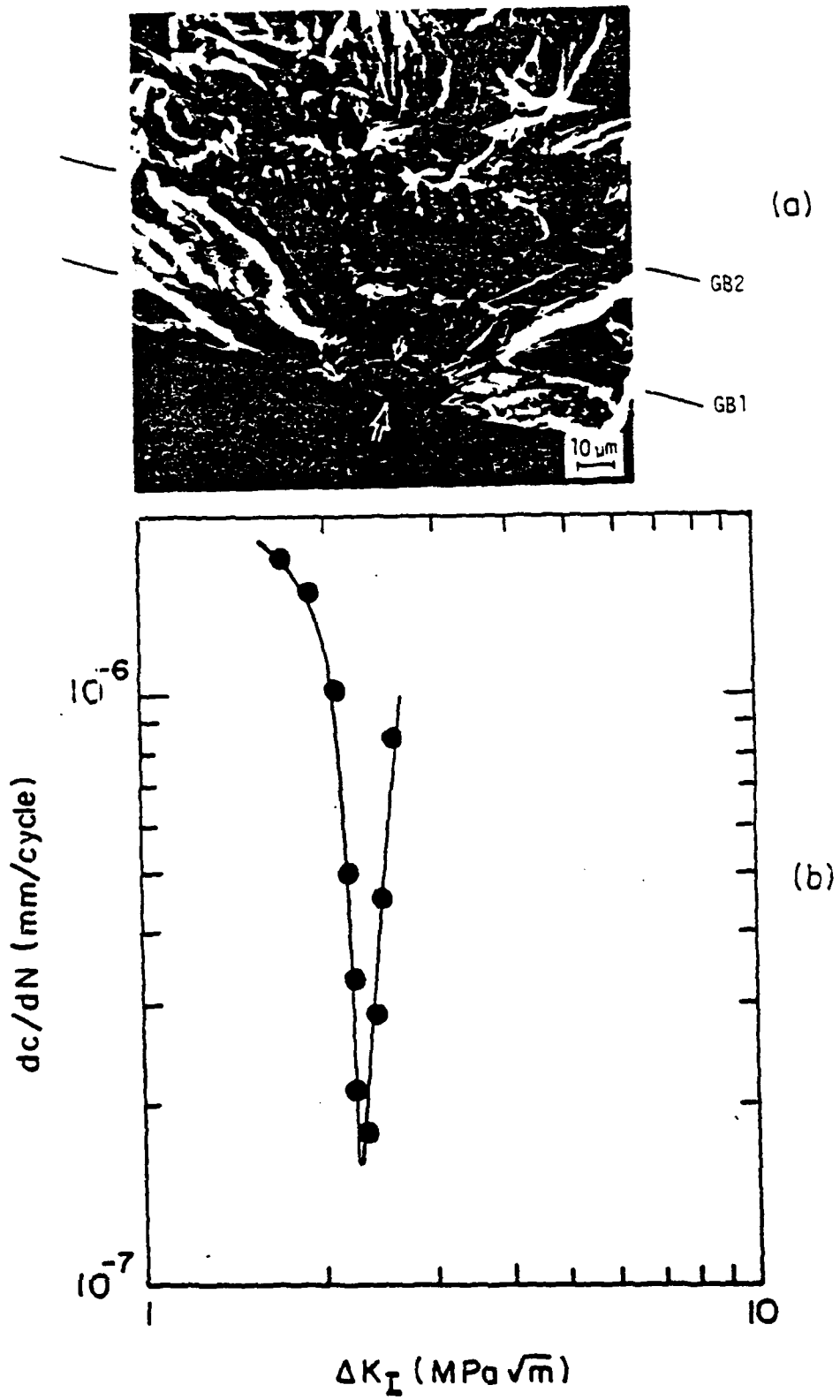

Fig. 10. a) Micrograph showing the changes in the direction of crack advance when the crack tip encounters a grain boundary; b) abrupt decrease in the rate of short fatigue crack growth due to crack tip-grain boundary interactions in 7075-T6 aluminum alloy (ref. 6).

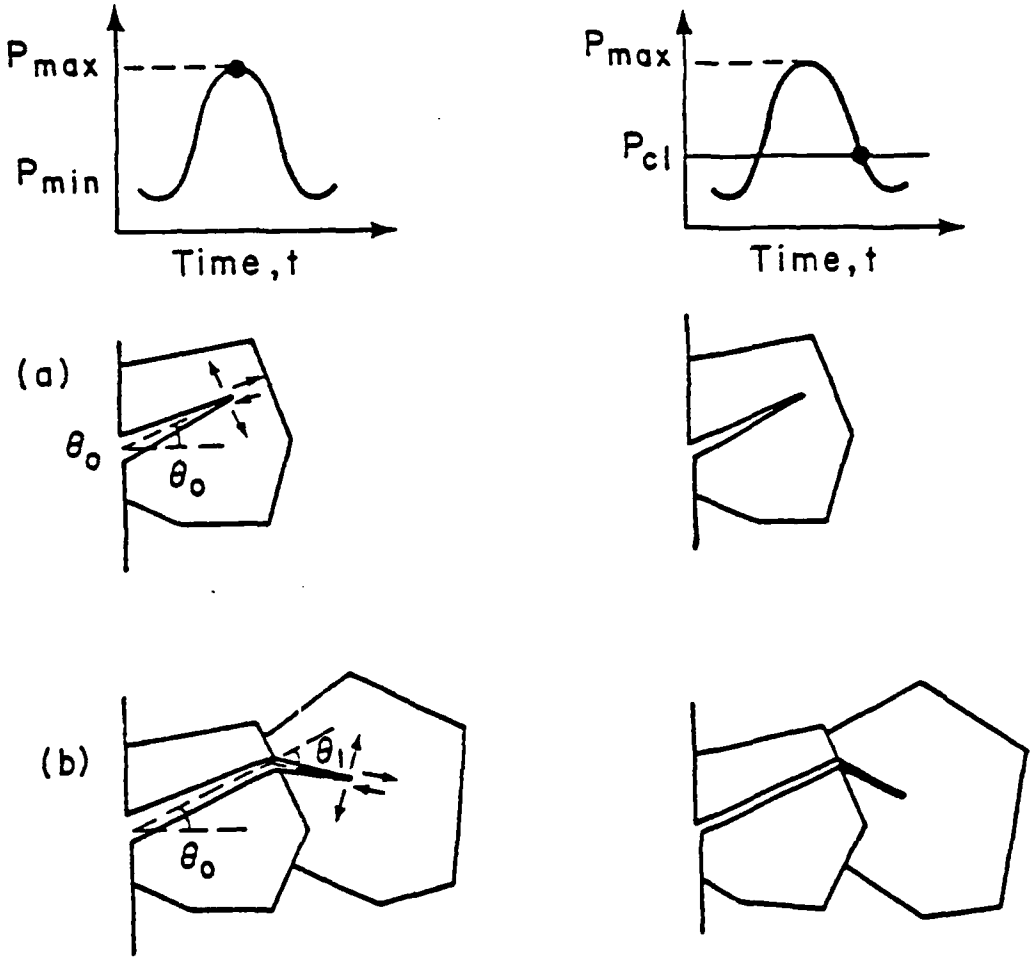

Fig. 11. Schematic illustrating the growth and deflection of microstructurally-short fatigue cracks and the resultant crack tip displacements and closure.

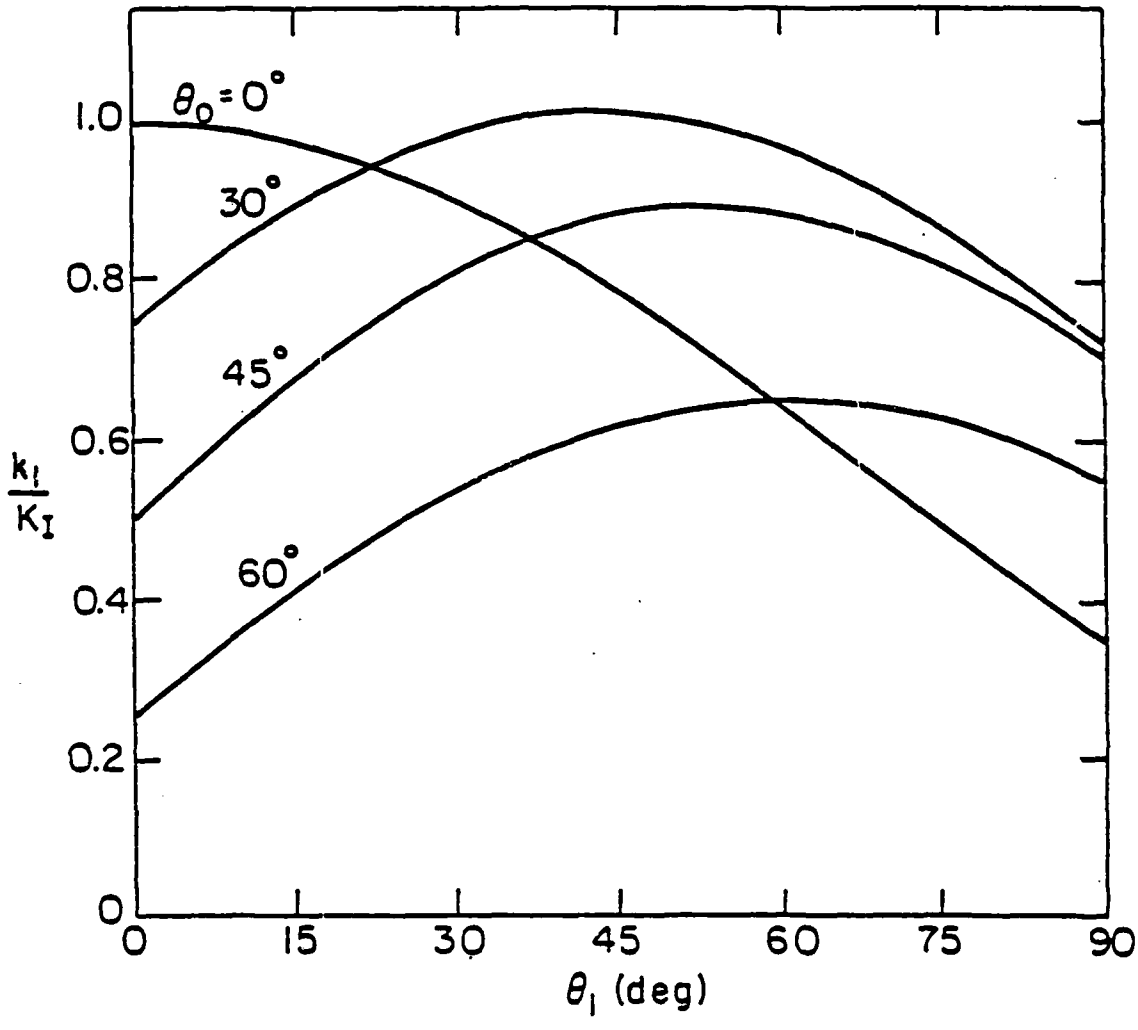

XBL 831-5137

Fig. 12a

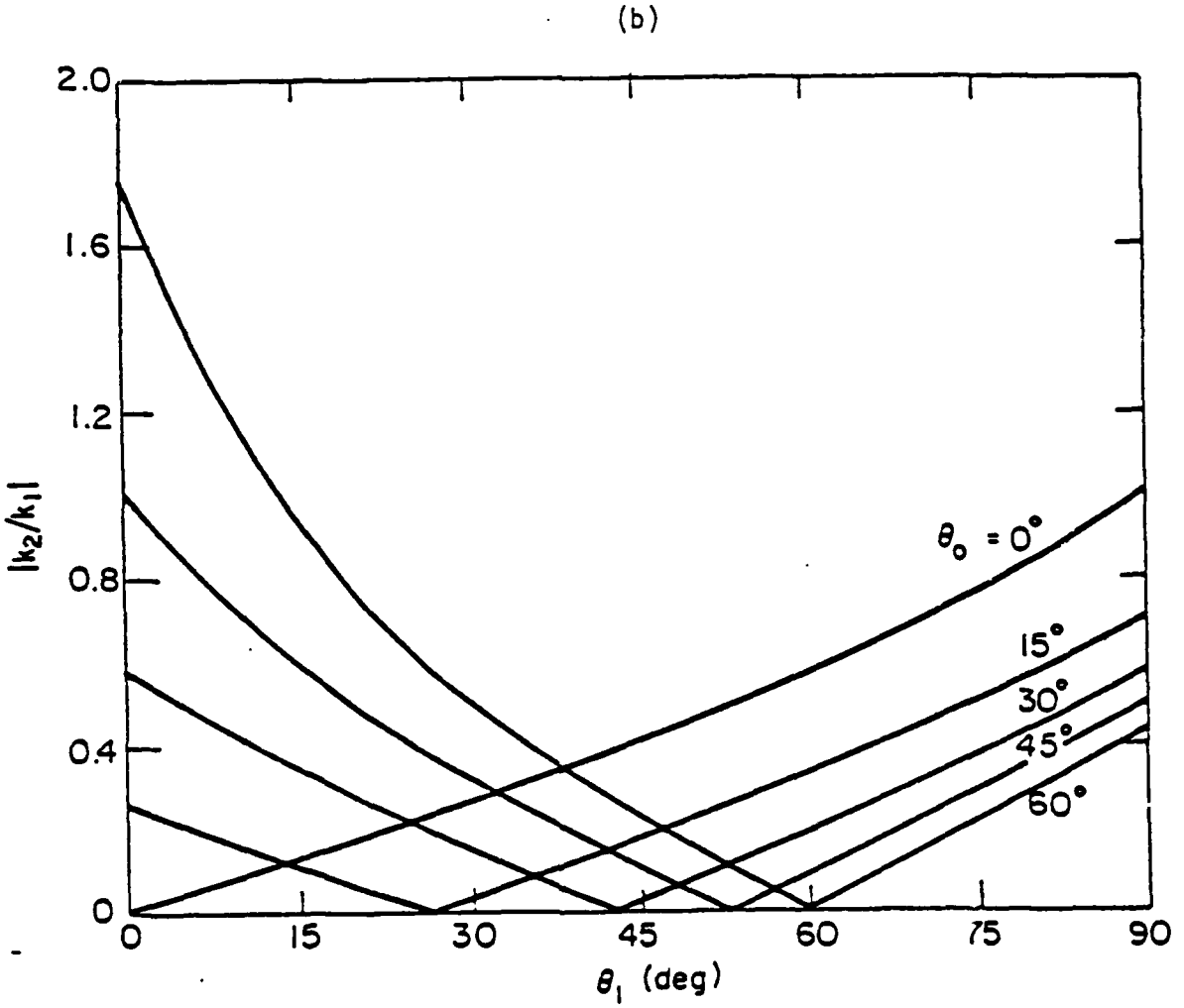

Fig. 12. Predicted variation of the a) normalized Mode I stress intensity factor and b) the ratio of Mode II to Mode I stress intensity factors for the deflection of initially inclined short elastic cracks; θ_0 is the angle of inclination and θ_1 is the angle of deflection.

Materials Science and Engineering, 57 (1983) L27-L30

Letter

The fracture mechanics similitude concept: questions concerning its application to the behavior of short fatigue cracks

R. O. RITCHIE and S. SURESH

Materials and Molecular Research Division, Lawrence Berkeley Laboratory, and Department of Materials Science and Mineral Engineering, University of California, Berkeley, CA 94720 (U.S.A.)

(Accepted November 29, 1982)

The application of fracture mechanics to the propagation of fatigue cracks is based on the premise that the governing parameter, such as the stress intensity factor K_I, used for the correlation of growth rates, fully describes the stress and deformation fields in the vicinity of the crack tip. In addition, it is implicitly assumed that the concept of *similitude* applies. The latter concept implies that, for two different sized cracks (Fig. 1) subjected to equal stress intensity values (under small-scale yielding) in a given material-microstructure-environment system, crack tip plastic zones will be equal in size and the stress and strain distributions along the borders of these zones (ahead of the crack) will be identical. Accordingly, equal amounts of crack extension Δa will be expected. For a cyclic load denoted by the maximum and minimum stress intensities, K_{max} and K_{min} respectively, this dictates that

$$\Delta a = \frac{da}{dN} = f(K_{max}, K_{min}) = f(\Delta K, R) \quad (1)$$

for each cycle N, where the stress intensity range $\Delta K = K_{max} - K_{min}$ and the load ratio $R = K_{min}/K_{max}$. However, as discussed at length elsewhere [1-3], this concept of similitude becomes violated (i) when crack sizes approach local microstructural dimensions, (ii) when crack sizes are comparable with the extent of local plasticity, (iii) when through-thickness out-of-plane stresses (which are independent of K_I) are different, (iv) when crack extension mechanisms are different, (v) when extensive fatigue crack closure is observed and (vi) when external environments significantly influence crack growth, to name but a few. Nowhere is this more evident than for the behavior of very short fatigue cracks. Experimental results to date (see for example refs. 1-13) have shown, almost without exception, that at the same nominal driving force (*i.e.* ΔK) the growth rates of short cracks (typically less than about 0.5 mm) are greater than the corresponding growth rates of long cracks (typically greater than about 25 mm). A schematic diagram illustrating these differences is shown in Fig. 2 and indicates a non-uniqueness between long and short crack growth rates both for physically small flaws and for flaws emanating from notches. Thus, for structures and components containing small cracks, where the initial growth of such defects will represent a large portion of the life, the current use of long crack data has the potential for ominously non-conservative defect-tolerant lifetime projections.

In general terms, cracks may be considered short when they are (i) small compared with the scale of the microstructure (a continuum mechanics limitation to current analysis

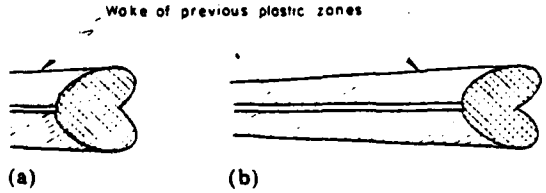

Fig. 1. Schematic representation of the similitude concept, in that cracks of differing length a at the same *nominal* driving force (*e.g.* ΔK) will possess equal plastic zone sizes r_y ahead of the crack and will thus extend equal amounts Δa per cycle: (a) short crack ($a \approx r_y$); (b) long crack ($a \gg r_y$).

0025-5416/83/0000-0000/$03.00

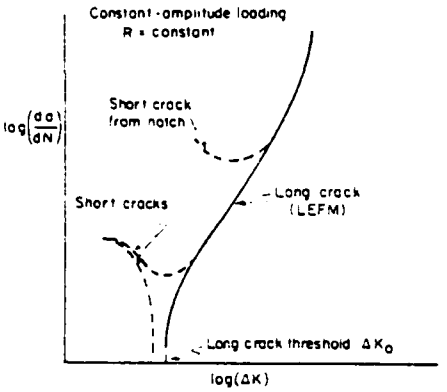

Fig. 2. Schematic representation of typical fatigue crack propagation rate da/dN data for long and short cracks as a function of the alternating stress intensity ΔK (constant-amplitude loading, R = constant): LEFM, linear elastic fracture mechanics.

procedures), (ii) small compared with the local plastic zone sizes (a linear elastic fracture mechanics limitation) and (iii) simply physically small (*i.e.* less than about 0.5 mm). Although related to the numerous factors listed above, the principal reasons associated with the breakdown of the similitude concept for such small cracks can be traced to (i) inappropriate fracture mechanics characterization (plasticity effects), (ii) fatigue crack closure (crack tip wake effects) and (iii) local crack tip environments (electrochemical effects).

The first of these factors is the most obvious in that, when short cracks are of a length a comparable with their crack tip plastic zone sizes r_y, or conversely totally embedded in the strain field of a notch, any analysis based on small-scale yielding through the use of K_I is clearly not valid. Accordingly, in such situations, alternative characterizations using elastic-plastic fracture mechanics (*i.e.* for large-scale yielding) through the use of the J integral or the crack-tip-opening displacements generally provide a much closer correspondence between long and short crack data [7].

Although this is an important first step in rationalizing the short crack similitude problem, the use of such large-scale yielding analyses cannot account for the non-uniqueness of short crack growth behavior at ultra-low growth rates. Here it has been observed [1, 3, 12, 13] that short cracks can propagate at progressively decreasing growth rates *below* the so-called fatigue threshold stress intensity ΔK_0 at which *long cracks* are considered to remain dormant or to grow at experimentally undetectable rates (Fig. 2). The latter observation highlights the fact that current fracture mechanics parameters such as K_I and J provide an adequate characterization of the *nominal* mechanical driving force* for crack extension based on stress and deformation fields *ahead* of the crack tip. However, they provide little information on the local *effective* driving force actually experienced at the crack tip, which is as much a function of irreversible plastic strains, fracture surface roughness and fracture surface corrosion debris effects in the *wake* of the tip [3]. Such wake effects are primarily described by the concept of fatigue crack closure where the nominal crack tip stress intensity ($\Delta K = K_{max} - K_{min}$) under small-scale yielding is considered to be reduced to some effective value ($\Delta K_{eff} = K_{max} - K_{cl}$) because of physical contact between the mating crack surfaces above the minimum stress intensity ($K_{cl} \geqslant K_{min}$). The origins of such closure can be related to three principal factors, namely residual inelastic deformation [14], excess corrosion debris [15] and irregular fracture morphologies (and the concomitant mode II displacements) which wedge the crack open [16–19]. Such phenomena are particularly relevant to the short crack similitude problem since all three closure mechanisms act in the wake of the crack, and by definition the short crack possesses only a limited wake (Fig. 1). Thus, short cracks in general are likely to be far less influenced by fatigue crack closure. In fact, recent experimental [19], analytical [18, 19] and numerical [20] modelling studies all conclude that the extent of closure is minimized at short crack lengths. Thus the non-uniqueness of near-threshold behavior, *i.e.* the progressively decreasing growth rates of short cracks *below* the long crack threshold ΔK_0 (Fig. 2), can be related to closure phenomena. Short cracks possess an initially higher ΔK_{eff} due to the absence of closure which progressively decreases with increasing crack length as closure forces build up to levels approaching those for long crack behavior, whereupon growth rates follow the

*Computed from the crack geometry and applied loads.

long crack curve. Such an explanation is consistent with the notion that long crack near-threshold behavior is markedly influenced by substantial fatigue crack closure [15, 20]. Thus, to circumvent the similitude problem for the near-threshold behavior of short and long cracks, one is forced with existing fracture mechanics procedures to resort to characterizing crack advance in terms of ΔK_{eff}. The practicality of such an approach is, however, extremely complex in view of the experimental (and theoretical) difficulty in defining the closure stress intensity K_{cl} (particularly for small cracks) and in isolating the individual role of the different closure mechanisms. Even this approach cannot totally solve the short crack similitude problem since *local* microstructural features, such as inclusions, second-phase particles and grain boundaries, are more likely to influence the growth of short cracks where their dimensions are comparable with the crack size [2, 3, 8, 9, 13, 21]. Such intrinsic microstructural effects, which are often specific to short cracks, have been considered to arise from such mechanisms as the blocking of slip bands [8, 9, 13] and crack deflection effects [21] at metallurgical discontinuities.

A further factor contributing to the non-uniqueness of long and short crack behavior can arise from environmental factors. Here corrosion fatigue crack growth rates of *physically short* cracks (less than 0.8 mm), well outside the near-threshold regime, have been observed in AISI 4130 steel to be one to two orders of magnitude faster than the corresponding growth rates of long cracks (25-60 mm) at the same ΔK values for tests in aqueous NaCl, whereas short and long crack growth behaviors were identical for tests in an inert atmosphere [10]. Explanations for this effect are currently unclear but have been attributed to differing local crack tip environments as a function of crack size. Specifically, the local concentration of embrittling species within the crack is reasoned to depend on the surface to volume ratio of the crack, on the diffusive and convective mass transport to the crack tip and on the distribution and coverage of active sites for electrochemical reaction, all processes sensitive to crack depth, opening displacement and crack surface morphology [10]. Since K_I, J or even ΔK_{eff} do not characterize such effects, existing macroscopic fracture mechanics procedures cannot be expected to describe the resulting behavior uniquely.

These examples of the differences in behavior of fatigue cracks of varying size provide a clear indication of where the fracture mechanics similitude concept breaks down. The stress intensity K_I, or J, although adequately describing the *nominal* mechanical driving force for crack extension, cannot account directly for local microstructural interactions, for closure effects in the wake of the tip or for chemical activity of the crack tip environment, all factors which are a strong function of crack size. It is thus unreasonable in these instances to expect unique crack growth behavior for long and short cracks, *i.e.* the similitude concept to apply. The correspondence of long and short crack data can be aided by appropriate fracture mechanics characterization (*e.g.* using large-scale yielding analysis where necessary) and by the use of the ΔK_{eff} concept (provided that experimental definition of K_{cl} is feasible), although for environmentally influenced crack growth this is clearly not the complete solution. Thus, in the absence of the similitude relationship, the analysis and utilization of laboratory fatigue crack propagation data to predict the performance of in-service components, where short cracks are present, become an extremely complex task which demands an immediate effort in fatigue research from both experimentalists and theoreticians alike.

ACKNOWLEDGMENTS

This work was supported under Grant AFOSR-82-0181 from the U.S. Air Force Office of Scientific Research with Dr. A. H. Rosenstein as technical monitor.

REFERENCES

1 D. Broek and B. N. Leis, in F. Sherratt and J. B. Sturgeon (eds.), *Materials. Experimentation and Design in Fatigue*, Westbury House, Guildford, 1981, p. 129.
2 J. Schijve, in J. Bäcklund, A. Blom and C. J. Beevers (eds.), *Fatigue Thresholds*, Vol. 2, EMAS, Warley, 1982, p. 881.
3 R. O. Ritchie and S. Suresh, *Behavior of Short*

AD-A131 324 FATIGUE BEHAVIOR OF LONG AND SHORT CRACKS IN WROUGHT AND POWDER ALUMINUM..(U) CALIFORNIA UNIV BERKELEY DEPT OF MATERIALS SCIENCE AND MINERA.. R O RITCHIE MAY 83 2/2

UNCLASSIFIED UCB/RP/IE/A1013 AFOSR-TR-83-0616 F/G 11/6 NL

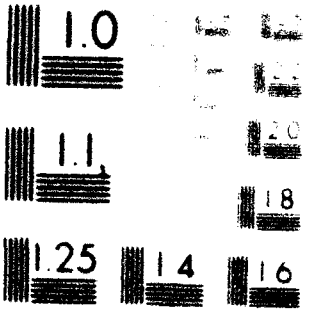
1.0
1.1
1.25
1.4
1.6
2.0
1.8

...Cracks in Airframe Components*, Proc. 54th Specialists Meet. of AGARD Structures and Materials Panel, 1982, Advisory Group for Aeronautical Research and Development, France (in the press)

4 S. Pearson, *Eng. Fract. Mech.* 7 (1975) 235

5 R. A. Smith, *Int. J. Fract.* 13 (1977) 717

6 J. Lankford, *Int. J. Fract.* 16 (1980) R7

7 M. H. El Haddad, N. E. Dowling, T. N. Topper and K. N. Smith, *Int. J. Fract.* 16 (1980) 15

8 K. Tanaka, Y. Nakai and M. Yamashita, *Int. J. Fract.* 17 (1981) 519

9 W. L. Morris, M. R. James and O. Buck, *Metall. Trans. A* 12 (1981) 57

10 R. P. Gangloff, *Res Mech. Lett.* 1 (1981) 299

11 J. F. McCarver and R. O. Ritchie, *Mater. Sci. Eng.* 55 (1982) 63

12 M. M. Hammouda and K. J. Miller, *ASTM Spec. Tech. Publ.* 675 (1979) p. 703

13 J. Lankford, *Fatigue Eng. Mater. Struct.* 5 (1982) (in the press)

14 W. Elber, *ASTM Spec. Tech. Publ.* 486 (1971) p. 230

15 S. Suresh, J. F. Zamiski and R. O. Ritchie, *Metall. Trans. A* 12 (1981) 1435

16 N. Walker and C. J. Beevers, *Fatigue Eng. Mater. Struct.* 1 (1979) 135

17 K. Minakawa and A. J. McEvily, *Scr. Metall.* 15 (1981) 633

18 S. Suresh and R. O. Ritchie, *Metall. Trans. A* 13 (1982) 1627

19 M. R. James and W. L. Morris, *Metall. Trans. A* (1982) (in the press)

20 J. C. Newman, Jr., *Behavior of Short Cracks in Airframe Components*, Proc. 54th Specialists Meet. of AGARD Structures and Materials Panel, 1982, Advisory Group for Aeronautical Research and Development, France (in the press)

21 S. Suresh, unpublished results, University of California, Berkeley, 1982


DATE
ILME